Response to Referee #1 (updated)

General Comments

This paper assesses the effect of riverine nutrient and C inputs on C cycling in global oceans, and notably on CO2 outgassing in a pre-industrial state. The work includes quantification of riverine inputs of different elements under inorganic and organic forms, regional coastal shelves analysis, and global ocean biogeochemical modelling. Finally, the authors derive a global land-ocean-atmosphere pre-industrial budget, and discuss the effect of riverine inputs and gaps that need to be further addressed in the future (e.g., including volcanic emissions and the effect of shale organic oxidation). I believe this is a substantial piece of work, improving the current understanding of global C cycling, and totally fitting Biogeosciences' scope.

Response: We would like to thank the reviewer for the comments and very helpful contributions to improving the manuscript. In this response, we first address the individual comments and then refer to the changes made for the revised manuscript.

Specific Comments

1) In general, the paper is extremely dense and would benefit from being shortened and making it more to the point. Major conclusions should be better highlighted, and repetitions avoided. Also, consider deleting sections with discussions out of the main scope of the study and already addressed in previous work (e.g., on weathering). A few suggestions to improve this point are also listed hereafter, in the specific comments.

Response: We think that the suggestion to streamline and shorten the manuscript is a good point that has been mentioned by both reviewers, and we therefore considered this for the revised manuscript.

We restructured the manuscript with a shortening of the introduction (section 1), the elimination of repetitions in the methods section (section 2), and the merging and shortening of pre-industrial weathering and riverine loads sections (-> section 3), and the merging of information from previous sections into a section 5 (Coastal region analysis).

2) Further details should be provided on the construction of 2 ocean simulations, RIV and REF. The understanding of the differences between these 2 simulations is key to understand the paper's major conclusions.

Response: While this was partly done in paragraphs in the methods and in the results and discussion, we also see the need to further highlight the main differences between REF and RIV, and discuss the analysis strategy. These are two things: Firstly, the geographical differences of inputs to the ocean (riverine inputs vs inputs to the open ocean), and secondly magnitudes of the increased carbon inputs to the ocean due to the transfer of carbon from land to ocean.

We more clearly stated these points in the revised manuscript (section). We also believe that the improvements from comment 1) help improve the overview of important points.

Minor comments

L7-8p1. “Thirdly, we quantify the terrestrial origins. . . in the framework, . . .” -> It is not clear from this sentence if this is purely a modelling exercise of if you are assessing global oceanic C budgets using the coupled land-atmosphere-ocean model.

Response: Here, we solely budget for the carbon fluxes from the “stand-alone” models, which are forced with the same pre-industrial atmospheric state. The models do not however give a feedback, which alters the atmospheric state, since the atmospheric CO2 concentration would decline due to the carbon imbalance of the atmosphere (Figure 11). On the terrestrial side, the carbon fluxes are derived from the weathering and the organic carbon export models. On the ocean side, they are derived from the the ocean biogeochemistry model HAMOCC. We therefore do not take into account for feedbacks in the system, as would be done in a fully coupled land-atmosphere-ocean model, but if so, one would need to consider further carbon outgassing sources (long-term volcanic emissions, shale oxidation), in order to have a balanced budget for the pre-industrial atmosphere.

This is clarified in the revised manuscript, although the discussion exceeds the scope of the abstract.

L11p1. “leads to a global oceanic source of CO2” -> “leads a net global CO2 emission to the atmosphere of”. To be consistent with the following sentence, the “source” would be 183+128 TgC/yr (Fig. 11).

Response: We implemented this correction in the revised manuscript.

L14p1. It is not clear what a sink due to a model drift is without reading the whole paper in depth. . .
Response: This is a good point, and we think that the word “model disequilibrium” is more understandable for the reader.

Introduction. The introduction provides a lot of information, some of it not totally relevant to the focus of the study. It should be shortened and re-organized to better highlight current state of knowledge, gaps and how they are addressed in this work.

Response: We will improve the structure and points of focus of the introduction in the revised manuscript. We will shorten the “background information” paragraphs to only include the most relevant information for the study and to increase the focus on what has been done/not done.

L15p2. “these knowledge gaps” -> all knowledge gaps are presented in paragraph 7.

Response: We agree that this part of the sentence was redundant and therefore removed it.

Paragraphes 2-6. These present in detail processing in watersheds, gaps in knowledge on tDOM and POM degradation and transfers, etc. These could be substantially shortened, since these are not points tackled in the paper, which waters down the main message/focus of the paper. Parts of it (e.g., uncertainties on degradation of different OM forms, desorption of P as it enters saline waters etc.) could however be used in the Discussion (e.g., subsection 7.2).

Response: We understand the point of view of the reviewer, and also therefore shortened the paragraphs. However, some of the information within these paragraphs is also vital in order to understand the assumptions chosen later in the methods section. For instance, due to the previous degradation of tDOM within rivers, we assume it is less reactive once it reaches the ocean than oceanic DOM, but not completely inert. Therefore it`s remineralization rate was chosen for it to have a longer lifetime than oceanic DOM.

In the revised manuscript, we will shorten these paragraphs and increase their focus.

L2p5. "Pre-industrial" could be defined here (state in 1850).

Response: We defined pre-industrial here in the revised manuscript.

L5p5. "spatially explicit quantification of global riverine loads" -> "spatially explicit quantification of riverine exports to global coasts". It is not clear otherwise if the loads within watersheds are quantified as well.

Response: The loads are indeed quantified for every watershed. We agree this might be somewhat unclear here and corrected this in the revised manuscript.

L10p5. "We first briefly..." -> Description of the Method's content is already described in the previous paragraph. These introductory sentences could be most of the time removed to make the paper shorter and more to the point.

Response: We removed this sentence, along with other needless repetitions in the revised manuscript.

L12p5. Define what you consider like alkalinity here.

Response: Alkalinity (which is carbonate alkalinity in this case of our derived riverine loads) is more clearly defined in the revised manuscript. This is however more suited in section for the riverine alkalinity loads, and section for alkalinity in the ocean.

L20-32p5. This is described in detail in the subsections; it could be deleted to avoid repetitions.

Response: We believe it is important to give a brief overview of all derived loads before addressing the individual elements. We think that the reader will be missing the "big picture" if we start with individual details of every compound load. We however removed large parts of the paragraph, which might be unnecessarily repeating information from later in the revised manuscript.

Fig.1. Precise that the C from weathering sources is DIC (OC assumed to originate only from the uptake of atmospheric CO2).

Response: This has been added to the figure in the revised manuscript.

L12-14p7. Doesn't river damming affect POM loads between pre-industrial and the 1970s? This point could be considered later in the discussion on river loads.

Response: We assume in the whole study that the organic matter loads have remained constant globally since the pre-industrial time period. While increased organic matter supplies to catchments have been suggested in literature (for instance in Regnier et al. 2013), increased retention and remineralization (for instance due to damming, Maavara et al., 2017) has also been reported. There is however yet a study to spatially quantify these combined effects, while

comparing the pre-industrial time-frame to the present day. This is briefly already discussed in 4.1. and we believe a more comprehensive discussion of these combined anthropogenic influences escape the scope of our study.

L13p8. "Pre-industrial runoff..." -> this is already explained L1-5p7, not necessary. This repetition occurs several times throughout the paper.

Response: We removed these repetitions in the revised manuscript.

L24p8. Are the soil types listed here those with typically low erosion rates? Is the 0.1 factor also used for wetlands and areas with a high groundwater table? If yes, what definition did you use for "high water table"?

Response: The soil types listed here are indeed the ones assumed to have very low weathering rates. The wetland areas are the Gleysols. These (along with the other soil types) are defined in the Harmonized World Soil Database (Fao et al., 2009). The description found in the database is that gleysols are soils with permanent or temporary wetness near the surface. The derivation of the soil shielding factor is extensively described in Hartmann et al. (2014). In our opinion, further details escape the scope of our study.

L4p9. What do the 1.6 TgP/yr used here correspond to? Fertilizer P in surface runoff reaching rivers? Hart et al. (2004) report an annual fertilizer consumption of 873 TgP in 1913.

Response: This number was wrongly cited. The 1.6 Tg P to catchments was derived from Figure 3 in Beusen et al. (2016), which on its side derived from inputs described in Hart et al. (2004), as is cited in the corresponding technical manuscript (Beusen et al., 2015). Assuming 873 Tg of P inputs of fertilizer to agricultural land for the year 1913 (Hart et al., 2004), this relatively high value seems plausible.

L7-9p9. Why is it reasonable to assume P equilibrium in soils at pre-industrial state (besides that state-of-the-art models usually use this initialization)?

Response: We agree this assumption is a limitation of our study. For instance, Filipelli et al. (2008) suggest an increase of P inputs to catchments due to increased soil erosion caused by deforestation and land use change. This likely already had an impact on land-ocean fluxes prior to industrialization, although it is completely unknown how large these fluxes could be. This point goes hand-in-hand with our assumption that the organic matter fluxes remain near constant, which is at least consistent within our study.

L9-11p9. The assumption that spatial distribution of P river loads is the same in pre-industrial and 1970 is quite strong. For example, agriculture was probably much more developed in North America and Western Europe than in Asia at the beginning of the 20th century. Implications of this assumption should be discussed later in the discussion on river loads. Why not use load distribution from models describing earlier states (e.g., Beusen et al., 2016)?

Response: This is a good point, we therefore performed an analysis comparing the assumed anthropogenic input distribution in this study (directly derived from NEWS2 year 1970), with the distribution of 1900 and 2000 inputs from the Beusen et al. (2016) study. The global distribution of all three cases are very similar, although there is an increase in some parts of Southeast Asia between 1900 and 2000, which can be observed from the results of the Beusen et al. (2016) study. At the global scale, we deem our assumption to be plausible enough. The analysis can be found in Supplementary information S.1.1.

L23-24p9. Molar C:P ratios are already provided earlier. You can just say L19 that P is incorporated in organic matter accordingly to C:P molar ratios for tDOM and POM.

Response: We corrected this in the revised manuscript to avoid repetition.

L6-12p10. Precise here that DIN export was calculated by subtracting the part contained in organic matter. Was DFe export equal to Fe inputs to catchments?

Response: The Fe composition of the organic matter is also subtracted from the Fe inputs to the catchments, which results in DFe. It is clarified in the revised manuscript.

L11-16p11. This is not totally clear. Do you assume that only HCO3- affects alkalinity and that DIC is only HCO3- as well (Alk:DIC = 1:1)?

Response: We asumed that only HCO_3^- release from weathering affect the alkalinity and that the Alk:DIC ratio is 1:1. This was already stated and justified in the paragraph, but we have made some modifications to the paragraph to make it more understandable.

Sub-subsection 2.1.5 Silica. Why not use the same weathering model type as for P (Hartmann et al., 2011)?

Response: In theory, this would be possible, but the model would first need to be calibrated for Si. Since the Beusen et al. (2009) model is already calibrated for Si, we used this one out of simplicity.

Sub-subsection 2.2.1 Ocean biogeochemistry. A scheme with model state variables and processes would be helpful here (as well as a description of biogeochemical processing equations and parameters as Supplementary Information).

Response: We added an overview of biogeochemical processes in Figure 1, a scheme which illustrates the main processes represented in HAMOCC (Appendix A) in the revised manuscript. Regarding the equations, this is too extensive in the case of this manuscript. We refer in our manuscript to the model description study of Ilyina et al. (2013) for equations and parameters, with more recent model developments described Paulsen et al. (2017) for cyanobacteria, and in Mauritsen et al. (2019). This has been already published, and in case of further interest, the model code can be requested. We however nevertheless provide a list of parameters in comparison to the ones given in Ilyina et al. (2013) study in a Supplementary Information S.2.

L22p13. How did you choose the 0.003 d-1 value for tDOM degradation? 0.008 d-1 for the oceanic DOM is also in the literature range for tDOM degradation.

Response: The assumption chosen here was that the tDOM entering the ocean at the river mouths is less reactive than the "freshly produced" oceanic DOM, since tDOM is reported to have been strongly degraded previously during its transport in rivers. The tDOM is however also not inert in the ocean. This is stated in paragraph p11.l25-p11.l30.

2.2.3 Pre-industrial ocean biogeochemistry model simulations. Please provide more details here, since the distinction between the REF and RIV simulations is key to understanding the paper's results. In the REF simulation, are input fluxes (per surface area?) globally homogeneous? Or do they compensate sediment losses to reach equilibrium locally (at the cell scale)? In the RIV simulation, are there also open ocean surface inputs in addition to river inputs?

Response: In short, the REF inputs are added globally homogeneously (per surface area) to the ocean surface. This represents oceanic inputs by (to a major part) passing the coastal ocean and does not at all represent geographic riverine inputs. Their magnitudes are dictated by losses to the

sediment: every few hundreds of years, the averaged global burial loss of biogeochemical compounds was computed, and these were the fluxes added to the surface ocean. They are indeed homogeneous per surface area. In the RIV simulation, there is no open ocean surface inputs, since these were replaced by riverine inputs, derived as shown in the previous sections of the manuscript.

We added clarification to these points extensively in the revised manuscript section 2.2.3 and also in the results section 4.1.

L1-6p14. What do you call quasi-equilibrium? How were the lengths of the different simulation chosen? Why did you perform a succession of 3 runs for the RIV simulation? Does "standard simulation" (L4) refer to REF?

Response: The lengths of the simulations were chosen accordingly to the model state, meaning the simulation were performed until no strong drifts of model variables was remaining. Since biogeochemical processes in the ocean, and especially in the sediment, likely need larger simulation time-periods to perfectly equilibrate than is feasibly possible with current computing resources, there will however always remain a small drift in model variables in such simulations. Therefore, this is a state of quasi-equilibrium and not a perfect equilibrium state.

The 3 sequential simulations for the RIV simulation were done in order to achieve a more stable state in the ocean sediment. The motivation here is that it is much less expensive in terms of computing power to simulate the sediment separately from the ocean, and since the time-scales of processes taking place in the sediment are much longer than in the water-column, it makes sense to perform simulations for the sediment alone once the oceanic water column has reached a state close to equilibrium. We therefore firstly performed a simulation of 4'000 years including both the water column and sediment biogeochemistry, until the global particulate fluxes from the water column to the sediment were approximately stable. Then simulations of the sediment component of the model, while being given the stable global particulate fluxes from the previous simulation. Finally, the sediment state was re-coupled to the ocean water-column for the final 2000 year simulation.

We have added some clarification in the revised manuscript, but the discussion of the computational expenses of performing of the model spin-up is too technical for the scope of this journal, and would substantially unnecessarily lengthen the manuscript.

Are the 100-year means (output results) calculated on the last 100 simulated years for each simulation? What are the simulation timesteps?

Response: The last 100 year mean of both REF and RIV were used to the analysis. Using a 100 year mean prior to this would not affect the results much. The simulation timestep is one hour. This was added to the revised manuscript.

It is mentioned that water loads vary inter-annually based on runoff inputs from OMIP. Are the ocean physics' inter-annual variations modelled with the same patterns for every simulated year?

Response: The parameters within the physical circulation model MPI-OM remain the same. We would like to point out that the model simulates the response of the ocean physics dynamically to the atmospheric state, from which the information is given to the model for every time-step. There is therefore inter-annual variation in the physical features of the ocean, and even variation at every model time-step.

It escapes the scope of our study to completely explain mechanisms of such an ocean circulation model in the scope of our study; this has been done many times before and we would like to refer to the cited references for our specific model (Junclaus et al., 2013 and Mauritsen et al., 2019).

L20-24p16. For which periods were these Si loads from the literature estimated?

Response: These estimates are for the present day. We will mention this in the revised manuscript.

L26-32p16. Comparison with Mackenzie et al. (1998) does not seem necessary here, especially since they assess only the TIC load.

Response: We agree and therefore removed this comparison in the revised manuscript.

Subsection 3.1 Runoff, precipitation and temperature patterns. Hydrology model performance is not the scope of the paper; this section seems to water down once more the message/goal of the study. The scaling of the MPI-ESM runoff should be detailed earlier, in the Methods section. How is the factor 1.59 chosen? Why is the runoff not scaled to the OMIP one, to be fully consistent with the freshwater inputs?

Response: Factor 1.59 was chosen in order to scale the average of Fekete et al. (2002) and Dai and Trenberth (2002) In the revised manuscript, this is more clearly stated. In order to shorten the manuscript, we will merge sections 3 with section 4, while shortening both with only the most central information for the next parts of the manuscript remaining. The discussion of the weathering model input parameters runoff, temperature and precipitation was moved to Appendix B.

Subsection 4.1 Global loads in the context of published estimates L2p19. Does the Fe-P load given in Table 3 only corresponds to the fraction that is desorbed when entering the estuary?

Response: The Fe-P loads refer to desorbed P loads both for the given modelled estimates (Model. Global load), as well as for the Compton et al. (2000) values. This was stated in the Table 3 caption in the revised manuscript.

Table 3p19. Precise for the POP comparison that the 5.9 value (for 1970) is for PP, and not only POP.
Response: This was added to the Table 3 caption in the revised manuscript.

L20-23p20. Doesn't the potential increase in Si retention at the end of the 20th century mainly concern particulate forms?

Response: This is not correct. Global reservoirs have also been suggested to retain a significant amount of DSi (Lauerwald et al, 2013; Maavara et al., 2014). This is due to in-reservoir formation of biogenic silica, which is then in turn also increasingly retained.

L20-26p21. Please better organize text.

Response: We restructured part of the paragraph and removed unimportant information in the revised manuscript.

L4p22. Could the discrepancies also be due to the fact that weathering formalisms are less adapted to Arctic regions?

Response: This is indeed very likely, with weathering mechanisms in the Arctic being likely more complex than is modelled here (for instance due to permafrost, Hartmann et al., 2014). We briefly mentionen this in the revised manuscript.

5.1 Ocean state – An increased biogeochemical coastal sink L14-15p25. "There is a higher carbon load originating from organic matter, since tDOM C:P ratio is higher than the oceanic DOM C:P ratio" -> This explanation is not straight-forward, since the estimation of DOC is not related to P in the model.

Response: This is correct, the outgassing is caused by the higher higher carbon loads contained in tDOM, which were not accounted for in REF. However, if the C:P ratio in tDOM were the same as for oceanic organic matter, the DIP and DIN released would drive the biological production to take up DIC, which would compensate the additional DIC originating from remineralization of tDOM in the long term. For oceanic organic matter exported to the sediment, 122 mol C is also exported for every mol P. For the river inputs however, for every mol P 2583 mol C are added. Therefore there is an accumulation of DIC when tDOM is mineralized, which leads to higher pCO_2 and outgassing. This is shown in equation C2 in Appendix C1. We have also clarified the sentence in the revised manuscript.

L15p25-L2p26. Comparison with other studies was already discussed earlier.

Response: The central point here is that the carbon inputs are increased in RIV comparison to REF (the model version used up to now), which is an agreement with previous estimates. This is why carbon outgassing takes place and therefore we believe this is central information here, even if it has been stated before since we improve the model with regards to its carbon inputs.

L17-19p26. Isn't the effect of large oxygen minimum zones on DIN concentrations also visible in WOA dataset?

Response: This is indeed the case and a sign that a substantial magnitude of denitrification takes place in the region.

What explains the major differences in DIP, DIN and DSi concentrations in the Southern Ocean?

Response: This is likely due to the relatively poor representation of the complex ocean circulation of the Southern Ocean in global ocean circulation models. An improved representation would require high enough resolution to better represent vertical mixing taking place in the Southern Ocean and a better representation of the effects from storms.

Table 5.p27. Do N inputs include N2 uptake from the atmosphere in the two simulations?

Response: **Both simulations consider dynamical N_2 fixation by cyanobacteria as well as (natural) nitrogen deposition. This is already stated in the methods (section 2.2.1, p10.l19 in revised manuscript): "The changes were made to incorporate dynamical nitrogen fixation through cyanobacteria (Paulsen et al., 2017), .."**

L12-14p28. Comparison of Arctic concentrations to the WOA database could be presented earlier in text, with the rest of the comparisons.

Response: We agree and implemented this change in the revised manuscript, along with eliminating unnecessary information in the section.

7.1 Rivers in an Earth System Model setting. Paragraph 2 (L12-17p36). These improvements could further avoid strong assumptions, such as globally constant N:P ratios for river inputs, and on the spatial distribution of non-weathering sources.

Response: These are both very good points and we added a brief discussion of these to the subsection in the revised manuscript, as well as an analysis in Supplementary Information S.1.1 (anthropogenic input distribution), S.1.2 (allochthonous input distribution) and S.1.3 (N:P ratios).

L11-14p37. Is the need for a runoff scaling factor a major conclusion of this work?

Response: This is a more technical conclusion, and therefore we have eliminated it.

L17-21p37. "Even for present-day..." -> comparison with literature is already discussed earlier, this could be removed.

Response: We agree and the sentence will be removed in the revised manuscript.

L26-27p37. "which have been identified to be more strongly controlled by extreme hydrological events than other C species" -> Was this considered in the study? What does it imply? It seems that this belongs to some discussion (that should be more developed if added).

Response: The NEWS2 model results, which we derive POC exports from, calculate the year-means of these exports. Therefore, these extreme events are not at all grasped in the model. We see this more as a conclusion than a discussion point: One might need to better resolve the intra-annual variability of riverine loads for regions with high annual POC exports.

L17p38. "despite previously being sinks" -> be more explicit by explaining that this is without accounting for river inputs, and not "previously" in a temporal way.

Response: We corrected this statement in the revised manuscript.

L27-29p38. Interhemispheric C transfers are already mentioned earlier in this section (L1-3p38). Please focus in this last paragraph only on the major points that this study shows have to be included in ESMs to better assess land-ocean-atmosphere C transfers.

We removed this second discussion interhemispheric C transfer and improved the final paragraph.

Appendix C L4p42. "Table 3" -> "Table 2". How do you get to the 280 Tg/yr of CO2 drawdown? Some calculations could be shorter explained (e.g., CO2 emissions explained L16- 20p42 and L9-12p43).

The drawdown of CO2 is calculated from directly from the weathering model (See equations (9) and (10) in section 2.1.4 and explanations in the text p14l5-p14l7 in the revised manuscript.

Minor Comments

L5p1. "in a regional shelf analysis" -> "in regional shelf analysis"; there are more than one.

This is not correct. It is one analysis of many shelf regions. Therefore "in a regional shelf analysis" is correct.

L10-11p1. "total C" -> "global C"

Corrected.

L13p2. “exported to the sediment” -> “stored in the sediment”

Corrected.

L18p2. Define NPP L25p5.

This sentence was removed, but we now define NPP later in the revised manuscript.

“their its ratios” -> “their ratios”

Corrected.

L30p5. “a fraction P” -> “a fraction of P”

Corrected.

L4p11. “and that 2 HCO3-” -> “and of 2 HCO3-”

Corrected.

L11p12. “dynamical nitrogen fixation through cyanobacteria” -> “dynamic N fixation by cyanobacteria”

Corrected.

L14p13. “its consistence” -> “its composition”

This sentence was removed.

L11p17. “much stronger gradients of variation” -> “much higher spatial variability”

This sentence was removed.

L21p17. End of sentence is missing or “which” should be deleted.

This sentence was modified.

L17p20. Start new sentence at “Dürr et al. . .”

Corrected.

L2p21. “and to a framework” -> “and could be fed/incorporated into a framework”

It is not the river loads that would be incorporated into a framework, but the framework that we present here could be incorporated into an Earth System Model.

L2p30. “compensate” -> “counterbalance”

Corrected.

L15p30. “due higher” -> “due to higher”

This sentence has been removed.

L18 p36 “consistence” -> “composition”

Corrected.

L19- 25p43. Check parentheses.

Corrected.

References (excluding cited references in the manuscript):

Beusen, A. H. W. Et al.: Coupling global models for hydrology and nutrient loading to simulate nitrogen and phosphorus retention in surface water – description of IMAGE–GNM and analysis of performance, Geosci. Model Dev., 8, 4045-4067, https://doi.org/10.5194/gmd-8-4045-2015, 2015.

Lauerwald et al.: Retention of dissolved silica within the fluvial system of the conterminous. Biogeochemistry, 112,637-659. 2013.

Response to Review#2 (updated)

General Comments

The manuscript addresses an important question about material transport across the land-ocean aquatic continuum, and is of particular interest given its global application. I appreciate the substantial amount of work presented here, which includes a synthesis of existing methods to derive a global data set of riverine sources of nutrients and carbonate species to the ocean, long-term simulations of a global ocean-biogeochemical model, and analyses of CO2 outgassing hotspots and the origins and fates of riverine carbon from land/atmosphere to the ocean/atmosphere. I am particularly impressed that the authors were able to run the global model simulations for several thousand years long (even though the model is relatively coarse). The scope of this study is certainly appropriate for publication in Biogeosciences, however the manuscript in this current format requires clarifications in some places while in others the text needs to be shortened and/or streamlined in order to avoid distraction and help readers better capture the key points of this study.

Response: We would like to thank the reviewer for their helpful comments and criticisms, and are also pleased with the acknowledgement of effort put into synthesizing the state of knowledge of land-ocean biogeochemical exports, as well as our computational expenses to simulate such long time-periods.

We agree the manuscript should be streamlined and shortened to a certain extent to improve the reader's understanding of the main points.

In this response, we first address the individual comments and then refer to the changes made for the revised manuscript.

Major Comments

Authors note: The comments found in the next paragraph of the reviewer's comment will be addressed individually.

My major concern about the study is the comparison of carbon (and other) budgets between the standard simulation (RIV, what does it stand for?) and reference simulation (REF), which led to most key conclusions made in the manuscript.

Response: In short, the reference simulation REF represents a previous model version of the ocean biogeochemistry model, which is lacking in terms of its constraints and geographical locations of "riverine" inputs. In the simulation RIV, we consider the magnitudes of the pre-industrial riverine inputs as well as their geographic input locations to the best of our knowledge. The focus is to analyze how adding riverine fluxes plausibly in terms of magnitudes, as well as at their correct geographical location (RIV) affected the ocean's biogeochemical state. This is done in comparison to REF, where these inputs are added to the open ocean. As a note, the overarching goal of having biogeochemical inputs

in REF is to compensate losses to the sediment; without these inputs, all biogeochemical variables would strive to an equilibrium state equal to zero. This however does not mean that these inputs must be added at the sediment interface (nor is this a more "realistic" solution to the problem), we will revisit this as a response to a later comment.

We improved the explanations of REF and RIV in the methods section 2.2.3., as well as the main differences in the results & discussion section 4.1.

The authors described REF as a configuration where no river inputs are added to the ocean but "the burial loss of biogeochemical tracers was compensated by a global homogenous flux to the surface ocean", such that REF is "fully constrained by the loss of the sediment layer" (P13L26-29). This REF configuration seems a bit odd or at least not so clear to me.

Response: We would like to note that the REF simulation is the state-of-the-art previous model version, which is lacking in terms of its representation of terrestrial nutrient and carbon inputs to the ocean, since it considers these inputs solely at magnitudes to compensate for sediment losses, and they are added to the open ocean. We improve the model in RIV in order to represent the riverine loads magnitudes and geographical locations. We did not design the REF model setup for this study in particular, but it is adequate in order to assess the impacts of riverine loads added at their geographical river mouths (RIV) in comparison to biogeochemical inputs added to the open ocean (REF).

Is this addition of homogenous flux occurs during the same or next time step?

Response: The loss of biogeochemical compounds to the sediment is not computed dynamically within the model, but we approximated the sediment loss fluxes for a 100 year mean around every 1000 years of the REF simulation. The resulting fluxes are added to the model at every timestep.

We added this information to the revised manuscript.

Why choosing to use a homogenous flux instead of a spatially varying flux that directly compensates for the bottom loss at the same location? Wouldn't this framework to some degree arbitrarily homogenize the resource distribution across the ocean?

Response: In theory, this could be the case. We however show in the paper that the global open ocean distributions of for instance nutrients (DIN, DIP, DSi) and NPP are to a greater extent dictated by ocean circulation. Firstly, the distributions of these variables (for instance DIN oceanic concentrations) are not homogeneous in REF, which does not reflect the distributions of the inputs. Therefore, the locations of the inputs clearly do not strongly dictate the distribution. Secondly, the difference between RIV-REF is relatively small compared to the "background" signal (For instance in the case of the NPP: Figure 8b). The mechanisms explaining the stronger importance of ocean circulation are that the fluxes added to the ocean to compensate for the sediment losses are small, especially per area, in comparison to the oceanic inventories of the compounds. We show this in an analysis in the Supplementary Information S.5; the P inputs are for instance only a fraction of only the surface layer P inventories for various regions. This is because the P inputs are

added over such a large area (in fact, the entire ocean). Furthermore, the nutrients are transported away from their points of "addition" relatively rapidly, since we do not observe accumulation in the open ocean at the points of inputs (-> the distribution of the nutrients and NPP in the ocean is not at all homogeneous).

The reviewer is however to a certain degree correct, since adding nutrient fluxes homogeneously to the open ocean artificially increases nutrient concentrations and NPP to a certain degree due to the addition of nutrients to the open ocean. In reality, there are no homogeneous surface fluxes to the open ocean. This is what we improve with the simulation RIV by eliminating biogeochemical compound fluxes to the open ocean and adding them to river mouths.

Why adding the flux at the surface instead of evenly distributing it throughout the water column?

Response: Our approach to add nutrient fluxes to the surface (REF) is slightly more realistic than adding them through the water column, since riverine fluxes also enter the ocean at the (near-) surface. Furthermore, adding biogeochemical compounds within all of the water column would also create an artificial signal: in areas where upwelling (rising of water masses from deeper layers to the surface) takes place, there would be an unwanted increase of compounds supply. For instance, nutrients added to the deeper water column layers would artificially increase the NPP at the surface of upwelling areas, which is also not at all realistic. That being said, the RIV scenario is the most realistic of all mentioned scenarios, since it also considers the correct geographical location of river inputs.

How about distributing this flux only along the coastline (acting as a riverine source)?

Response: This is indeed a more realistic solution than was chosen in REF, but it would not allow us to investigate the effects caused by adding rivers to their correct geographical location in contrast to adding them in the open ocean, which is part of what we want to investigate in this manuscript. The difference between RIV and the suggested simulation would not be as large as between RIV and REF, since adding the flux to the coastline resolves to a certain degree the geographic distribution of the riverine fluxes. We are also not aware of any model approaches that tackle riverine inputs as a homogeneous coastline source, and therefore the found differences would not be of great use to assess what models are missing by misrepresenting riverine inputs.

It seems that in this framework carbon (and other materials) is being relocated from the bottom to the surface and from some places to others without any explicit transport processes involved. And this would potentially make a HUGE impact on NPP and CO2 outgassing patterns regardless of riverine inputs.

Response: We show in Figure 8 that the impacts on the NPP between RIV-REF are relatively small, despite this large difference in distributions of the biogeochemical inputs. Therefore, the changes suggested by the editor are unlikely to be huge. We also would like to point out that this mentioned re-location is what happens in reality: riverine inputs at

the surface are thought to approximately compensate sediment losses in the ocean sediment (the bottom). Thus, a "reflecting" sediment is not a more realistic scenario.

We already state in the manuscript the dominant role that the physical circulation in dictating open ocean biogeochemical distributions and would like to avoid extending the manuscript with further discussions on other scenarios that we do not perform.

Also, what are other inputs to the REF beside this surface flux? Does REF also include N2 fixation? How is carbon synthesis associated with N2 fixation being handled in the model?

Response: Both model simulations include N_2 fixation, nitrogen deposition and dust deposition. These are all unchanged between in the simulations RIV and REF. At low DIN concentrations and favorable conditions, cyanobacteria fix N_2 in order to produce organic matter. The detailed description of cyanobacteria activity and their effects on the ocean state can be found in Paulsen et al. (2017).

While we state that N_2 is fixed dynamically by cyanobacteria in section 2.2.1, we will add revised manuscript the inputs of nitrogen deposition and dust deposition (in both model simulations), and from which literature sources the values for the inputs were derived. Both these atmospheric deposition fluxes are however identical for REF and RIV, so they do not impact the differences between the simulations.

Depending on these details and whether the comparison between RIV and REF is justifiable, I recommend either a major (which would require a re-configuration run of the 5000-year REF experiment) or a moderate revision (which would be focused on streamlining and shortening the text plus clarification on some details as suggested below) of the paper before considering it for publication in Biogeosciences.

Response: Leaning on our previous responses, we do not see the need for an additional reference simulation. Using the current simulations enables us to assess the differences between biogeochemical riverine inputs as derived in the manuscript and adding the biogeochemical inputs to the open ocean, as was done previously in simulations in HAMOCC.

Minor Comments

P2L13: and also released to the atmosphere

Response: This is corrected in the revised manuscript.

P2L19-P2L6: introductory information in these a few paragraphs needs to be streamlined. I suggest shortening it to 5-8 lines and expand Fig.1 to include more details on the processes to be considered or discussed.

Response: We assume the reviewer is addressing the whole introduction. The introduction was streamlined and shortened in the revised manuscript.

P3L9: without reading the referenced literature, it is not so clear to me why riverine DIC would cause CO2 outgassing. Is it due to solubility change? Would riverine DOC/POC be also, if not more, likely to cause CO2 outgassing as a result of microbial respiration?

Response: The exact mechanisms which cause pre-industrial carbon outgassing, are often unclearly explained in literature. In this manuscript, we explain this in detail in section C2. Riverine DIC inputs consist majorly of HCO_3^- inputs (or DIC:Alk = 1:1). In the process of carbonate production, HCO_3^- is consumed while increasing the pCO_2 during its lifetime in the ocean:

$$Ca^{2+} + 2HCO_3^- => CaCO_3 + CO_2 + H_2O$$

The remineralization of DOM and POM also cause an increase in pCO_2, the released nutrients through the remineralization process however enhance the biological productivity, which counterbalances this effect and decreases the pCO_2. Therefore, it is the C:nutrients ratio within the organic matter which determines the extent of the pCO_2 and of the outgassing. As an example, for tDOM remineralization (first reaction) and the subsequent uptake of the released nutrients (second reaction):

$$C_{2583}N_{16}P^* \rightarrow 2583DIC + DIP + 16DIN + ..^* \rightarrow C_{122}N_{16}P + 2461CO_2$$

The extent of the long-term net outgassing is therefore strongly dependent on the carbon to nutrients ratio within POM and DOM. This is all found with more detailed explanation in Appendix C.2.

P3L20: where does photodegradation most likely occur? In the rivers? Coastal margins? Is this process not reflected in the extremely high C:P ratio (2584:1) considered here?

We would like to note that we found that the C:P ratio of tDOM was often wrongly stated (2584:1 instead of 2583:1). This was corrected in the revised manuscript.

Response: The degradation of the tDOM during its transit time within rivers is likely mostly biotic, thus explaining the low C:nutrients ratios found in tDOM at river mouths. Since the tDOM is already strongly degraded and has a very high C:P ratio, it has been strongly debated how reactive tDOM is within the ocean, since these characteristics hint that biological breakdown might be unfavorable. However, tDOM is also not found in substantial in the open ocean and in the sediment pore water. Therefore, photooxidation might play a strong role in breaking down tDOM in the ocean. Aarnos et al. (2018) derive from field measurements at 8 major river plumes globally that a substantial amount (around 30%) of tDOM is photodegraded within these plumes. In Fichot et al. (2014), which focuses on the Louisiana shelf, it is suggested that 40-50% of tDOM is mineralized on the shelf, with combined photodegradation and subsequent biotic breakdown being the major pathway for the degradation.

We believe this unfortunately exceeds the scope of our manuscript, since it is already very information-dense.

P3L24: why does POM control the availability of nutrients? By being remineralized?

Response: Indeed, POM contains nutrients that are released during mineralization of the POM. The strength of this control depends on various factors (other nutrient sources, POM composition, POM reactivity etc.).

This is very shortly mentioned in the revised manuscript.

P4L13: which 10 years? Contemporary?
Response: The mentioned study performs a 10-year simulation only for the present day and for present-day riverine inputs. We clarify this in the revised manuscript.

P5L8: Is there a particular reason to use 250m rather than the more commonly defined 200m?

Response: Using a depth threshold of 250m yields a better areal representation of the shelves in our relatively coarse resolution. This is especially the case for the narrower shelves.

P7L18: C:P=1000:1 here but 2584:1 in P9L23.

Response: C:P = 1000 is weight ratio and 2583:1 (corrected in revised manuscript) is the mole ratio. We however consistently only state mole ratios in the revised manuscript.

P10 section 2.1.3: why not deriving N:P ratios for different rivers from Global NEWS data set? Or at least to make a comparison with?

The Global NEWS data set prescribes very high N:P ratios, especially for dissolved inorganic species (approximately N:P = 29). This is plausible since this dataset represents inputs before their processing in estuaries. In estuaries, substantial denitrification and N outgassing takes place (i.e. Seitzinger et al., 2006), but these systems are not representable in the current state of global models due to resolution. We therefore do not have a choice but to simplify the ratios.
We added a brief discussion of these limitations in section 7.1. and an analysis in Supplementary Information 1.3. There, we show that the magnitudes of the global N sink through denitrification in estuaries (Seitzinger et al., 2006) could counterweight the additional N induced by a higher N:P ratio (for instance, from Beusen et al., 2016).

P12L7: “river freshwater model” -> is this the MPI-ESM model mentioned in P7L3?

The inputs of the Ocean-Model-Intercomparison-Project do indeed originate from the Hydrological Discharge (HD) which is a component of the global Max-Planck-Institute Earth System Model MPI-ESM.

P12L9-18: need some clarification on the biogeochemical model configuration and references for different versions of the model. The original model is described in Ilyina et al. 2013, and the version being used in this study is the same with Mauritsen et al., 2018? The major changes include cyanobacterial N2 fixation and incorporation of DOM? Was the DOM improvement also made in Mauritsen et al., 2018? What about Paulsen et al., 2017 and Six and Maier-Reimer, 1996? Are these studies relevant to the HAMOCC model development?

Response: The core of the model, which is essentially still the same, is described in Ilyina et al. (2013). The model developments that were incorporated since the Ilyina et al. (2013) manuscript were published are described in Mauritsen et al., 2018. As stated in our manuscript, the major changes were "to incorporate dynamical nitrogen fixation through cyanobacteria (Paulsen et al., 2017), to follow recommendations from the OMIP protocol (Orr et al., 2017) and to correct errors in the model. "

The references are cited more clearly in the revised manuscript, and we added a list of all model pools. We improved the understandability the last part of the paragraph in order to improve clarity in the revised manuscript. We will also add a general scheme of the main processes represented in HAMOCC in Appendix A. Furthermore, an updated list of the biological parameters can be found in the Supplementary Information S.2.

Also, is the model (e.g. photosynthesis) N or P or C based?

Response: We do not fully understand this question. The standard model is an extended NPZD type model (represents nutrients, phytoplankton, zooplankton, detritus), which was extended with DOM and cyanobacteria. The nutrients inorganic pools are DIP, DIN, DSi and DFe and can all be limiting. The phytoplankton and cyanobacteria produce organic matter at a fixed C:N:P ratio (122:16:1) taking up dissolved inorganic nutrients and DIC. The remineralization processes (grazing, or bacterial remineralization) then release dissolved inorganic nutrients and DIC back to the water column. For more information, we refer to the technical manuscript of the model (Ilyina et al., 2013). This should be clearer with the list of pools and the process scheme in the revised manuscript.

Are there different pools for D/POC, D/PON, D/POP, etc?

Response: For the composition of the organic matter (phytoplankton, cyanobacteria, zooplankton, detritus, DOM), the model solely uses the globally fixed C:N:P ratios. This is mostly due to the computational expenses associated with having to compute 3x5 additional tracers to represent D/POC, D/PON, D/POP.

Beside river inputs, are there other inputs from e.g. atmosphere deposition? Is N2 fixation also a carbon input or just N? These important details, particularly on the sinks and sources of N,P,C, need to be provided here.

Response: This is a good point that was forgotten in the submitted manuscript; the model also represents atmospheric dust and nitrogen deposition. These are estimated datasets

for the pre-industrial time frame. Regarding the second question, at low enough DIN concentrations and favorable growth conditions for cyanobacteria (see Paulsen et al. 2017 for details), cyanobacteria produce organic matter (thus take up DIC, DIP, DFe from the water column), while fixing (atmospheric) N_2.

We added the description of the dust and nitrogen inputs from atmospheric and their literature sources in the revised manuscript.

Abstract: focus on the riverine impact on CO2 outgassing and NPP hotspots in the ocean and leave the details of the river export (e.g numbers in P1L8) to the result section. P1L15-19 can be removed or shortened to one sentence.

Response: This is a good point, but our results are strongly dependent on our estimation of the inputs, which is a substantial part of the manuscript, and we therefore believe it is important to give the reader a grasp of the magnitudes of the exports.

References:

Seitzinger et al. : Denitrification across landscapes and waterscapes: a synthesis. *Ecological Applications*, 16(6), 2064-2090, 2006.

Oceanic CO_2 outgassing and biological production hotspots induced by pre-industrial river loads of nutrients and carbon in a global modelling approach

Lacroix Fabrice[1,2], Ilyina Tatiana[1], and Hartmann Jens[3]

[1]Ocean in the Earth System, Max Planck Institute for Meteorology, Hamburg, Germany
[2]Department of Geoscience, Université Libre de Bruxelles, Brussels, Belgium
[3]Institute for Geology, Center for Earth System Research and Sustainability, University of Hamburg, Hamburg, Germany

Correspondence to: Fabrice Lacroix (fabrice.lacroix@mpimet.mpg.de)

Abstract. Rivers are a major source of nutrients, carbon and alkalinity ~~for~~ to the global ocean~~, where the delivered compounds strongly impact biogeochemical processes~~. In this study, we firstly estimate pre-industrial riverine ~~fluxes~~ loads of nutrients, carbon and alkalinity based on a hierarchy of weathering and ~~land-ocean~~ terrestrial organic matter export models, while identifying regional hotspots of the land-ocean exports. Secondly, we implement the riverine loads into a global biogeochemical ocean model and describe their implications for oceanic nutrient concentrations, the net primary production (NPP) and air-sea CO_2 fluxes globally, as well as in a regional shelf analysis. Thirdly, we ~~quantify~~ quantitatively assess the terrestrial origins and the long-term oceanic fate of riverine carbon in the framework~~, while assessing the potential implementation of riverine carbon fluxes in a fully coupled land-atmosphere-ocean model. Our approach leads to~~ . We quantify annual pre-industrial riverine ~~exports~~ loads of 3.7 Tg P, 27 Tg N, 158 Tg Si and 603 Tg C~~, which were derived from weathering and non-weathering sources and were fractionated into organic and inorganic compounds~~. We thereby identify the tropical Atlantic catchments (20% of global C), Arctic rivers (9% of ~~total~~ global C) and Southeast Asian rivers (15% of ~~total~~ global C) as dominant providers of carbon to the ocean. The riverine exports ~~lead to a global oceanic source of CO_2 to the atmosphere (~~leads to a net global oceanic CO_2 source of 231 Tg C yr^{-1} ~~), which is largely a result of~~ to the atmosphere, which mainly results from a source from inorganic riverine carbon loads (183 Tg C yr^{-1}), and from organic riverine carbon inputs (128 Tg C yr^{-1}). Additionally, a sink of 80 Tg C yr^{-1} is caused by the enhancement of the biological carbon uptake by dissolved inorganic nutrient inputs, resulting alkalinity production and a slight model ~~drift~~disequilibrium. While large outgassing fluxes are mostly ~~found~~ simulated in proximity to major river mouths, substantial outgassing fluxes can also be ~~observed~~ found further offshore, most prominently in the tropical Atlantic. Furthermore, we find evidence for the interhemispheric transfer of carbon in the model; we detect a stronger relative outgassing flux (49% of global river induced outgassing) in the southern hemisphere in comparison to the hemisphere's relative riverine inputs (33% of global river inputs), as well as an outgassing flux of 17 Tg C yr^{-1} in the Southern Ocean. Riverine ~~exports~~ loads lead to a strong increase in NPP in the tropical West Atlantic, Bay of Bengal and the East China Sea (+166%, +377% and +71% respectively). While the NPP is not strongly sensitive to riverine loads on the ~~light-limited~~ light-limited Arctic shelves, the CO_2 flux is strongly altered due to substantial dissolved carbon supplies to the region. While our study confirms that the ocean circulation is the main driver for open ocean biogeochemical distributions, it reveals the necessity to

consider riverine exports for the representation of heterogeneous features of the coastal ocean, to represent riverine-induced carbon outgassing, as well as to consider the long-term volcanic CO_2 flux to close the atmospheric carbon budget in a coupled land-ocean-atmosphere setting.

1 Introduction

Rivers deliver substantial amounts of land-derived biogeochemical compounds to the ocean. For the present-day, they provide 4-11 Tg P yr^{-1} of carbon (C), phosphorus (P), 37-66 Tg N yr^{-1} of nitrogen (N), 158-200 Tg Si yr^{-1} of dissolved silica (Si)and , iron (Fe, no estimate available) as dissolved and particulate inorganic and organic compounds to the ocean (Seitzinger et al., 2005, 2010; Dü They also supply carbon (C) as dissolved inorganic carbon (260-550 Tg C yr^{-1}), dissolved organic carbon (130-380 Tg C yr^{-1}), as well as particulate organic carbon (100-197 Tg yr^{-1}) and alkalinity (Alk) to the ocean (Meybeck, 1982; Amiotte Suchet and Probst, 1995; These loads, which originate from natural and anthropogenic sources, strongly affect the biogeochemistry in the coastal ocean, where nutrients and carbon are transformed during biogeochemical processes, are exported to (Seitzinger et al., 2005, 2010; Dürr et al., 201 In the ocean, these compounds are either stored in the sediment, or are exported offshore (Stepanauskas et al., 2002; Froelich, 1988; Dagg et are outgassed (Froelich, 1988; Stepanauskas et al., 2002; Dagg et al., 2004; Krumins et al., 2013; Sharples et al., 2017). In global ocean models however, biogeochemical riverine exports and their contributions to the cycling of carbon have been strongly simplified or ignored. In this study, we attempt to reduce these gaps of knowledge by improve the understanding of the long-term effects of riverine loads in the ocean, by firstly estimating the magnitudes of biogeochemical riverine exports as a function of Earth System Model variables for the pre-industrial time periodby using a hierarchy of weathering and land-export models. We then describe , and secondly by assessing their long-term implications for oceanic biogeochemical cycles, with the NPP and CO_2 fluxes as focal pointsocean biogeochemical cycles.

Natural riverine carbon and nutrients originate from the export of organic matter from the terrestrial biosphere and the inputs from weathering of the lithosphere , which both consume atmospheric CO_2 while supplying freshwaters with carbon (Ludwig et al., 1998).

Weathering directly releases nutrients (P, Si and Fe) that can be taken up by the terrestrial ecosystems, or exported directly to aquatic systems (Hartmann et al., 2014). In these ecosystems, they are reported to enhance the carbon uptake due to their limitation of the biological primary production (Elser et al., 2007; Fernández-Martínez et al., 2014). Furthermore, alkalinity and carbon are released in the weathering process, while CO_2 is drawn down from the atmosphere (Amiotte Suchet and Probst, 1995; Meybeck and Vörösmarty, 1999; Hartmann et al., 2009). Spatially explicit approaches that quantify the weathering release weathering models have a strong potential for providing weathering release fluxes of nutrients, alkalinity and carbon for Earth System Models (e.g. for P in Hartmann et al. (2014)). They also have been used in the past to provide valuable information regarding the Hartmann et al. (2014)), as well as to quantify the weathering-induced drawdown of atmospheric CO_2 and its transformation to surface water alkalinity (Ludwig et al., 1998; Roelandt et al., 2010). It is acknowledged that (Ludwig et al., 1998; Hartmann et al., 2009; Roelandt et al., 2010; Hartmann et al., 2014). These approaches rely on estimating chemical weathering rates are as a first-order function of hydrology, lithology, rates of physical erosion, soil properties and tem-

perature (Amiotte Suchet and Probst, 1995; Hartmann et al., 2009, 2014). ~~Approaches to estimate chemical weathering yields therefore depend on quantifying these controls (Hartmann et al., 2014).~~

The terrestrial biosphere ~~is also a source of~~ also provides carbon and nutrients to ~~freshwater systems~~ rivers, dominantly through organic matter exports (Meybeck and Vörösmarty, 1999; Seitzinger et al., 2010; Regnier et al., 2013). The formation of organic matter through biological primary production on land firstly consumes atmospheric CO_2 (Ludwig et al., 1998). Leaching and physical erosion can then mobilize dissolved and particulate organic matter from soils and peatlands, and export it to rivers. While the natural P and Fe within the organic matter ~~originates~~ originate from weathering, C and N mostly originate from atmospheric fixation (Meybeck and Vörösmarty, 1999; Green et al., 2004). ~~Within rivers, autochthonous production can take place, which further transforms inorganic nutrients to organic matter while taking up CO_2. In soils and in rivers, organic matter remineralization also occurs, which transforms the organic matter back to dissolved inorganic nutrients and carbon.~~

~~Rivers therefore export P, N, Si, Fe and C as dissolved and particulate inorganic and organic compounds, as well as alkalinity to the ocean. It is known that dissolved~~ Dissolved inorganic nutrients enhance the primary production in the ocean, and thus cause an uptake of atmospheric CO_2 (Tyrrell, 1999). The riverine inputs of dissolved inorganic carbon on the other hand causes carbon outgassing in the ocean (e.g. Sarmiento and Sundquist (1992)). ~~The fate and contributions of terrestrial organic matter to the oceanic carbon cycle~~ Terrestrial organic matter releases dissolved inorganic carbon and nutrients during its remineralization, but its dynamics and composition in the ocean have been open questions for over two decades (Ittekkot, 1988; Hedges et al., 1997; Cai, 2011; Lalonde et al., 2014). ~~While the nutrients contained in reactive organic matter can control phytoplankton and bacterial growth in given regions (Seitzinger and Sanders, 1997; Stepanauskas et al., 2002; Björkman and Karl, 2003), the reactivity of organic matter has been strongly debated (Ittekkot, 1988; Hedges et al., 1997; Lalonde et al., 2014), since it is thought to already have undergone substantial degradation in rivers (Ittekkot, 1988; Vodacek et al., 2003).~~ In the case of terrestrial dissolved organic matter (tDOM), ~~the previous riverine degradation~~ its previous degradation in rivers leads to high carbon to nutrients ratios found in tDOM at the river mouths (i.e. C:P weight ratios of over 500, Meybeck (1982); Seitzinger et al. (2010)). The degradation of tDOM could cause substantial regional outgassing due to its large transfer of carbon in relation to its nutrient supplies (Cai, 2011; Müller et al., 2016; Aarnos et al., 2018). Although the strong previous degradation of tDOM and its high carbon to nutrients ratios imply low biological reactivity in the ocean, ~~yet~~ tDOM is not a major constituent of organic mixtures in open ocean sea-water or sediment pore water (Ittekkot, 1988; Hedges et al., 1997; Benner et al., 2005), ~~Recent studies have suggested that photodegradation might be responsible for partly or completely degrading tDOM to dissolved CO_2, thus possibly closing this gap of knowledge (Vodacek et al., 2003; Fichot and Benner, 2014; Lalonde et al., 2014; Aarnos et al., 2018). The degradation of tDOM could cause substantial regional outgassing due to its large transfer of carbon (Cai, 2011; Müller et al., 2016; Aarn~~ it is also not inert in the ocean. In the case of terrestrial particulate organic matter (POM), even stronger gaps in knowledge exist (Cai, 2011). POM has however been reported to affect coastal ocean biogeochemistry regionally by ~~firstly~~ controlling the availability of nutrients ~~and secondly by altering the optical properties of aquatic systems~~ through its remineralization (Froelich, 1988; Dagg et al., 2004; Stramski et al., 2004). Furthermore, a substantial proportion of weathered P is exported to the ocean bound to iron (Fe-P, Compton et al. (2000)). Within ~~estuaries and the coastal~~ the ocean, a fraction of P in Fe-P is thought to be desorbed, and thus converted to a bioavailable compound (dissolved inorganic phosphorus).

~~The cycles of~~ Pre-industrial P and N ~~and their land-ocean exports have been strongly perturbed over the 20th century, leading to a doubling of P and N riverine loads at the least (Seitzinger et al., 2010; Beusen et al., 2016). In the case of C and Si, the perturbations have been reported to be far less substantial at the global scale, although regional changes could have large implications for the coastal ocean (Seitzinger et al., 2010; Regnier et al., 2013; Maavara et al., 2014, 2017). It has furthermore been suggested that riverine~~ riverine loads strongly differ to present-day loads due to a dramatic anthropogenic perturbation of inputs to catchments over the 20th century (Seitzinger et al., 2010; Beusen et al., 2016). Riverine P and N exports ~~were already substantially~~ are suggested to even have already been perturbed prior to 1850-1900 due to increased soil erosion from land-use changes, fertilizer use in agriculture and sewage sources (Mackenzie et al., 2002; Filippelli, 2008; Beusen et al., 2016). In the case of C and Si, the perturbations have been reported to be far less substantial at the global scale (Seitzinger et al., 2010; Regnier et al., 2013; Maavara et al., 2014, 2017). Since global modelling studies ~~that tackle anthropogenic perturbations~~ of the climate are usually initialized for 1850 (Giorgetta et al., 2013) or 1900 (Bourgeois et al., 2016), these exports due to non-natural sources should also be taken into account in ~~the~~ initial pre-industrial model states.

Until now, riverine point sources of biogeochemical ~~tracers~~ compounds have been omitted or poorly represented in global ocean biogeochemical models, despite being suggested to strongly impact the biogeochemistry of coastal regions ~~(Stepanauskas et al., 2002~~ to cause a ~~natural~~ pre-industrial source of atmospheric CO_2 in the ocean (Sarmiento and Sundquist, 1992; Aumont et al., 2001; Gruber et al., 2009; Resplandy et al., 2018). This 'background' CO_2 outgassing flux of 0.2 to 0.8 Gt C yr^{-1} is significant in the context of the present-day oceanic carbon uptake of around 2.3 Gt C yr^{-1} (IPCC, 2013). In a modelling study~~tackling the interhemispheric transfer of carbon~~, Aumont et al. (2001) derived carbon loads from an erosion model and analyzed the oceanic outgassing caused by the riverine carbon. The impacts of nutrients and alkalinity were however not considered and carbon was only added to the ocean as dissolved inorganic carbon, omitting terrestrial organic matter dynamics in the ocean. Da Cunha et al. (2007) analyzed the impacts of present-day river loads on the oceanic primary production in a global biogeochemical model for an analysis period of 10 years, which does not suffice to assess long-term implications of river loads on the ocean's biogeochemistry. Bernard et al. (2011) added ~~river~~ present-day biogeochemical riverine loads to an ocean biogeochemistry model to focus on their implications for global opal export distributions, ignoring other aspects of the implications of these loads. In a global coastal ocean study, Bourgeois et al. (2016) quantified the coastal anthropogenic CO_2 uptake, but did not analyze the impacts of riverine loads. To our knowledge, a study has yet to give a comprehensive overview of pre-industrial land-ocean river exports and their long-term global impacts on oceanic biogeochemical cycling in a 3-dimensional framework. In previously published literature, riverine loads were added according to present-day estimates, despite severe perturbation of the land-ocean N and P exports having taken place during the 20th century (Beusen et al., 2016). An initial ocean state ~~with~~ that considers pre-industrial riverine supplies would however be necessary to truly assess the temporal dynamical impacts associated with these perturbations. Studies ~~until now~~ have also not considered differing characteristics of terrestrial organic matter to those of oceanic organic matter. Furthermore, it is often unclear under which criteria the alkalinity supplies to the ocean were constrained in global ocean models. Regional sensitivities of coastal regions to biogeochemical riverine loads have not been assessed at the global scale, largely due to the incapability of the global models to represent plausible continental shelf sizes in the past (Bernard et al., 2011).

In this study, we **1.** implement a representation of pre-industrial riverine loads into a global ocean biogeochemical model, considering both weathering and non-weathering sources of nutrients, carbon and alkalinity. We compare our estimates with a wide range of published literature values, while also determining regions of ~~strong riverine exports and their~~ disproportionate contributions to global exports. **2.** The implications of riverine fluxes for the oceanic ~~NPP~~ net primary production (NPP) and CO_2 flux are assessed globally, as well as regionally in an analysis of shallow ~~shelves~~shelf regions. **3.** We evaluate the origins and fate of riverine carbon quantitatively, while assessing the balance between the land carbon uptake and the oceanic carbon outgassing in the individual models. This balance of the land carbon uptake and the oceanic outgassing is then used to assess the potential implementation of riverine fluxes in a fully coupled land-atmosphere-ocean setting.

2 Methods

To address the objectives of this study, we derived the most relevant pre-industrial ~~land-ocean fluxes~~ (1850) riverine loads of biogeochemical compounds ~~dependently on~~ to the ocean in dependence of pre-industrial ~~output of~~ Earth System Model ~~simulations. We used a hierarchy of models to derive biogeochemical compound sources from weathering and non-weathering to catchments, and estimated their terrestrial transformations to organic matter. This resulted in a spatially explicit quantification of global riverine loads~~simulation variables. The derived riverine loads were then ~~implemented~~ incorporated into a global ocean biogeochemical model in order to assess their global and regional impacts~~on the ocean biogeochemistry~~. In order to quantify the effects of the riverine supplies on coastal regions, we also defined 10 ~~shelves with~~ regions with ocean depths of less than 250m.

2.1 Deriving pre-industrial riverine loads

We ~~first briefly describe the framework used to derive pre-industrial riverine exports here, while the individual models and assumptions are explained in detail in the next subsections. We~~ focused on the exports of ~~phosphorus (P), nitrogen (N), silica (Si), iron (Fe), carbon (C) and alkalinity (Alk)~~ P, N, Si, Fe, C and Alk for global catchments. The catchments were defined by using the largest 2000 catchments from the Hydrological Discharge (HD) model (Hagemann and Dümenil, 1997; Hagemann and Gates, 2003), a component of the Max Planck Institute Earth System Model (MPI-ESM). The catchments were derived from the runoff flow directions of the model at a horizontal resolution of 0.5 degrees. The exorheic river catchments (catchments, which discharge into the ocean) were considered to be catchments with river mouths that have a distance of less than 500 km to the coastline in the HD model. Catchments with larger distances were considered to be endorheic catchments (catchments, which do not discharge into the ocean). The biogeochemical tracers released in these ~~in the endorheic catchments in our framework~~ catchments were assumed to be retained permanently, whereas the riverine exports ~~from~~ of exorheic catchments were added to the ocean.

We considered both weathering sources as well as non-weathering sources of P, N, Si, Fe, C and Alk to river catchments (Figure 1). These were derived, if possible, from spatially explicit models. Within the catchments, we accounted for transformations of P, N and Fe to organic matter through biological productivity on land and in rivers~~. These biological transformations~~

were however not modelled dynamically in our approach. Instead, the net amounts of catchment P, N and Fe to have been transformed to organic matter on land or in rivers , which were derived from globally fixed ratios to C depending on the tDOM and POM composition (see (Figure 1). The composition of tDOM and POM and their its ratios of C, P, N and Fe were assumed to be identical for every catchment out of simplicity. The amounts of P, N and Fe that were transformed to organic matter were subtracted from their inorganic catchment pools, in order to avoid double counting. The organic carbon in tDOM and POM , which was derived from river mouth load estimations of the NEWS2 study (Seitzinger et al., 2010), was assumed to ultimately originate from terrestrial biological CO_2 uptake (Ludwig et al., 1998) and was therefore not subtracted from the catchment DIC pools. Additionally, a fraction of P was also assumed to have been adsorbed to Fe-P. The rivers in our approach therefore deliver terrestrial organic matter (tDOM and POM), inorganic compounds (DIP, Fe-P, DIN, DSi, DFe and DIC) and alkalinity (Alk) to the ocean (Figure 1).

The surface runoff, surface temperature and precipitation data used to drive the framework submodels weathering release models were obtained from output of a fully coupled coupled Max Planck Institute Earth System Model (MPI-ESMCMIP5) pre-industrial simulation (Giorgetta et al., 2013). We thereby used the annual 100 year means of model pre-industrial runoff, temperature and precipitation data computed by the MPI-ESM on a 1.875 degree Gaussian grid. We scaled the runoff data by a factor of 1.59 to account for the runoff model bias with regards to global estimations (Fekete et al., 2002), which is discussed in Section 3.1Appendix B.

2.1.1 Terrestrial dissolved and particulate organic matter characteristics

We assumed that the pre-industrial loads of tDOM and POM did not strongly differ to their present-day loads at the global scale. In the NEWS2 study (Mayorga et al., 2010; Seitzinger et al., 2010), in which Seitzinger et al. (2010), who analyzed anthropogenic perturbations to riverine loads were analyzed, only for 1970-2000, only found small changes in POC and DOC loads to the ocean were found over the 1970 to 2000 over this time period. Regnier et al. (2013) suggest an a total anthropogenic perturbation of the total carbon flux to the ocean of around 10%, for which we did not account in this study.

The riverine loads of tDOM and POM were therefore derived from the DOC and POC river loads for the reference year 1970 (NEWS2), which were in turn determined from the models of Harrison et al. (2005) and Beusen et al. (2005). The Harrison et al. (2005) model quantifies the DOC catchment yields as a function of runoff, wetland area and consumptive water use. The Beusen et al. (2005) describes the POC catchment yields as a function of catchment suspended solids yields, which depend on grassland and wetland areas, precipitation, slope and lithology.

The riverine organic matter exported to the ocean consisted of globally constant fractions of C, P, N and Fe. The tDOM C:P consistence was based on a C:P weight ratio of 1000mole ratio of 2583:1 derived from Meybeck (1982) and Compton et al. (2000). The global tDOM total N:P mole ratio was chosen to be 16:1, which is in accordance to natural and pre-industrial estimations of previous studies (Seitzinger et al., 2010; Beusen et al., 2016). For the P:Fe ratio , the same mole ratio in order to represent the same N:P ratio as of the organic matter export to the sediment, as well as for the Fe biological uptake in the ocean was chosen P:Fe ratio (1:3.0 10^{-4}). The total C:N:P:Fe mole ratio of tDOM was therefore 25842583:16:1:3.0 10^{-4}. The C:P ratio of riverine POM is highly uncertain, but global C:P mole ratios from observational data (56-499) (Meybeck, 1982;

a)

	Source	Model/Study		Source	Model/Study
	Weathering (DIC)	Hartmann et al. (2009)	**Si**	***Weathering***	Beusen et al. (2009)
C	***Non-Weathering***				
	DOC (Atmospheric)	NEWS2		***Non-Weathering***	
	POC (Atmospheric)	NEWS2	**N**	Atmospheric	Fixed ratio to P
				Anthropogenic	
	Weathering	Hartmann et al. (2014)	**Fe**	***Weathering***	Fixed ratio to P
	Non-Weathering				
P	Fertilizer (1900)	Hart et al. (2004)	**Alk**	***Weathering***	Hartmann et al. (2009)
	Sewage (1900)	Morée et al. (2013)			Goll et al. (2014)
	Allochtonous (1900)	Beusen et al. (2016)			

b)

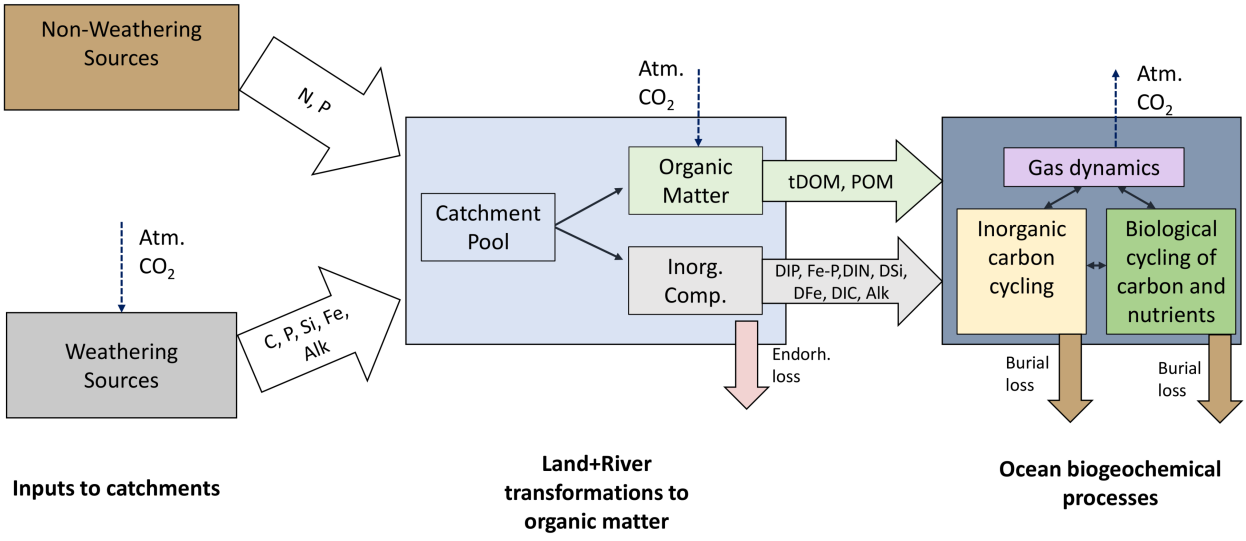

Figure 1. (a) Table of sources of nutrient, carbon and alkalinity inputs to the catchments and (b) scheme of origins~~and~~, transformations of the catchment compounds and biogeochemical processes in the ocean. The abbreviations are: Inorg. Comp.: Inorganic Compounds, tDOM: terrestrial dissolved organic matter, POM: particulate organic matter , DIP: dissolved inorganic phosphorus, Fe-P: Iron-bound phosphorus, DIN: dissolved inorganic nitrogen, DSi: dissolved silica, DFe: dissolved iron, DIC: dissolved inorganic carbon, Alk: alkalinity.

Ramirez and Rose, 1992; Compton et al., 2000) suggest a much closer ratio to the oceanic production and export ratios (mole C:P = 122:1, Takahashi et al. (1985)) than for tDOM. Due to this and the gaps of knowledge on POM composition, we chose a C:N:P:Fe ratio analogous to that of oceanic POM (122:16:1:3.0 10^{-4}).

2.1.2 Phosphorus

P weathering yields

We derived the P weathering yields from a spatio-temporal model (Hartmann et al., 2014), which quantifies the P weathering release in relation to the SiO_2 and cation release. The model core is dependent on runoff and lithology (Hartmann and Moosdorf, 2011) and was calibrated for the extensive dataset of 381 river catchments of the Japanese Archipelago. The model was then corrected globally for temperature and soil shielding effects (Hartmann et al., 2014):

$$F_{Prelease} = \sum_{i=lith} b_{P,i} * q * F_i(T) * F_S \quad (1)$$

where $F_{Prelease}$ is the chemical weathering rate of P per area (t km^{-2} yr^{-1}), $b_{P,i}$ is an empirical factor representing the rate of P weathering of lithology i, q is the runoff (mm yr^{-1}), F(T) is a lithology-dependent temperature function and F_S is a parameter for soil shielding.

The lithology types consisted of 16 lithological classes from the lithological map database GliM (Hartmann and Moosdorf, 2012), which have different weathering parameters $b_{P,i}$ as well as temperature functions $F_i(T)$. The ~~release of P was assumed to be proportional to the release of SiO_2 + cations, as in Hartmann et al. (2014). The~~ factor $b_{P,i}$ represents the chemical weathering rate factor for SiO_2 + cations (b_{SiO_2+Cat}) multiplied with the relative P content ($b_{Prel,i}$):

$$b_{P,i} = b_{SiO_2+Cat,i} * b_{Prel,i} \quad (2)$$

The parameters $b_{SiO_2+Cat,i}$ and $b_{Prel,i}$ for each lithology i can be found in Hartmann et al. (2014).

~~Pre-industrial runoff model output of the MPI-ESM was used to force the model for q.~~ The temperature correction function F(T) is an Arrhenius relationship for basic (rich in iron and magnesium) and acid (high silica content) lithological classes, with activation energies normalized to the average temperature of the calibration catchments of the study (Hartmann et al., 2014). For acid rock lithologies, an activation energy of 60 kJ/mole was assumed, whereas for basic rock types 50 kJ/mole was used. Carbonate lithologies do not have a temperature correction due to the absence of a clear relationship to field data, as well as uncertainties in the mechanisms of a temperature effect on carbonate weathering ~~(Plummer and Busenberg, 1982; Hartmann et al., 2014; Romero~~

A soil shielding factor F_S was considered due to the inhibition of weathering by certain types of soils. These soils with low physical erosion rates develop a chemically depleted thick layer, which shields them from water supply, thus preventing the maximum weathering of the soil aggregates (Stallard, 1995). ~~Wetlands and areas with a high groundwater table have also been shown to partially inhibit weathering (Edmond et al., 1995; Goudie and Viles, 2012).~~ The average soil shielding factor of 0.1 was estimated for the soils Ferrasols, Acrisols, Nitisols, Lixisols, Histosols as well as Gleysols~~from the Harmonized World~~

~~Soil Database (Hartmann et al., 2014). The factor used for these soils is 0.1~~, which was found to be the best global estimate for the calibration catchments in Hartmann et al. (2014)~~, after having iteratively altered the parameter from 0 to 1.~~ .

Non-weathering P sources

Since the P cycle was already perturbed in the assumed pre-industrial state (1850) due to anthropogenic activities (Mackenzie et al., 2002; Filippelli, 2008; Beusen et al., 2016), we also accounted for P sources other than weathering ($P_{nw,catch}$). Similarly to Beusen et al. (2016), we derived the global non-weathering source of P as the sum of fertilizer ($P_{fert,~~global~~catch}$), sewage ($P_{sew,~~global~~catch}$) and allochthnonous P inputs ($P_{alloch,~~global~~catch}$):

$$P_{nw,global}{}_{nw,catch} = P_{fert,global}{}_{fert,catch} + P_{sew,global}{}_{sew,catch} + P_{alloch,global}{}_{alloch,catch} \quad (3)$$

$P_{fert,~~global~~catch}$ was the input ~~to the non-weathering $P_{nw,global}$ pool~~ from the agricultural application of fertilizers, manure and organic matter (1.6 Tg P yr^{-1} globally, from ~~Hart et al. (2004)~~Beusen et al. (2016)), $P_{sew,~~global~~catch}$ was the P input from sewage (0.1 Tg P yr^{-1} globally, Morée et al. (2013)) and $P_{alloch,~~global~~catch}$ represented allochthnous organic matter P inputs (1 Tg P yr^{-1} simplified as vegetation in floodplains in Beusen et al. (2016))~~. The~~ , all estimated for year 1900 ~~was used as a reference,~~ due to previous ~~estimates or data~~ robust estimates not being available to our knowledge. Since our framework was developed with the aim of being used in Earth System Models, we assumed soil equilibrium since this is the initial state criteria used in state-of-the-art model simulations. Therefore, P exports due to soil perturbations ~~reported in Filippelli (2008) and Beusen et al. (2016)~~ were not considered. The distribution of ~~P inputs from catchment non-weathering sources~~ anthropogenic P inputs (agriculture+sewage) to catchments was assumed to be the same as the global distribution of contemporary anthropogenic P inputs, which was derived from the NEWS2 study:

$$P_{nw,catch}{}_{ant,catch} = P_{nw,global}{}_{ant,global} * DIP_{ant,catch}{}_{ant\text{-}pd,catch} / DIP_{ant,global}{}_{ant\text{-}pd,global} \quad (4)$$

where $P_{~~nw~~ant,catch}$ is the ~~non-weathering~~ anthropogenic catchment P pool, whereas $DIP_{~~ant~~ant\text{-}pd,catch}$ and $DIP_{~~ant~~ant\text{-}pd,global}$ are anthropogenic inputs from the NEWS2 study for every catchment and their global sum, respectively. For allochtonous P inputs, we assumed the same distribution as for the organic matter yields. Both of these distributions are shown and discussed in the Supplementary information S.1.1. and S.1.2.

P river loads

For each catchment, we estimated the total annual P inputs to the catchments ($P_{total,catch}$), as the sum of the catchment weathering yields ($P_{w,catch}$) and of non-weathering sources ($P_{nw,catch}$):

$$P_{total,catch} = P_{w,catch} + P_{nw,catch} \quad (5)$$

$P_{total,catch}$ was then fractionated into inorganic P (IP_{catch}) and P contained in tDOM ~~and POM~~(DOP) and POM (POP), which was assumed to have been taken up on land or in rivers by the biology ~~(Figure ??)~~at the globally fixed prescribed P:C ratios. After considering this net P transformation~~to organic matter~~, the remaining P was assumed to be ~~inorganic P (IP_{catch})~~ IP_{catch}

for every catchment:

$$IP_{\text{catch}} = P_{total,catch} - P_{tDOM,catch} DOP_{total,catch} - P_{POM,catch} POP_{total,catch} \quad (6)$$

~~The mole ratios of C to P in tDOM and POM were assumed to be 2584:1 (Meybeck, 1982; Compton et al., 2000) and 122:1, respectively.~~ The IP was then fractionated into DIP and Fe-P with a ratio r_{inorg} (DIP:Fe-P = 1:3) ~~derived~~ approximated from the global natural P river export estimates of Compton et al. (2000):

$$DIP_{catch} = r_{inorg} * IP_{catch} \quad (7)$$

and:

$$Fe - P_{catch} = (1 - r_{inorg}) * IP_{catch} \quad (8)$$

We did not consider ~~shale derived~~ particulate inorganic phosphorus exports in this study, since it originates from physical erosion, which does not chemically transform the shale. The resulting shale-derived material is considered to not be bioavailable in rivers or the coastal ocean (Compton et al., 2000). ~~We also did not consider in-stream retention and sinks of P, although in-stream processes might retain nutrients within river catchments (Beusen et al., 2016).~~

~~Scheme of catchment sources of P ($P_{w,catch}$ and $P_{nw,catch}$) and the export fractionation of catchment P ($P_{POM,catch}$,$P_{tDOM,catch}$,Fe-P_{catch} and DIP_{catch}).~~

2.1.3 Nitrogen and iron

The inputs of N to ~~riverine~~ river catchments were derived from the total P inputs to catchments at a globally fixed mole N:P ratio of 16:1 for all species ~~, which is the same as of their oceanic removal as organic matter (Takahashi et al., 1985). While the model study of Beusen et al. (2016) suggests~~ (Takahashi et al., 1985). The nitrogen contained in organic matter were subtracted from its dissolved inorganic nitrogen pool. Beusen et al. (2016) suggest a total pre-industrial N:P mole ratio of ~~15.5~~21:1 ~~,~~ and a synthesis of global obervations by Turner et al. (2003) ~~suggests a~~ report higher N:P ~~ratio for bioavailable N and P species~~ ratios for in most major rivers. However, ~~processes such as denitrification~~ denitrification also removes N in river estuaries ~~take place that remove N primarily (Meybeck, 1982; Nixon et al., 1996; Beusen et al., 2016), which exceeds the scope of our study~~(3-10 Tg N yr^{-1}, Seitzinger et al. (2005)) globally, which could compensate the higher N loads than at a N:P ratio of 16:1 (Supplementary Information S.1.3). For Fe, we used a Fe:P mole ratio of 3.0 10^{-4}:1 to quantify Fe inputs to the catchments for all species, which is the Fe:P export ratio of organic material in the ocean biogeochemical model. The dissolved Fe inputs were also formed from subtracting iron from organic matter to the catchment Fe pool.

2.1.4 Dissolved inorganic carbon and alkalinity

The C and Alk weathering release was derived from weathering CO_2 uptake equations that originate from the studies of Hartmann et al. (2009) and Goll et al. (2014). Weathering reactions take up atmospheric CO_2 and release carbon in the form of

HCO_3^- during carbonate weathering:

$$CaCO_3 + CO_2 + H_2O => Ca^{2+} + 2HCO_3^- \quad (9)$$

and silicate weathering:

$$Mg_2SiO_4 + 4CO_2 + 4H_2O => 2Mg^{2+} + 4HCO_3^- + H_4SiO_4 \quad (10)$$

The equations (9) and (10) dictate the release of 1 HCO_3^- (thus 1 DIC and 1 Alk) for each mole of CO_2 taken up in the weathering of silicate lithologies, and ~~that~~ of 2 HCO_3^- (thus 2 DIC and 2 Alk) are released during the uptake of each mole of CO_2 drawn down during the weathering of carbonate lithologies.

The release equations from Hartmann et al. (2009) and Goll et al. (2014) quantify the lithology (i) dependent HCO_3^- weathering release as a function of runoff (q), temperature ($F_i(T)$), soil shielding F_S and a weathering parameter $b_{C,i}$:

$$F_{HCO_3^-} = \sum_{i=lith} b_{C,i} * q * F_i(T) * F_S \quad (11)$$

~~Modelled pre-industrial runoff from the MPI-ESM was used for q.~~ The parameter $b_{C,i}$ is dependent on the weathering rate of the lithology and the composition of the lithology.

~~We derived the catchment Alk exports to the ocean as~~ The catchment Alk and DIC catchment loads were the HCO_3^- weathered annually within the catchments, assuming conservation of Alk along the land-ocean continuum. We therefore consider carbonate alkalinity exports solely and a DIC:Alk loads ratio of 1:1. Riverine HCO_3^- is thereby considered to mainly originate from the products of silicate and carbonate weathering reactions (Amiotte Suchet and Probst, 1995; Meybeck and Vörösmarty, 1999). We did not consider additional DIC sources, for instance of CO_2 from respiration of organic matter in soil pore water, groundwater or in rivers. River observational data however show that the riverine HCO_3^- and total DIC mole exports rarely deviate by more than 10% (Araujo et al., 2014). ~~Our assumptions lead to riverine exports of DIC and Alk at a mole ratio of 1:1.~~

2.1.5 Silica

To quantify the spatial distribution of Si export yields, we used the model of Beusen et al. (2009), which describes the dissolved silica (DSi) river export as:

$$F_{DSiO_2} = b_{prec} * ln(prec) + b_{volc} * volc + b_{bulk} * bulk + b_{slope} * slope \quad (12)$$

where F_{DSiO_2} is the export of DSi in Tg SiO_2 yr^{-1} km^{-2}, ln(prec) is the natural logarithm of the precipitation in mm d^{-1}, volc is the area fraction covered by volcanic lithology (no dimension), bulk is the bulk density of the soil in Mg m^{-3}, slope is the average slope based on global Agro-ecological zones (FAO/IIASA) in m km^{-1}, and b_{prec}, b_{volc}, b_{bulk}, b_{slope} are the estimated regression coefficients in Beusen et al. (2009). For the precipitation, we used pre-industrial model output from the MPI-ESM,

whereas the volcanic area originated from Dürr et al. (2005), the soil density from Batjes (1997) and Batjes (2002), and the average slope from the Global Agro-Ecological Zones database (FAO/IIASA). The exports were aggregated for the HD model catchments, while taking into account catchment areas. The loads that were generated by the Beusen et al. (2009) model were converted to Tg DSi loads and are given accordingly in the rest of our study. We also neglected the land-ocean export of particulate silica physically eroded from land.

2.2 Ocean Model Setup

2.2.1 Ocean Biogeochemistry

The Max Planck Institute Ocean Model (MPIOM, Jungclaus et al. (2013)), which was used to simulate oceanic physics, is a z coordinate global circulation model that solves primitive equations under the hydrostatic and Boussineq approximation on a C-grid with a free surface ~~(Jungclaus et al., 2013)~~for every model time step (1 h). The grid configuration ~~used was (~~GR15~~, which consists of)~~ is a bipolar grid with poles over Antarctica and Greenland, ~~and a grid resolution of about~~ resolving the surface at around 1.5 degrees. Vertically, the configuration consists of 40 uneven spaced layers, with increasing thicknesses at greater depths. The atmospheric surface boundary data, as well as river freshwater model inputs originate from the ~~Ocean-Model-Intercomparision-Project~~ Ocean-Model-Intercomparison-Project (OMIP, Röske (2006)). The flow fields of the MPIOM dictate the advection, mixing and diffusion biogeochemical tracers in the ocean.

~~We used the~~ Hamburg Ocean Carbon Cycle model (HAMOCC)~~to simulate the major biogeochemical processes that affect carbon as well as nutrients~~, which is coupled to MPIOM, simulates the inorganic carbon chemistry, biological transformations, nutrient cycling and gas dynamics in the ocean ~~. The standard model used was an extension of the model~~ water column, sediment and at the air-sea interface. The model core along with its equations are described in Ilyina et al. (2013), ~~which is~~ but we also accounted for more recent modifications explained in Mauritsen et al. (2018). ~~The changes were made to incorporate dynamical nitrogen fixation through~~ These included incorporating dynamic nitrogen fixation by cyanobacteria (Paulsen et al., 2017), ~~to follow recommendations from~~ following recommendations of the OMIP protocol (Orr et al., 2017)~~and to correct~~, nitrogen deposition according to the Coupled Model Intercomparison Project 6 (CMIP6) database (https://esgf-node.llnl.gov/projects/input4mips/) and correcting errors in the model. The ~~model represents processes in the water column, sediment, as well as air-sea exchange fluxes. All biogeochemical tracers found in the water column are thereby fully advected, mixed and diffused by the flow fields of MPIOM. The biogeochemistry of the water column includes both organic~~ pools of the model consist of DIP, DIN, DFe, oxygen, DSi, DIC, Alk, opal, calcium carbonate ($CaCO_3$), phytoplankton (PHY), cyanobacteria (CYA), dissolved organic material (DOM) and particulate organic material (POM) (Appendix A1).

The inorganic carbon chemistry is based on Maier-Reimer and Hasselmann (1987), with adjustments in the calculation of chemical constants as described in the OMIP protocol (Orr et al., 2017). Total DIC and total Alk are thereby prognostic tracers from which the carbonate species are determined diagnostically. The total DIC includes all carbonate species and total Alk is defined as carbonate as well as ~~inorganic carbon cycle processes. The dynamics for the organic carbon cycle~~ borate alkalinity.

The dynamics of the biological organic matter cycling are based on ~~a NPZD (~~an extended NPZD type model with pools of nutrients, phytoplankton, zooplankton~~and detritus) model approach, which was extended to incorporate the compartments of oceanic dissolved organic material (DOM) and cyanobacteria(Six and Maier-Reimer, 1996; Ilyina et al., 2013).~~

~~A constant Redfield ~~, detritus (POM), DOM and cyanobacteria. The phytoplankton growth follows Michaelis-Menten kinetics as a function of temperature, light and nutrient availability and a constant ratio (C:N:P:Fe = 122:16:1~~, Takahashi et al. (1985))~~ and Fe:P ratio of :~~3.0 10^{-4}~~:1 dictate ~~, Takahashi et al. (1985)) dictates the composition of all oceanic organic matter. ~~The phytoplankton growth follows Michaelis-Menten kinetics as a function of temperature, light and nutrient availability. The phytoplankton produce opal when dissolved silica is available, and calcium carbonate ($CaCO_3$) when dissolved silica is depleted. The $CaCO_3$ and opal thereby sink at constant rates.~~

~~The mortality of the phytoplankton and its exudation as DOM, as well as the zooplankton grazing of phytoplankton is included. DOM can also be formed due to sloppy feeding. POM is formed from dead cells of phytoplankton and zooplankton, as well as fecal pellets from zooplankton activity.~~ Both oceanic DOM and POM are advected according to the ocean physics, and the POM also sinks as a function of depth (Martin et al., 1987). Aerobic remineralization takes place when the oxygen concentration is above a threshold oxygen concentration, whereas at low enough oxygen concentrations, denitrification and sulfate reduction can take place.

~~The inorganic chemistry is based on Maier-Reimer and Hasselmann (1987), with adjustments in the calculation of chemical constants as described in the OMIP protocol (Orr et al., 2017). Total DIC and total Alk are thereby prognostic tracers from which the carbonate species are determined diagnostically~~Furthermore, the phytoplankton produce opal shells when dissolved silica is available, and $CaCO_3$ shells when dissolved silica is depleted. The $CaCO_3$ and opal thereby sink at constant rates.

HAMOCC also contains a 12 layer sediment module where the same remineralization and dissolution processes as in the water column take place for the solid sediment constituents (Heinze et al., 1999). The sediment consists of a fraction of pore water, which contains dissolved inorganic compounds (e.g. DIC and DIP). POM, $CaCO_3$ and opal fluxes from the water column are deposited to the top sediment layer. There is a diffusive inorganic compound flux at the water sediment-water column interface and a particulate flux from the bottom layer to a diagenetically consolidated burial layer.

Dust is added through atmospheric deposition according to input fields of Mahowald et al. (2006). The model considers the ~~gas exchange~~ dynamics of CO_2, O_2, N_2O and N_2 and their exchange at the ocean-atmosphere interface. Since we model a pre-industrial state of equilibrium in this study, we used constant atmospheric concentrations for CO_2 of 278ppmV (Etheridge et al., 1996).

2.2.2 Treatment of the river loads in the ocean biogeochemistry model

The biogeochemical riverine loads were added to the ocean surface layer in HAMOCC constantly over the whole year. The locations of major river mouths were corrected manually on a case to case basis for large rivers in order to reproduce the same locations as the freshwater inputs from ~~OMIP. The riverine freshwater discharge on the other hand varied intra-annually according to the prescribed OMIP freshwater loads (Röske, 2006)~~the OMIP model inputs.

The dissolved riverine inorganic compounds (DIC, DIP, DIN, DSi, DIC, DFe, Alk) were added to the model in their dissolved species pools in HAMOCC. We added 80% of P contained in the riverine Fe-P to the oceanic DIP pool, in order for the amount of bio-available Fe-P to be comparable with the given range in Compton et al. (2000) (1.1-1.5 Tg P yr^{-1}). The rest of the Fe-P pool was considered to be unreactive in the ocean and was eliminated. The riverine POM was added to the oceanic POM pool in the ocean model~~, since we assumed its consistence to be the same (P:N:C:Fe mole ratio of 1:16:122:3.0 10^{-4})~~.

For tDOM, we extended HAMOCC with a new tracer that was characterized with ~~a~~ the described C:N:P:Fe mole ratio~~of 2584:16:1:3.0 10^{-4} (Meybeck, 1982; Compton et al., 2000)~~. tDOM was mineralized as a function of the tDOM concentration at a rate $k_{rem,tDOM}$ and also of an oxygen limitation factor (Γ_{O2}), which decreases the maximum potential remineralization rate as a function of the oxygen concentration:

$$dtDOM/dt = k_{rem,tDOM} * tDOM * \Gamma_{O2} \quad (13)$$

Since a large fraction of tDOM delivered by rivers is already strongly degraded, it is to a certain extent resistent to microbial degradation (Ittekkot, 1988; Vodacek et al., 2003). We ~~consequently~~ therefore assumed a slightly slower remineralization rate of tDOM ($k_{rem,tDOM}$) compared to oceanic DOM (0.003 versus ~~to~~ 0.008 d^{-1} for oceanic DOM), ~~which~~ in order to have a slower degradation rate than oceanic DOM. This rate is within the tDOM degradation range provided in Fichot and Benner (2014) for the Louisiana shelf (0.001-0.02 d^{-1}). The oxygen limitation function used (Γ_{O2}) was analogous to that of the oceanic DOM which is described in Mauritsen et al. (2018).

2.2.3 Pre-industrial ocean biogeochemistry model simulations

We performed ~~a reference simulation~~ two ocean model simulations in order to assess the impacts of biogeochemical riverine fluxes in terms of their magnitudes and locations.

The first (REF) ~~, where the burial loss of biogeochemical tracers was compensated by a global homogeneous flux to the surface ocean , as in the standard configuration of the model. This flux served~~ was the standard model version until now (for instance in Mauritsen et al. (2018)), which was lacking in terms of its representation riverine inputs: Biogeochemical inputs were added in the open ocean in order to compensate for burial losses in the sediment at the global scale. In HAMOCC, biogeochemical inputs are needed in order to maintain a stable ocean state~~. Thus in REF, the delivery of biogeochemical inputs were added directly in the~~ , since the burial loss in the sediment induces a loss of of $CaCO_3$, opal and organic matter. Without these inputs, ocean biogeochemical inventories would thrive to zero. In order to maintain a state close to equilibrium in the the standard model version (REF), inputs representing the re-dissolution of $CaCO_3$ (added in a mole Alk:DIC ratio of 2:1), inputs of dissolved silica (DSi) and inputs of oceanic DOM were added homogeneously per surface in all of the ocean to compensate for sediment burial. Therefore, inputs were almost solely added to the open ocean ~~while bypassing the coastal ocean , and were fully constrained by the loss of the sediment layer. Our simulation RIV however included riverine loads of inorganic compounds ((~~See Supplementary Information S.5.). REF was simulated for 5'000 years, where burial fluxes were computed approximately every 1'000 years. The resulting fluxes of these calculations were added to the ocean as inputs.

The simulation RIV replaced the homogeneous inputs of biogeochemical compounds with riverine inputs of DIP, Fe-P, DIN, DSi, DFe, DIC, Alk~~) and organic matter (tDOM, POM), which were constrained by our framework and added to their geographical river mouth locations.~~

~~REF was simulated for 5000 years to quasi-equilibrium. RIV~~ , tDOM and POM, derived in the described approach at their corrected geographical locations. The major differences to the REF simulation originate from the geographic locations of the inputs, the magnitudes of carbon loads to the ocean, as well as the mole ratios of Alk:DIC in comparison to the $CaCO_3$ burial compensation inputs (1:1 for RIV and 2:1 for REF) and of tDOM in comparison to the oceanic DOM inputs. Since the inputs to the ocean were fully constrained by our described approach, long simulations were needed in order for both the water column and especially the sediment to equilibrate to the new biogeochemical inputs. We firstly performed the simulation was simulated for ~~4000~~ 4'000 years first including both the water column and sediment model components~~, then for~~ . Once particulate fluxes to the sediment were approximately stable, we performed a 10'000 years in a model version simulating only ~~sediment processes. In these 10'000 years, the inputs to the sediment were the means of $CaCO_3$, POM and opal from the water column of the last 100 years of~~ the ~~standard~~ sediment sub-model, which was forced with the stable 100 year mean of particulate fluxes from the previous simulation. The sediment was then coupled back to the ocean water column, with a simulation performed for ~~2000~~ 2'000 more years in the full model version.

We used REF as a reference simulation in order to compare RIV to, which enabled us to compare the impacts of riverine fluxes at plausible pre-industrial magnitudes and locations (RIV) to REF, where the vast majority of inputs were added directly to the open ocean. For the analysis of the resulting ocean biogeochemistry, we used the last 100 year means of ~~model output~~RIV and REF.

2.3 Definitions of coastal regions for analysis

To investigate the impacts of riverine exports on coastal regions, we chose 10 coastal regions characterized by shallow continental shelves and high riverine loads that cover a variety of latitudes (Table 1). The shelves were defined to have depths shallower than 250m. The cutoff sections perpendicular to the coast were done according to MARgins and CATchements Segmentation (MARCATS) (Laruelle et al., 2013), except for the Beaufort Sea, Laptev Sea, North Sea and Congo shelf, where we used the COastal Segmentation and related CATchments (COSCATs) definitions (Meybeck et al., 2006) due to the vastness of their MARCATS segmentations.

3 ~~Global weathering~~Pre-industrial rivers loads

~~The weathering yields provided in this study are dependent on the MPI-ESM pre-industrial spatial representation of surface runoff, surface temperature and precipitation (Figure B1a,b,c). For the modelled MPI-ESM CMIP5 100 year average, we observe high modelled precipitation and temperature in the tropics, whereas in the subtropics and temperate zones the patterns are much more spatially variable. Above the Arctic Circle, the model shows only moderate precipitation and cold annual temperatures. Spatial patterns of high precipitation are usually also reproduced in the spatial patterns of runoff. This is~~

Table 1. Comparison of the surface areas [10^9 m^2] of selected coastal regions with depths of under 250m in the ocean model setup and in segmentation approaches. The comparisons were done with the MARCATS (Laruelle et al., 2013) or ~~COSTCATs~~ COSCATs (Meybeck et al., 2006). The shelf classes were defined as in Laruelle et al. (2013).

Coastal Regions	Major Rivers	Model Area	MARCATS/COSCAT Area	Shelf Class
1. Beaufort Sea (BS)	Mackenzie	269	274	Polar
2. Laptev Sea (LS)	Lena	397	326	Polar
3. North Sea (NS)	Rhine	499	871	Marginal Sea
4. Sea of Okhotsk (OKH)	Amur	245	992	Marginal Sea
5. East China Sea (CSK)	Yangtze, Huang He	731	1299	Tropical
6. Bay of Bengal (BEN)	Ganges	245	230	Indian Margin
7. Southeast Asia (SEA)	Mekong	1795	2318	Indian Margin
8. Tropical West Atlantic (TWA)	Amazon, Orinoco	448	517	Tropical
9. Congo shelf (CG)	Congo	53	38	Tropical
10. South America (SAM)	Paraná	1553	1230	Subpolar

~~however not always the case due to evapotranspiration. For instance, in northern North America, northern Europe and Siberia, a pattern of high runoff can be observed despite relatively low precipitation in these regions, which is most likely due to these regions having low vegetation densities, as well as due to the negative temperature dependency of evaporation, both of which result in lower evapotranspiration rates than in lower latitudes. Modelled pre-industrial (a) surface runoff mm a^{-1}, (b) surface temperatureCand (c) precipitation mm a^{-1}annual means.~~

~~Previous work by Goll et al. (2014) describes the MPI-ESM performing well when estimating surface temperatures at single grid cells with regards to observations. The global precipitation is slightly higher than is reported in the Precipitation Climatology Project (GCPC) (Adler et al., 2003), which is discussed along with spatial biases of the precipitation in Stevens et al. (2013). Most notably, the precipitation is too strong over extratropical land surface and too little over tropical land surface. Runoff on the other hand is less well reproduced globally. For the given time period of the CMIP5 simulation, the global runoff is 23,496 km^3 yr^{-1}. This is significantly lower than the global runoff estimations of 36,600-38,300 km^3 yr^{-1} (Fekete et al., 2002; Dai and Trenberth, 20 The difficulty of representing several processes that control the runoff, such as evapotranspiration and condensation, is also reflected in the global runoff means of other Earth System Models, which range from 23,000~~ Global weathering inputs to ~~42,500 km^3 yr^{-1} (Goll et al., 2014). The spatial patterns in the CMIP5 simulation are however comparable with the mean annual runoff patterns reported in Fekete et al. (2002), with high surface runoff observed in the Amazon basin, West Africa, Indo-Pacific Islands, Southeast Asia, eastern North America, Northern Europe as well as in Siberia. Due to the strong underestimation of the model regarding the runoff in relation to the combined runoff mean of Fekete et al. (2002) and Dai and Trenberth (2002), we conclude that a scaling factor of 1.59 is necessary to produce runoff plausibly at the global scale. The global runoff from~~

~~OMIP which provides freshwater to the ocean model, is on the other hand more plausible (32,542 km^3 yr^{-1}), and was therefore not scaled.~~

3.1 ~~Global weathering yields and their spatial distribution~~

catchments]~~Runoff, precipitation and temperature patterns~~

~~The weathering yields provided in this study are dependent on the MPI-ESM pre-industrial spatial representation of surface runoff, surface temperature and precipitation (Figure B1a,b,c). For the modelled MPI-ESM CMIP5 100 year average, we observe high modelled precipitation and temperature in the tropics, whereas in the subtropics and temperate zones the patterns are much more spatially variable. Above the Arctic Circle, the model shows only moderate precipitation and cold annual temperatures. Spatial patterns of high precipitation are usually also reproduced in the spatial patterns of runoff. This is however not always the case due to evapotranspiration. For instance, in northern North America, northern Europe and Siberia, a pattern of high runoff can be observed despite relatively low precipitation in these regions, which is most likely due to these regions having low vegetation densities, as well as due to the negative temperature dependency of evaporation, both of which result in lower evapotranspiration rates than in lower latitudes. Modelled pre-industrial (a) surface runoff mm a^{-1}, (b) surface temperatureCand (c) precipitation mm a^{-1}annual means.~~

~~Previous work by Goll et al. (2014) describes the MPI-ESM performing well when estimating surface temperatures at single grid cells with regards to observations. The global precipitation is slightly higher than is reported in the Precipitation Climatology Project (GCPC) (Adler et al., 2003), which is discussed along with spatial biases of the precipitation in Stevens et al. (2013). Most notably, the precipitation is too strong over extratropical land surface and too little over tropical land surface. Runoff on the other hand is less well reproduced globally. For the given time period of the CMIP5 simulation, the global runoff is 23,496 km^3 yr^{-1}. This is significantly lower than the global runoff estimations of 36,600-38,300 km^3 yr^{-1} (Fekete et al., 2002; Dai and Trenberth, 20 The difficulty of representing several processes that control the runoff, such as evapotranspiration and condensation, is also reflected in the global runoff means of other Earth System Models, which range from 23,000~~ Global weathering inputs ~~to 42,500 km^3 yr^{-1} (Goll et al., 2014). The spatial patterns in the CMIP5 simulation are however comparable with the mean annual runoff patterns reported in Fekete et al. (2002), with high surface runoff observed in the Amazon basin, West Africa, Indo-Pacific Islands, Southeast Asia, eastern North America, Northern Europe as well as in Siberia. Due to the strong underestimation of the model regarding the runoff in relation to the combined runoff mean of Fekete et al. (2002) and Dai and Trenberth (2002), we conclude that a scaling factor of 1.59 is necessary to produce runoff plausibly at the global scale. The global runoff from OMIP which provides freshwater to the ocean model, is on the other hand more plausible (32,542 km^3 yr^{-1}), and was therefore not scaled.~~

3.1 ~~Global weathering yields and their spatial distribution~~

catchments

The ~~described~~ weathering release models provide global means for pre-industrial weathering release rates of P, Si, DIC and Alk (Table 2), as well as their spatial distributions (Figure 2).

For P, ~~which is derived from runoff and temperature data (Hartmann et al., 2014), the~~ the calculated global release is 1.34 Tg P yr^{-1} when considering the runoff scaling factor of 1.59~~, whilst it is 0.84 Tg P yr^{-1} when omitting the scaling factor~~. The release calculated when compensating the model's runoff underestimation fits within the range found in published literature of 0.8 - 4 Tg P yr^{-1} (Compton et al., 2000; Wang et al., 2010; Goll et al., 2014; Hartmann et al., 2014)~~, while it is on the lower end of this range without the scaling factor~~. The Hartmann et al. (2014) and Goll et al. (2014) estimates (1.1 and 0.8-1.2 Tg P yr^{-1}, respectively) originate from the same weathering model as is used here. The 1.9 Tg P yr^{-1} reported in Wang et al. (2010) was on the other hand constructed by upscaling measurement data points. In a further study, Compton et al. (2000) provide a quantification of the prehuman phosphorus cycle while distinguishing between land-ocean fluxes from shale-erosion as well as from weathering. Thereby, the total pre-human P riverine flux which originates from weathering is given by averaging P species concentrations from unpolluted rivers and multiplying them with global runoff estimates, yielding an estimate of 2.5 - 4 Tg P yr^{-1}. Both estimates originating from upscaling from river measurements are therefore higher than the P weathering flux provided in the modelling approach in this study, in Goll et al. (2014) and in Hartmann et al. (2014), which suggests further effort might be needed to better constrain the global P weathering release.

~~Deriving the Si export from the Si model (Beusen et al., 2009) forced with MPI-ESM precipitation output amounts to~~ We derive a DSi global yield of 168 Tg Si yr^{-1}. This is within the range estimated by Beusen et al. (2009) (158-199 Tg Si yr^{-1}), who used the same model while using present-day observational data to drive the model for precipitation. Our estimate is also comparable with the 173 Tg Si yr^{-1} estimate provided by Dürr et al. (2011). ~~In a synthesis of the global oceanic silica cycle, Tréguer and De La Rocha (2013) conclude that rivers deliver around 200 Tg DSi to estuaries annually.~~

The modelled DIC and Alk release amounts to 374 Tg C yr^{-1}, which also takes into account the runoff scaling factor. By extrapolating from measurement data of 60 large river catchments, Meybeck (1982) suggests that the DIC export to the ocean is around 380 Tg yr^{-1} and originates directly from weathering. Further modelling studies also provide similar estimates of 260 to 300 Tg yr^{-1} (Berner et al., 1983; Amiotte Suchet and Probst, 1995). ~~Mackenzie et al. (1998) provide an inorganic carbon flux of 720 Tg C yr^{-1} in a conceptual model that considers mass balance. Since this estimate considers both particulate and dissolved inorganic carbon fluxes, the DIC flux is however significantly lower. Accounting for a particulate inorganic carbon flux of around 170 Tg C yr^{-1} (Meybeck and Vörösmarty, 1999), the value provided by the Mackenzie et al. (1998) study would result in a global DIC load of around 550 Tg C yr^{-1}.~~

The atmospheric CO_2 drawdown induced by weathering is directly related to the release of HCO_3^- since silicate weathering draws down 1 mole of CO_2 per mole HCO_3^-, and carbonate weathering draws down 0.5 mol of CO_2 per mole HCO_3^- released (Eq. (9) and Eq. (10)). While we ~~provide a modelled~~ model a CO_2 drawdown of 280 Tg C yr^{-1} induced by weathering, previously estimated drawdown fluxes are suggested in the range of ~~220 and 440~~ 220-440 Tg C yr^{-1} (Gaillardet et al., 1999; Amiotte Suchet et al., 2003; Hartmann et al., 2009), Goll et al. (2014)). ~~As for the DIC release, the modelled estimate is therefore comparable to what was previously suggested in published literature.~~ The results imply that of the 374 Tg C yr^{-1} DIC released by weathering, 280 Tg C ~~drawdown~~ yr^{-1} originates from atmospheric drawdown, while the rest originates from the weathering of the carbonate lithology (94 Tg C yr^{-1}).

Table 2. ~~Weathering~~ Pre-industrial weathering release of P, Si, DIC and Alk, as well as CO_2 drawdown, quantified by the combination of models used in this study in comparison to published literature estimates.

Species	Modelled weathering flux	Estimates	Source
P release [Tg yr^{-1}]	1.34	1.2 - 1.8	Wang et al. (2009); Hartmann et al. (2014)
Si release [Tg yr^{-1}]	168	158 - 200	Beusen et al. (2009); Dürr et al. (2011); Tréguer and De La Rocha (2013)
DIC release [Tg yr^{-1}]	374	260 - 550	Berner et al. (1983); Amiotte Suchet et al. (1995); Mackenzie et al. (1998); Hartmann et al. (2009)
Alk release [10^{12} mole yr^{-1}]	18.8	-	-
CO_2 drawdown [Tg yr^{-1}]	*280*	*220 - 440*	*Gaillardet et al., 1999; Amiotte-Suchet et al., 2003 Hartmann et al., 2009, Goll et al., 2014*

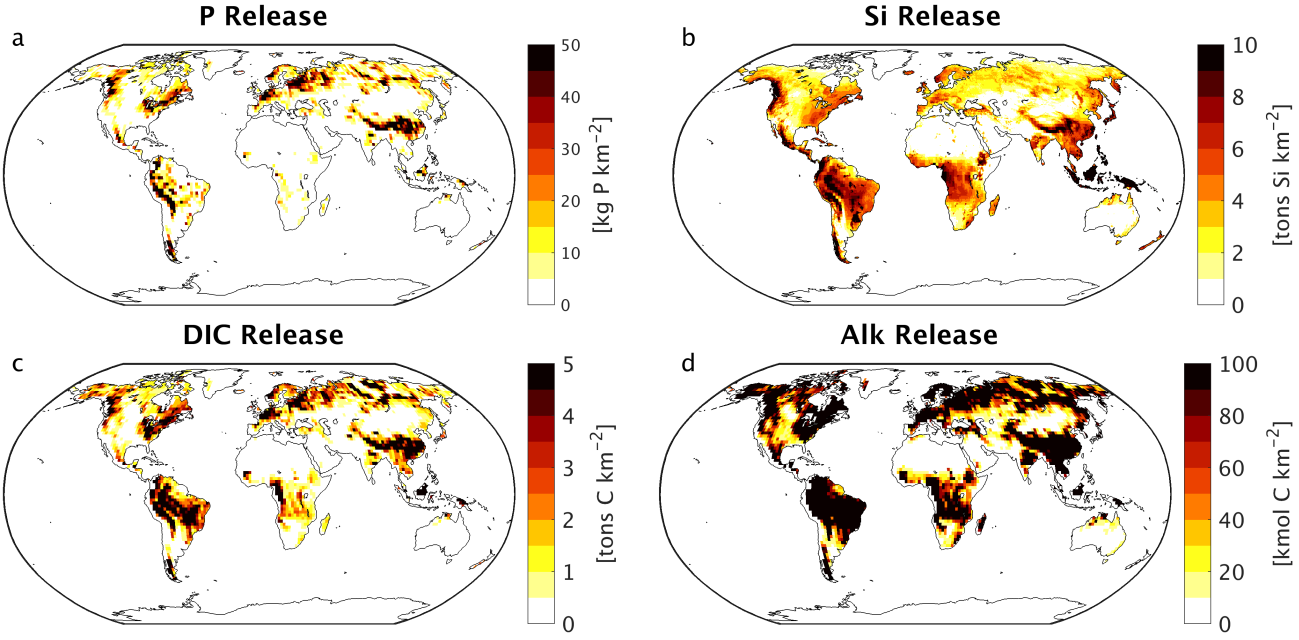

Figure 2. Weathering release rates of (a) P [kg P km^{-2}], (b) Si [tons Si km^{-2}], (c) DIC [tons C km^{-2}] and (d) Alk [kmol km^{-2}].

~~The spatial distributions of the modelled weathering release of nutrients, carbon and alkalinity (Figure 2) show strong agreement with Hartmann et al. (2009), Hartmann et al. (2014) as well as Beusen et al. (2009), where the same models were used, but were forced with observational datasets. Generally, the patterns mostly follow the runoff and precipitation patterns, whereas the lithologies play a secondary role in explaining the spatial variability patterns. This is most likely due to runoff~~

and precipitation having much stronger gradients of variation than the nutrient and carbon content in the different lithologies. Hartmann et al. (2014) suggest that in the case of the P release model, the temperature effect on the spatial variability is of similar magnitude as the P-content of the lithologies.

Furthermore, we We observe hotspots that contribute disproportionally to the nutrients and carbon release, as is also suggested in Hartmann et al. (2009) and Hartmann et al. (2014). The spatial distributions of the weathering release yields indicate the dominance of with the Amazon, Southeast Asia as well as Northern Europe and Siberia as strong sources of weathering , despite substantial soil shielding in these regions. The Amazon and Southeast Asian regions have also been identified in other studies as regions of strong carbon yields due their the (Figure 2). The dominance of these regions regarding their weathering release is often due to a wet and warm climate, as well as due to their lithology (Amiotte Suchet and Probst, 1995). The Southeast Asian islands are also areas of weathering rates significantly higher than average, due to the combination of the warm and wet climate in the region, as well as the regional abundance of volcanic and carbonate lithologies, which (Gaillardet et al., 1999; Hartmann and Moosdorf, 2011). The northern hemispheric hotspots in eastern North America and western Europe can be explained by the carbonate lithology in these regions. While the weathering and export rates over the 6 major Arctic catchments do not appear as high as other hotspots such as in the Amazon or in Southeast Asia, the vastness of the Arctic catchments could still lead to large exports to the Arctic Ocean, and the shallowness of the Arctic shelf could result in stronger implications of the exports on the ocean carbon cycle of the Arctic Ocean (Le Fouest et al., 2013)(Amiotte Suchet and Probst, 1995

4 Pre-industrial rivers loads

In this section, we report the modelled riverine loads at the global scale, as well as their regional distributions, while comparing them to a wide range of estimates made for pre-industrial riverine loads until now. We also compare the modelled loads of P and N to contemporary estimates (NEWS2, reference year 1970), in order to grasp the magnitude of their anthropogenic perturbations. Since we focus on the implications of land-sea fluxes for the ocean carbon cycle in this study, our validation analysis revolves around the nutrient, carbon and alkalinity loads at the river mouths, omitting validation of river concentrations further upstream.

3.1 Global loads in context of published estimates

3.1 Global river loads in the context of published estimates

The cumulative The modelled global pre-industrial catchment loads riverine exports to the ocean amount to 3.7 Tg P yr $^{-1}$, 27 Tg N yr $^{-1}$, 158 Tg Si yr^{-1} and 603 Tg C yr^{-1} delivered to the ocean globally. We thereby estimate , resulting from the retention of 0.3 Tg P, 2.2 Tg N, 10 Tg Si and 19 Tg C through endorheic catchments, which do not discharge into the ocean. These values do not account for particulate inorganic compounds and in the case of P, the . The fraction of Fe-P assumed to not be not desorbed in the ocean was also subtracted from the total global loads (0.2 Pg P yr^{-1}).

Table 3. Comparison of modelled global riverine loads (Model. global loads) with previous estimates [Tg yr^{-1}], except for the 1970 POP estimate, which includes all particulate P compounds from the NEWS2 study. The total loads thereby exclude particulate inorganic loads. Fe-P only considers P that is assumed to be desorbed in the ocean. The PP value from the NEWS2 study considers both POP as well as particulate inorganic phosphorus. [1] Compton et al. (2000), [2] Beusen et al. (2016), [3] NEWS2 (Seitzinger et al., 2010), [4] Beusen et al. (2009), [5] Dürr et al. (2011), [6] Tréguer and De La Rocha (2013), [7] Green et al. (2004), [8] Jacobson et al. (2007), [9] Meybeck and Vörösmarty (1999), [10] Resplandy et al. (2018), [11] Regnier et al. (2013), [12] Berner et al. (1983), [13] Amiotte Suchet and Probst (1995), [14] Mackenzie et al. (1998), [15] Cai (2011).

Species	Model. global load	Estimates and Source	Species	Model. global load	Estimates and Source
P [Tg P yr^{-1}]	3.7	4 - 4.8 (prehuman)[1]	N [Tg N yr^{-1}]	27	19-21 (pre-industrial)[27]
		2 (1900)[2]			37 (1970)[3]
		7.6 (1970)[3]			
DIP	*0.5*	*0.3 - 0.5 (prehuman)[1]*	*DIN*	*3.4*	*2.4 (pre-industrial)[7]*
		1.1 (1970)[3]			*14 (1970)[3]*
DOP	*0.1*	*0.2 (prehuman)[1]*	*DON + PON*	*24*	*19 (pre-industrial)[7]*
		0.6 (1970)[3]			*23 (1970)[3]*
POP	2.2	*0.9 (prehuman)[1]*			
		5.9 (PP, 1970)[3]	C [Tg C yr^{-1}]	603	450 - 950 (present-day)[8,9,10,11]
Fe-P	*0.8*	*1.1 - 1.5 (prehuman)[1]*	*DIC*	*366*	*260 - 550 (present-day)[12,13,14]*
		-	*DOC*	*134*	*130 - 250 (present-day)[3,9,15]*
			POC	*103*	*100 - 140 (present-day)[3,9]*
DSi [Tg Si yr^{-1}]	158	158 - 200 (present-day)[4,5,6]			

~~The~~ In the following, we compare the magnitudes of modelled land-ocean exports of P, N, Si and C, as well as their fractionations ~~, largely agree with the~~ with a wide range of estimates found in published literature (Table 3). This was done in comparison to pre-industrial estimates directly, as well as for the 1970 estimates by the NEWS2 study to assess the loads in the context of present-day estimations.

~~For instance, the~~ The modelled global P loads fluxes are close to the higher P export estimate range of 4 - 4.7 Tg P yr^{-1} reported in Compton et al. (2000), which was constructed by upscaling natural river catchment P concentrations to the global river freshwater discharge (thus prehuman). A recent modelling study by Beusen et al. (2016), which takes ~~into account~~ a more complex retention scheme within rivers ~~than is done in our framework~~into account, suggests a lower load of 2 Tg P yr^{-1} for

year 1900. The 1970 estimate (7.6 Tg P yr^{-1}) provided by the NEWS2 study, which considers substantial anthropogenic inputs, nevertheless suggests a steep 20th century increase in the global P flux to the ocean for all three cases.

The modelled DIP export to the ocean (0.5 Tg P yr^{-1}) is at the top range of prehuman estimates (0.3 - 0.5 Tg yr^{-1}) and well below 1970 estimates (1.1 Tg P yr^{-1}). A direct fractionation of the global P flux to DIP, DOP and POP is not provided in the Beusen et al. (2016) study. We estimate similar global loads of DOP as Compton et al. (2000) (around 0.1 and 0.2 Tg P yr^{-1}). The modelled DOP value is also much lower than the 1970 value (0.6 Tg P yr^{-1}), which was also strongly anthropogenically perturbed for 1970 (Seitzinger et al., 2010). The modelled POP global load is larger than the estimate of Compton et al. (2000), which could be due to the POM C:P ratio of 122:1 chosen in our study. Strong uncertainties exist in the global C:P ratios for riverine POM, with Meybeck (1993) suggesting a ~~weight~~ mole ratio of around ~~57~~ 140 C:P, whereas Ramirez and Rose (1992) estimate a ratio of around ~~500.~~ 1500, which would strongly affect the results given here. The particulate P load given in the NEWS2 study is vastly higher than the POP load modelled in our study, but a large fraction of the estimate is likely to be directly shale-derived particulate ~~inorganic~~ P and thus biologically unreactive in the ocean. The modelled Fe-P (1.0 Tg P yr^{-1}) is slightly below the range estimated in Compton et al. (2000) (1.5 - 3.0 Tg P yr^{-1}). However, the assumed reactive fraction of the Fe-P loads (0.8 Tg P yr^{-1}) here is close to how much P is suggested to be desorbed in the coastal ocean in Compton et al. (2000) (1.1-1.5 Tg P yr^{-1}).

Despite our simplified assumption of N loads being coupled to P loads, the modelled global N load is also situated within the pre-human and contemporary land-ocean N loads given in the modelling study of Green et al. (2004) (21 and 40 Tg N yr^{-1} respectively). The modelled annual DIN load (3.4 Tg N) is slightly higher than the prehuman load given in the Green et al. (2004) study (2.4 Tg N yr^{-1}). In Beusen et al. (2016), the global pre-industrial N load is suggested to be lower (19 Tg N yr^{-1}) due to in-stream retention and removal.

The modelled global load of DSi is 158 Tg Si yr^{-1}, which is at the lower boundary of the range of present-day estimates of 158-200 Tg Si yr^{-1}. We thereby assume that the change in the global DSi load over the 20th century is small, and therefore compare our pre-industrial estimate with present-day estimates from published literature. The NEWS2 study used the same Beusen et al. (2009) silica export model forced with present-day observational precipitation data~~,~~. Dürr et al. (2011) and Tréguer and De La Rocha (2013) upscaled discharge weighted DSi concentrations at river mouths. Substantial amounts of particulate silica, which aren't considered in this study, are suggested to be delivered to the ocean, yet it is not clear how much is dissolvable and biologically available (Tréguer and De La Rocha, 2013). Another point of uncertainty is the increase in river damming during the 20th century, which might have strongly increased the global silica retention in present-day rivers (Ittekkot et al., 2000; Maavara et al., 2014). The pre-industrial loads therefore might have been higher than for the present-day, but the implications of damming on the retention of biogeochemical compounds escape the scope of this study.

The modelled total C, DIC, DOC and POC fluxes are within, albeit on the lower side of the present-day estimate ranges shown in Table 3. While the carbon retention along the land-ocean continuum might have increased during the 20th century, enhanced soil erosion through changes in land use might have also increased the carbon inputs to the freshwater systems, leaving question marks on the magnitude of the net anthropogenic perturbation (Regnier et al., 2013; Maavara et al., 2017).

The agreement of the DOC and POC loads with estimates is not surprising, since they originate directly from the NEWS2 study, which already validated the global loads extensively.

The large spread found in the literature estimates regarding all species points towards difficulties in constraining pre-industrial river fluxes. Even for the present-day, Beusen et al. (2016) note large differences between the outcomes of their study and the previous global modelling study NEWS2. Upscaling approaches, on the other hand, are often based on data collected by Meybeck (1982) for pre-1980s without taking into account more recent river measurement data. They also rely on the assumption of a linear relationship between river runoff and river specie loads. While we acknowledge a certain degree of uncertainty in the numbers provided in this study, ~~and that possibly significant riverine processes such as in-stream retention are omitted,~~ the modelling approach chosen nevertheless leads to pre-industrial global river loads that are in line with what was suggested previously and to a framework that could be ~~used~~ incorporated within state-of-the-art Earth System Models.

3.2 ~~Spatial load distribution and identified hotspots~~Hotspots of riverine loads

Riverine loads of the major catchments show similar spatial distributions with regards to areas of high weathering rates (Figure 3), with warm and wet regions yielding the largest river exports to the ocean. We observe large differences between the northern and southern hemispheres. The northern hemisphere accounts for an annual total carbon input of 404 Tg C to the ocean, vastly dominating the global loads (67% of total global C). ~~The northern hemisphere also contributes overproportionally to the oceanic nutrient supply (69% for DIP and DIN, 60% for DSi). The dominance of northern hemispheric riverine C land exports to the ocean is also reported in Aumont et al. (2001) and Resplandy et al. (2018).~~

We furthermore observe several regions of disproportionate contributions to global riverine loads. For one, rivers that drain into the tropical Atlantic consist of a major fraction of the global ~~biogeochemical oceanic~~ oceanic biogeochemical supply. This is due to major rivers of the South American continent debouching into the ocean basin, as well as considerable exports provided by the west African ~~Volta, Congo and Niger~~ rivers (Table 4). According to our framework, the seven largest rivers unloading in the region (Orinoco, Amazon, São Francisco, Paraíba do Sul, Volta, Niger and Congo) amount to a total yearly carbon ~~flux~~ loads of 123 Tg C (58 Tg DIC, 44 Tg DOC, 21 Tg POC), which consists of around 20% of the global carbon riverine exports. These regional carbon loads agree very well with estimated values derived from monthly river discharge and carbon concentrations data in Araujo et al. (2014) (53 Tg DIC, 46 Tg DOC). In terms of catchments, the pre-industrial Amazon river provides the largest inputs of biogeochemical tracers to the ocean in the region (modelled annual loads of 0.07 Tg DIP, 0.5 Tg DIN, 15.2 Tg DSi, 33.2 Tg DIC , 28.3 Tg DOC Tg, 17.1 Tg POC)~~. Present-day data from Araujo et al. (2014) suggests annual Amazon river loads of~~ , which compares well with the present-day data (0.22 Tg DIP, 17.8 Tg DSi, 32.7 Tg DIC, 29.1 Tg DOC~~. Since DIP loads are suggested to have strongly increased due to anthropogenic inputs (NEWS2, Seitzinger et al. (2010)), the pre-industrial and present-day difference in the DIP loads is plausible~~). For the other tropical Atlantic catchments, the modelled DIC loads are close to estimated values for the Congo, Orinoco and Niger, but are overestimated for the smaller catchments of the Paraíba, Volta and São Fransisco. The DIP loads of the tropical Atlantic catchments tend to show much lower values with regards to present-day data, suggesting the realistic increase in the region's DIP loads from pre-industrial exports of 81.8 10^9 g P yr^{-1} to present-day loads of 276 10^9 g P yr^{-1} due to anthropogenic inputs.

Although less significant in terms of global loads, the major Arctic rivers (Yukon, Mackenzie, Ob, Lena, Yenisei) provide a large carbon supply ~~, which consists~~ to the Arctic Ocean, thereby consisting of a dominant fraction of DIC~~, to the shallow basin of the Arctic Ocean~~. The Arctic rivers thereby provide 37.5 Tg DIC (10% of global DIC), 14.4 Tg DOC (11 % of global DOC) and 4.4 Tg POC annually to the Arctic Ocean. The total C loads of the Arctic therefore amount to 56 Tg C yr^{-1}, thus 9% of global C loads. The DIC, DOC and POC load levels are comparable to estimates of 29 Tg DIC yr^{-1} (Tank et al., 2012), 17 Tg DOC yr^{-1} (Raymond et al., 2007) and 5 Tg POC (Dittmar and Kattner, 2003). Total Arctic DIP loads (40.8 10^9 g P yr^{-1}) derived from our modelling approach are slightly higher with regards to published literature estimates of 35.8 10^9 g P yr^{-1}. DIP inputs from anthropogenic sources are considered to be small for Arctic catchments (NEWS2), which explains why the modelled pre-industrial DIP loads are of comparable magnitudes to observed DIP loads for the present-day. ~~River loads originating from weathering models (~~DIC and DIP loads~~) thereby show~~ , which are strongly affected by inputs from weathering models, where a global runoff correction term of 1.59 was applied thereby shows a slight overestimation in the Arctic with regards to published literature estimates~~. Since both of these modelled exports mostly originate from weathering models due to the low anthropogenic contributions to Arctic catchment riverine loads, the runoff correction of the P and DIC weathering release models~~ , suggesting that a scaling factor of 1.59 might be too high for this region. Furthermore, the dynamics of weathering in the region also remain largely uncertain, for instance due to the implications of permafrost on the weathering rates.

Southeast Asian rivers also provide large exports of biogeochemical tracers to the ocean. The Huang He, Brahmaputra-Ganges, Yangtze, Mekong, Irrawaddy and Salween, which have catchment areas characterized by warm and humid climates, provide 92.4 Tg C yr^{-1} to the ocean (15% of global C loads). We observe vastly elevated DIP levels for the present-day estimates with regards to our pre-industrial modelled levels. The NEWS2 data suggests a strong present-day perturbation of the DIP loads due to anthropogenic inputs to the region's catchments, which can plausibly explain these differences.

The Indo-Pacific Islands have been identified as a region with much higher weathering yields than average ~~Hartmann et al. (2014)~~(Hartma Although this region only accounts for around 2% of the global land surface, it provides 7% (39 Tg) of C and in particular 10% (10 Tg C) of the global POC delivered to the ocean annually, making the region a stronger land source of POC than the entire Arctic basin. This implies that POM mobilization through soil erosion is a substantial driver of land-sea carbon exports in the region~~, in addition to weathering~~.

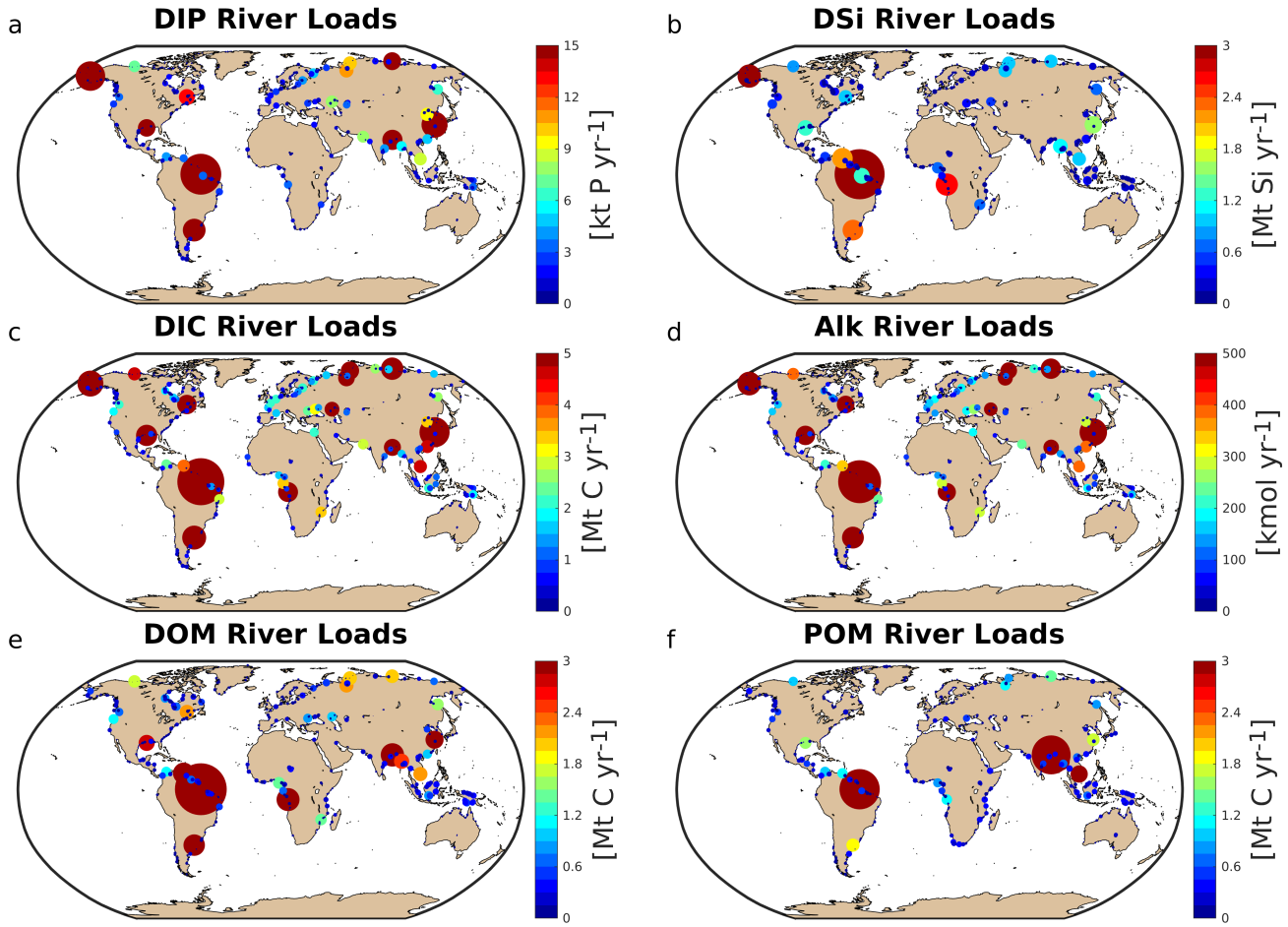

Figure 3. Modelled ~~dissolved~~ annual river loads of DIP (a), DSi (b), DIC (c), Alk (d), DOM (e) and POM (f).

3.3 ~~Exports to chosen coastal regions~~

~~With respect to the 10 shallow shelf regions chosen for this study (Table 1), the catchments of the low latitude regions (5. CSK, 6.BEN, 7.SEA, 8.TWA, 9.CG) provide substantially more carbon and nutrients to the coastal ocean than the high latitude regions (Figure 7), although the differing size of the coastal regions and of their drainage catchments might play a strong role in explaining these differences. The tropical West Atlantic (8.TWA) has the largest input of biogeochemical tracers due to the Amazon and Orinoco rivers being a dominant source of nutrients and carbon. In the tropical regions of the Bay of Bengal (6.BEN) and Southeast Asia (7.SEA), the fraction of carbon delivered as POC is substantially higher than for the rest of the regions (Figure 7b). Furthermore, in the high latitude regions (1.BS, 2. LS, 3.NS, 10.SAM), the DIC loads are the major source~~

Table 4. Regional hotspot of C loads [Tg C yr^{-1}] and DIP loads [10^9 g P yr^{-1}] compared with regional estimates: [1] Araujo et al. (2014), [2] Bird et al. (2008), [3] Tank et al. (2012), [4] Raymond et al. (2007), [5] Dittmar and Kattner (2003), [6] Le Fouest et al. (2013), [7] Li and Bush (2015), [8] Yoshimura et al. (2009), [9] Tao et al. (2010), [10] Seitzinger et al. (2010). Modelled DIP is from our approach to represent pre-industrial fluxes, whereas the DIP literature estimates are from present-day data and are strongly affected by anthropogenic perturbations.

Hotspots	**Modelled**				**Estimates**			
	DIC	DOC	POC	DIP	DIC	DOC	POC	DIP
Tropical Atlantic								
Amazon	33.2	28.2	17.1	73	32.7[1]	29[1]	6.1[2]	221[1]
Congo	9	5.6	1.2	2.3	13[1]	10.58[1]	2.0[2]	18 [1]
Paraíba	2.4	0.5	0.4	<0.1	0.3[1]	0.10[1]	-	0.6[1]
Volta	3	0.5	0.5	0.1	0.1[1]	0.13[1]	-	7.0[1]
Niger	1.1	1.5	0.9	1.0	2.2[1]	0.43[1]	0.8[2]	7.5[1]
São Fransisco	6	2.9	0.2	2.4	0.5[1]	0.35[1]	-	0.5[1]
Orinoco	3.3	4.8	1.1	2.9	5.0 [1]	3.9[1]	1.7[2]	21.4[1]
Total	**58**	**44**	**21**	**81.8**	**53**	**46**	**-**	**276**
Arctic								
Mackenzie	4.5	1.7	0.4	6.0	6.29[3]	1.4[4]	-	1.5[6]
Yukon	3.1	6.1	0.9	3.8	4.45[3]	1.7[4]	-	1.9[6]
Lena	12.7	2.0	1.1	8.23	5.82[3]	5.83[4]	0.47[4]	4.4[6]
Yenisei	8.6	2.0	1.2	8.8	6.96[3]	4.69[4]	0.17[4]	7.9[6]
Ob	8.6	2.6	0.8	14.1	5.90[3]	3.05[4]	0.3-0.6[4]	20.4[6]
Total	**37.5**	**14.4**	**4.4**	**40.8**	**29.4**	**16.7**	**1.09**	**35.8**
Southeast Asia								
Ganges	7.7	5.8	15.6	21.3	4.2[7]	1.4[2]	1.7[2]	165[10]
Irrawaddy	2.5	6.1	0.9	4.6	10.8[7]	0.89[2]	3.25[2]	8.7[10]
Salween	0.7	0.3	0.7	0.8	8.4[7]	0.26[2]	2.9[2]	1.9[10]
Mekong	4.4	2.1	3.1	7.2	4.5[7]	-	-	0.9[8]
Huang He	3.6	0.5	0.3	8.3	1.3[7]	0.1[2]	6.3[2]	5.0[9]
Yangtze	23	3.5	1.7	29.9	24[7]	2.1[2]	6[2]	92[10]
Xi River	8.6	0.9	0.4	4.3	-	4.6[2]	-	25[10]
Total	**50.5**	**19.2**	**22.7**	**76.4**	**-**	**-**	**-**	**298.5**
Indo-Pacific Islands								
Total	**19.4**	**10.2**	**10.1**	**24.7**	**-**	**-**	**-**	**-**

~~of carbon, whereas for the other regions, organic carbon is the largest contributor to the total carbon load. The increasing contribution of DIC loads to the total carbon load at high latitudes was moreover observed for Arctic catchments in Table 4.~~

~~(a) Total P (TP) and N (TN) and (b) C (DIC, DOC and POC) exports to the chosen coastal ocean regions. TP and TN are the total P and N modelled in their dissolved inorganic species (DIP, DIN) and organic species (tDOM and POM). DOC and POC are the carbon loads from tDOM and riverine POM, respectively.~~

4 Implications for the global ocean~~biogeochemistry~~

~~In this section, we investigate the long-term implications of considering the inputs of pre-industrial riverine loads in an ocean biogeochemical model. We thereby compare the RIV simulation, in which the described pre-industrial riverine loads were added, to the standard model REF simulation, where biogeochemical tracers were added homogeneously to the surface ocean to compensate for particulate losses ($CaCO_3$, opal and organic matter) in the sediment and thus were necessary to maintain a stable ocean state .~~

4.1 The ocean state - An increased biogeochemical coastal sink

4.2 ~~Ocean state - An increased biogeochemical coastal sink~~

We observe that the magnitudes of the nutrient inputs (P, N and Si) do not strongly differ between REF and R (Table 5). This implies that in REF, the amounts of P, N and Si added to the open ocean to maintain a plausible ocean state were similar to what is derived in our approach while deriving river exports. Despite slightly larger inputs of nutrients in RIV than in REF, RIV shows lower global surface dissolved nutrient concentrations and global NPP. The coastal ocean therefore must act as an increased biogeochemical sink in the model, since river-delivered or newly produced particulate organic matter reaches the shelf sea floor faster than in the open ocean, allowing for less time for the organic matter to be remineralized within the water column. This is confirmed by the increased organic matter flux to the global continental shelf sediment (defined as areas with less than 250m depth) in RIV, with an increase from 0.18 Gt C yr^{-1} to 0.25 Gt C yr^{-1}. The large range of global values (0.19-2.20 Gt C yr^{-1}) given in a review by Krumins et al. (2013) nevertheless hints that the coastal POM deposition flux is possibly improved in RIV.

~~We observe that the total REFand RIV nutrient magnitudes of the P, N and Si inputs to the ocean are very similar (Table 5) , implying that the differences in nutrient concentrations and NPP between RIVand REF originate from the geographic locations of inputs. Alk inputs are~~ While Alk inputs were also added at nearly the same levels ~~. The~~ in REF than in our derived riverine loads in RIV, the total carbon inputs are on the other hand increased by almost 100% in RIV in comparison to REF. ~~These larger carbon inputs originate firstly from higher DIC to Alk ratio of the riverine loads (1:1) than is exported through the net $CaCO_3$ production (1:2). Secondly, there is a higher carbon load originating from organic matter, since the tDOM C:P ratio is higher than the oceanic DOM C:P ratio. In both cases, the model~~ In comparison to REF, the inorganic (366 Tg C yr^{-1}) and organic (237 Tg C yr^{-1}) carbon inputs in RIV show stronger agreement with the riverine inorganic (260-550 Tg C yr^{-1}) and organic carbon

(270 - 350 Tg C yr^{-1}) global load estimates found in literature (Meybeck, 1982; Amiotte Suchet and Probst, 1995; Mackenzie et al., 1998; Meybeck and Vörösmarty, 1999; Hartmann et al., 2009; Seitzinger et al., 2010; Cai, 2011; Regnier et al., 2013), signifying an improvement in the model's carbon inputs. These higher carbon inputs also result in a net long-term outgassing flux (231 Tg C yr^{-1}), which ~~we will discuss in detail.~~

~~Despite slightly larger inputs of nutrients in RIV than in REF, lower global surface dissolved nutrient concentrations and lower global primary production rates are found in RIV. The coastal ocean therefore acts as an increased biogeochemical sink in the model, since river-delivered or newly produced particulate organic matter reaches the shelf sea floor faster than in the open ocean, allowing for less time for the organic matter to be remineralized within the water column. On shallow shelves (<250m depth), we find an increased organic matter flux of 0.25 Gt C yr^{-1} to~~ is suggested in literature for the pre-industrial time-period and is absent in REF. The net outgassing largely originates from higher DIC:Alk ratios of the riverine inputs (1:1) than is exported through the net $CaCO_3$ production (1:2), as well as higher C:P ratios of tDOM inputs (2583:1) than is exported in the oceanic organic ratio (122:1). Both of these inputs-output imbalances lead to increasing the pCO_2 in the ~~sediment in RIV versus a flux of 0.18 Gt C yr^{-1} for REF. Although strong uncertainties exist in literature regarding the coastal POM sediment deposition flux, the range of global values given in a review by Krumins et al. (2013) (0.19-2.20 Gt Cyr^{-1})hints that the coastal POM deposition flux is possibly improved in RIV~~long-term (Appendix C.2).

Table 5. Comparison of river inputs and the ocean state for REF and RIV. Additionally, we compare the modelled mean surface DIP, DIN and DSi concentrations with World Ocean Atlas 2013 (WOA) surface layer means. OMZ: Ocean minimum zone.

Variables	REF	RIV		REF	RIV	WOA
Open Ocean/River Inputs			***Global ocean variables***			
P [Tg P yr^{-1}]	3.49	3.7	NPP [Gt C yr^{-1}]	48.87	47.09	
N [Tg N yr^{-1}]	25.2	27	Air-Sea CO_2 flux [Gt C yr^{-1}]	-0.05	0.18	
Si [Tg Si]	115	158	Organic export 90m [Gt C yr^{-1}]	6.84	6.47	
Alk [Tg HCO_3^- yr^{-1}]	416	366	$CaCO_3$ export 90m [Gt C yr^{-1}]	0.66	0.61	
Inorganic C [Tg C yr^{-1}]	208	366	Surface DIC [mM C]	1.94	1.94	
Organic C [Tg C yr^{-1}]	106	237	Surface DIP [μM P]	0.439	0.413	0.48
			Surface DIN [μM N]	3.90	3.76	5.04
			Surface DSi [μM Si]	13.6	14.6	7.5
			OMZs volume [km^3]	2.61	2.45	

The global mean surface concentration is lower in RIV than in the observational data of the World Ocean Atlas 2013 (WOA, Boyer et al. (2013)) for DIP (0.439 and 0.480 μM P respectively) and DIN (3.90 and 5.04 μM N), and higher for DSi (13.6 and 7.5 μM Si). The WOA dataset is constructed from present-day observations of an ocean state that might already be perturbed by a substantial increase in riverine P and especially N loads, whereas the model shows pre-industrial concentrations. A

consideration of the substantial anthropogenic increase in DIN riverine loads ~~(Seitzinger et al., 2010; Beusen et al., 2016)~~ (e.g. Seitzinger et al. (2010)) could plausibly shrink some of the disagreement with the WOA dataset in the case of DIN. A large part of the DIN underestimation is however most likely due to notably large tropical Pacific oxygen minimum zones, which cause a large DIN sink due to denitrification and the consumption of DIN in the anaerobic breakdown of organic matter. Furthermore, the lower surface concentrations of DIP and DIN than found in the WOA dataset suggest that the coastal sink of biogeochemical tracers might be too large. Nevertheless, the surface DIN:DIP ratio in RIV is slightly improved in comparison to REF with regards to WOA, which is most likely due to the shrinking of the tropical Pacific oxygen minimum zones and the decrease of denitrification in the region.

The DIP and DIN underestimation bias with respect to the WOA datasets are also reflected in the spatial distributions of the surface concentrations (Figure 4), where in particular the DIN concentrations are underestimated in most major basins. The spatial patterns of differences with regard to WOA data are similar for RIV and for REF ~~, suggesting ocean physics being~~ (Appendix, Figure E1,F1,G1), suggesting that the ocean physics are the dominant driver of the nutrient distributions in the open ocean (see ~~Appendix, Figure E1,F1,G1~~also Supplementary Information S.5). Prominent bias of the model are lower surface DIP and DIN concentrations in the Southern Ocean, higher DSi concentrations in the Southern Ocean, and higher DIP concentrations in the tropical gyres in comparison with the WOA dataset.

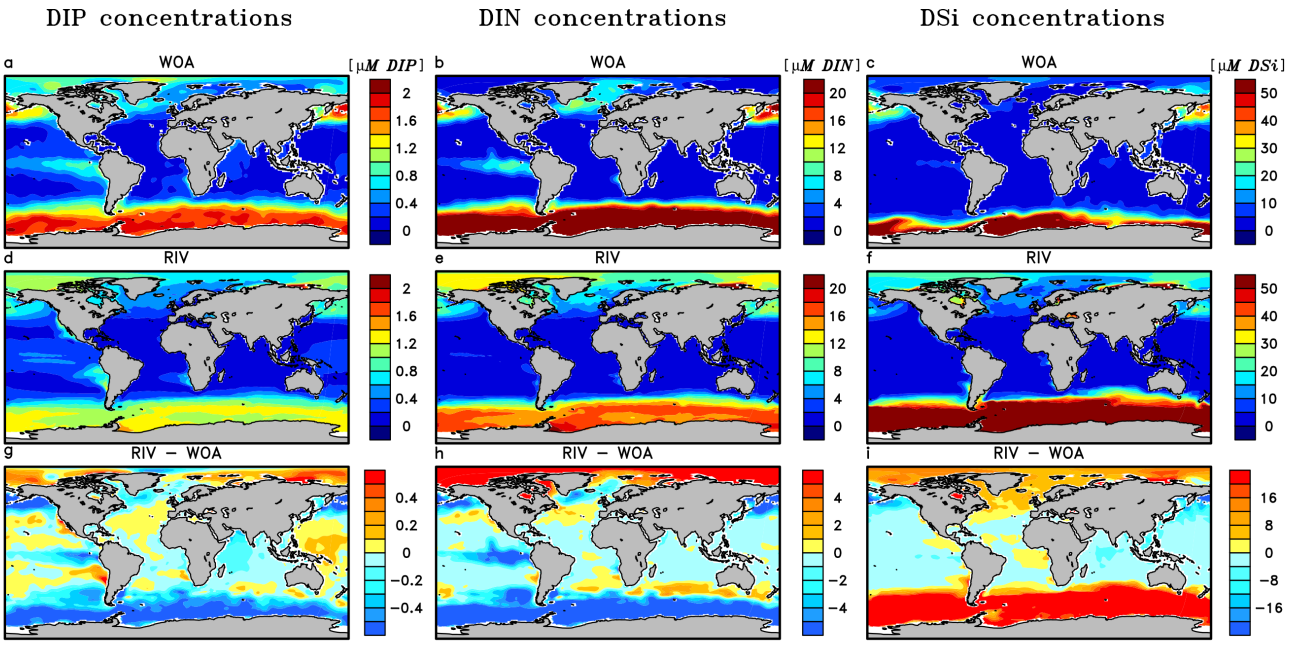

Figure 4. Surface DIP (a,d,g), DIN (b,e,h) and DSi (c,f,i) concentrations in WOA observations (a,b,c), RIV (d,e,f) and their differences ~~RIV-OBS~~RIV-WOA (g,h,i).

4.2 Riverine-induced NPP hotspots

The ~~net primary production (NPP) in the~~ most productive open ocean ~~regions (tropical Atlantic and Pacific, north Pacific, Southern Ocean) are reduced in RIV with respect to REF , but nevertheless~~ in regions REF remain the most dominant areas of biological production in RIV (Figure 5a,b)~~. However~~, signaling the major importance of the ocean physics in dictating major spatial patterns of the global NPP.

In comparison to when adding nutrients to the open ocean (REF), substantial enhancements in the NPP can be found near various major river mouths in RIV. In proximity to lower latitude rivers~~such as the Amazon~~, the uptake of nutrients by phytoplankton via primary production occurs efficiently due to favorable light conditions~~. This freshly produced organic matter, in addition to the terrestrial supplies of organic material delivered by rivers, leads to local increases in oceanic organic material concentrations~~ , thus adding to the local organic matter stock (Figure 5c,d).

~~In the tropical Atlantic , a region we identified to have major nutrient and carbon riverine supplies in section 4.2, the NPP is increased near the mouths of the major rivers. This is most notably the case in~~ This can be observed on the shallow shelves of the Tropical Atlantic basin, where major nutrient supplies are provided (see section 3.3), most notably for the Amazon plume~~, which mirrors the direction of the freshwater plume northwestwards (see Appendix, Figure ??). However, in the open ocean of the equatorial Atlantic, where upwelling takes place from deeper water layers~~. Moreover, the NPP is increased in certain semi-enclosed seas such as the Caribbean Sea, the Baltic Sea, the Black Sea and the Yellow Sea, where satellite observation data also suggest high chlorophyll concentrations (Behrenfeld and Falkowski, 1997).

In the tropical Atlantic and Pacific, north Pacific, Southern Ocean, the NPP is decreased ~~. While considering both effects, the NPP increases by only 2% for the whole region, while there are nevertheless substantial NPP increases along the western African and eastern South American tropical shelves.~~

in RIV, signaling that keeping ocean biogeochemical inventories stable with open ocean inputs led to a slight artificial enhancement of the NPP in REF in these regions. In the Equatorial Pacific, ~~we observe a strong decrease in NPP, a feature that could be partly~~ this could partly be explained by the South American river systems, which ~~majorly~~ almost solely discharge into the Atlantic (Figure 7). Although Southeast Asian rivers deliver substantial amounts of land-derived material to the ocean, the export to the open Pacific ~~appears to be~~ is likely inefficient, with model coastal salinity profiles in this region suggesting little mixing with the open ocean. Coastal parallel currents could be a key reason explaining ~~the inefficent~~ this inefficient export (Ichikawa and Beardsley, 2002). Furthermore, the riverine loads mostly supply semi-enclosed or marginal seas (East China, South China and Yellow Seas), which have limited exchange to the open ocean and which are affected by the relatively coarse GR15 model resolution in this region (Jungclaus et al., 2013). The resulting decrease in the Equatorial Pacific NPP is likely responsible for most of the shrinking of oxygen minimum zones (Table 5). ~~The NPP is decreased in the Benguela Current System, which is a major NPP hotspot in the model due to nutrients being entrained to the surface from deeper layers. Moreover, the NPP is increased in certain semi-enclosed seas such as the Caribbean Sea, Baltic Sea, the Black Sea and the Yellow Sea, where satellite observation data also suggest high chlorophyll concentrations (Behrenfeld and Falkowski, 1997).~~

~~Depth integrated annual NPP (a,b) and total annually accumulated organic concentration (c,d) in the surface layer in the RIV simulation and RIV - REF.~~

The Arctic Ocean does not show a noticeable increase in NPP, despite high nutrient concentrations in the basin. This can be explained by ~~the~~ light limitation, as well as sea ice coverage~~inhibiting~~ , which both inhibit the primary production ~~especially during the winter~~in the region during winter especially. In the entire basin, the nutrient concentrations are much higher than what is suggested in the WOA database. In Bernard et al. (2011), where nutrient inputs were added to the ocean according to the NEWS2 study, similarly high concentrations of DSi were found in the Arctic. Furthermore, Harrison and Cota (1991) suggest that nutrients limit phytoplankton growth in the late Summer in the Arctic Ocean. Although the summer ~~primary production~~ NPP in the model is substantially higher than for other seasons, the NPP is never ~~nutrient limited~~ nutrient-limited for the vast majority of the Arctic.

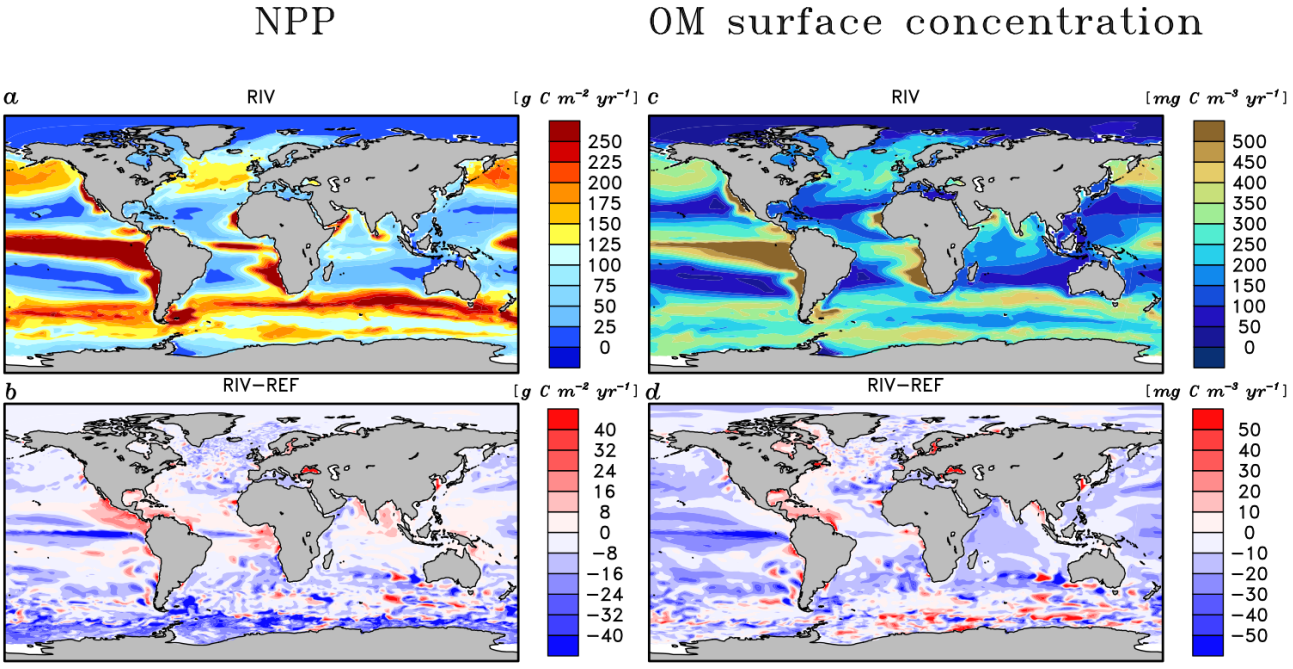

Figure 5. Depth integrated annual NPP (a,b) and total annually accumulated organic concentration (c,d) in the surface layer in the RIV simulation and RIV - REF.

4.3 Riverine-induced CO_2 Outgassing

The addition of riverine carbon loads causes ~~an~~ a net oceanic CO_2 source of 231 Tg C yr^{-1} to the atmosphere (Table 5). ~~The outgassing flux is thereby caused by carbon contained in tDOM, as well as considering the inputs of DIC.~~ While the hotspots

of the riverine-induced carbon outgassing are regions in proximity to major river mouths (Figure 6b), a widespread, albeit weaker outgassing signal can be observed in open ocean basins. The largest outgassing fluxes are found in the Atlantic and Indo-Pacific (31% and 43% of global outgassing flux respectively), likely due to the tropical Atlantic and Southeast Asian hotspots of riverine carbon supplies (see section ~~4.2~~3.2). In the Southern Ocean, we observe an increase in the outgassing flux of 17 Tg yr^{-1} when comparing RIV to REF, which is almost 10% of the total riverine-caused outgassing. The southern hemisphere shows an oceanic outgassing flux of 113 Tg yr^{-1} (49%), despite southern hemisphere land exports contributing only 227 Tg (36 %) of total riverine carbon loads to the ocean, which suggests a substantial interhemispheric transfer of carbon from the northern hemisphere to the southern hemisphere. The interhemispheric transfer of carbon in the ocean has been a topic of discussion in literature, with studies of Aumont et al. (2001) and Resplandy et al. (2018) also suggesting the transport of carbon between latitudinal regions of the ocean to compensate for ~~the heterogeneous terrestrial supplies~~unequal contributions of riverine carbon from the northern and southern hemisphere.

The high latitude Arctic rivers also (Lena, Mackenzie, Yenisei, Ob, Oder, Yukon) provide ~~a source of~~ carbon to their respective shelves, which causes outgassing on the Laptev shelf and in the Beaufort Sea (2.2 Tg C yr^{-1} and 2.3 Tg C yr^{-1}, respectively). The impacts of riverine carbon loads in these regions can also be observed in the present-day coastal ocean pCO_2 dataset of Laruelle et al. (2017), in which these regions display very high pCO_2 values ~~.~~ (>400ppm).

~~While all areas in proximity to the river mouths show increases in CO_2 outgassing caused by the addition of riverine inputs of carbon (Figure 6b), determining the net sign of the CO_2 of individual plumes in RIV is not as straightforward. A CO_2 undersaturation in many river plumes can still be observed despite the addition of riverine carbon (Figure 6a). Riverine nutrient, carbon, alkalinity and freshwater inputs, as well as physical and biogeochemical oceanic features all interact to affect the net CO_2 flux. The Amazon plume is a prominent example, which is a net carbon sink near the river mouth in the model despite being supplied by large amounts of carbon from the Amazon river. The near-shore Amazon plume is thereby also identified as an atmospheric carbon sink in literature (Cooley et al., 2007; Lefèvre et al., 2017).~~

4.4 ~~Sensitivity of the NPP and CO_2 flux in chosen coastal regions~~

5 Coastal region analysis

~~The areas of~~ With respect to the 10 ~~chosen coastal ocean regions~~ shallow shelf regions chosen for this study (Table 1~~in section 4.3)are better represented for the Atlantic shelves than eastern Asian shelves due higher resolutions of the GR15 model in the Atlantic (Jungclaus et al., 2013). We observe strong latitudinal differences in the regional riverine inputs (section 4.3) , and analyze their implications for the coastal ocean regions here. We observe strong differences in the regional responses to the riverine loads , with a tendency of stronger relative changes in NPP on lower latitudinal shelves, and stronger relative changes in CO_2 in the higher latitudes (Figure 8)~~), the catchments of the low latitude regions (5. CSK, 6.BEN, 7.SEA, 8.TWA, 9.CG) provide substantially more carbon and nutrients to the coastal ocean than the high latitude regions (Figure 7), although the differing size of the coastal regions and of their drainage catchments might play a strong role in explaining these differences. The tropical West Atlantic (8.TWA) has the largest supplies of biogeochemical tracers which are provided largely by the

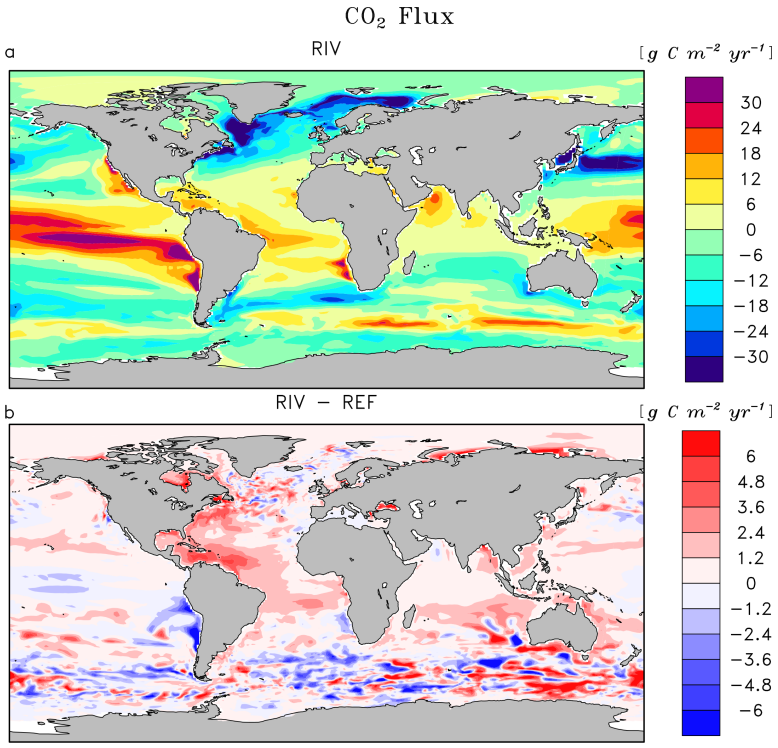

Figure 6. Annual pre-industrial air-sea CO_2 exchange flux of (a) RIV and (b) RIV-REF. A positive flux describes an outgassing flux from the ocean to the atmosphere, whereas a negative flux is from the atmosphere to the ocean.

Amazon and Orinoco rivers. In the tropical regions of the Bay of Bengal (6.BEN) and Southeast Asia (7.SEA), the fraction of carbon delivered as POC is substantially higher than for the rest of the regions (Figure 7b). Furthermore, in the high latitude regions (1.BS, 2. LS, 3.NS, 10.SAM), the DIC loads are the major source of carbon, whereas for the other regions, organic carbon is the largest contributor to the total carbon load. The increasing contribution of DIC loads to the total carbon load in the Arctic can also be observed in Table 4.

For tropical and subtropical regions, we observe major coastal ocean NPP increases of 166%, 377% and 71% for the tropical West Atlantic (3.TWA), Bay of Bengal (5.BEN) and East China Sea (6.CSK), ~~respectively~~caused by the consideration of riverine inputs, respectively (Figure 8b). The availability of light, as well as the large riverine supplies of nutrients to these regions provide optimal conditions to enhance the biological production. Surprisingly however, the Southeast Asian shelf (6.SEA) does not show a similar substantial NPP increase as the other tropical regions despite considerable riverine fluxes to the region (Table 4 in Section ~~4.2~~3.2). This is on one hand due to the large area of the defined region; the shelf is the largest that is analyzed in this study (1795 10^9 m^2), which reduces the impact of the river loads per area. Secondly, there is a larger connection area to the open ocean due to not sharing a coastal border with a continent, which implies a larger open ocean exchange, thus reducing the influence of the riverine supply with regard to open ocean supplies. The Congo shelf (9.CG) on

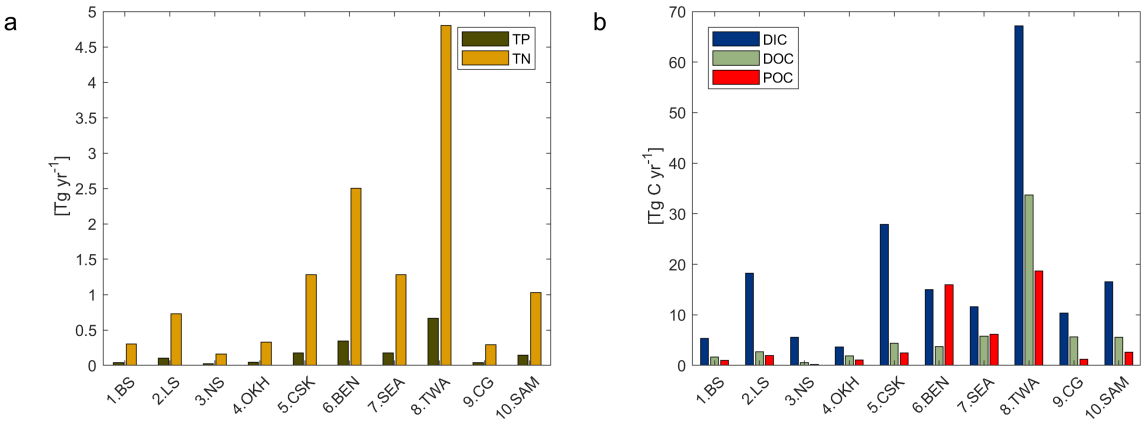

Figure 7. (a) Total P (TP) and N (TN) and (b) C (DIC, DOC and POC) exports to the chosen coastal ocean regions. TP and TN are the total P and N modelled in their dissolved inorganic species (DIP, DIN) and organic species (tDOM and POM). DOC and POC are the carbon loads from tDOM and riverine POM, respectively.

the other hand has a very small surface area (53 10^9 m^2) due to a steep coastal slope. The NPP here is however already one of the highest of the chosen regions without considering rivers, ~~suggesting~~ indicating that the region is already strongly supplied with nutrients from coastal upwelling.

On the temperate shelves, where there is a stronger seasonal cycle of the light limitation, the North Sea (2.NS) shows only weak enhancement in the NPP (2%) due to riverine inputs. The South American (10.SAM) and Sea of Okhotsk (4.OKH) also do not show significant NPP increases. Although the NPP is strongly enhanced in the direct proximity to the Paraná river (Figure 5b), the vastness of the South American shelf (1553 10^9 m^2) also makes the region less sensitive to river inputs. In published literature, the nutrient supply which drives the NPP on the Patagonian Shelf is also confirmed to be strongly controlled by ~~the~~ open ocean inflows, and not by river supplies (Song et al., 2016).

The Arctic shelf regions do not show a strong NPP response to the river inputs (8% and 5% increases for the Beaufort Sea ,1.BS, and Laptev Sea ,2.LS, respectively). We however do not consider seasonality of the riverine inputs. Larger inputs of nutrients in months of larger discharge (Le Fouest et al., 2013) of April to June, which are also months of better light availability, could cause a more efficient usage of the riverine nutrients, since the sea-ice coverage is strongly reduced in these months.

All regions show an increase in CO_2 outgassing due to the increased carbon inputs to the ocean. In the Arctic regions (Beaufort Sea and Laptev Sea), the relative change is ~~much more~~ very pronounced, whereas the impact is generally not as strong in the lower latitude regions due to the enhancement of biological carbon uptake by the nutrient inputs. The tropical West Atlantic is an exception to this latitudinal pattern, since the large carbon riverine supplies also cause a substantial change in the CO_2 flux ~~of~~ in the region. In the North Sea, we observe an enhancement of carbon outgassing caused by river loads, but the region remains a substantial sink of atmospheric CO_2, as is still suggested for the present-day by Laruelle et al. (2014).

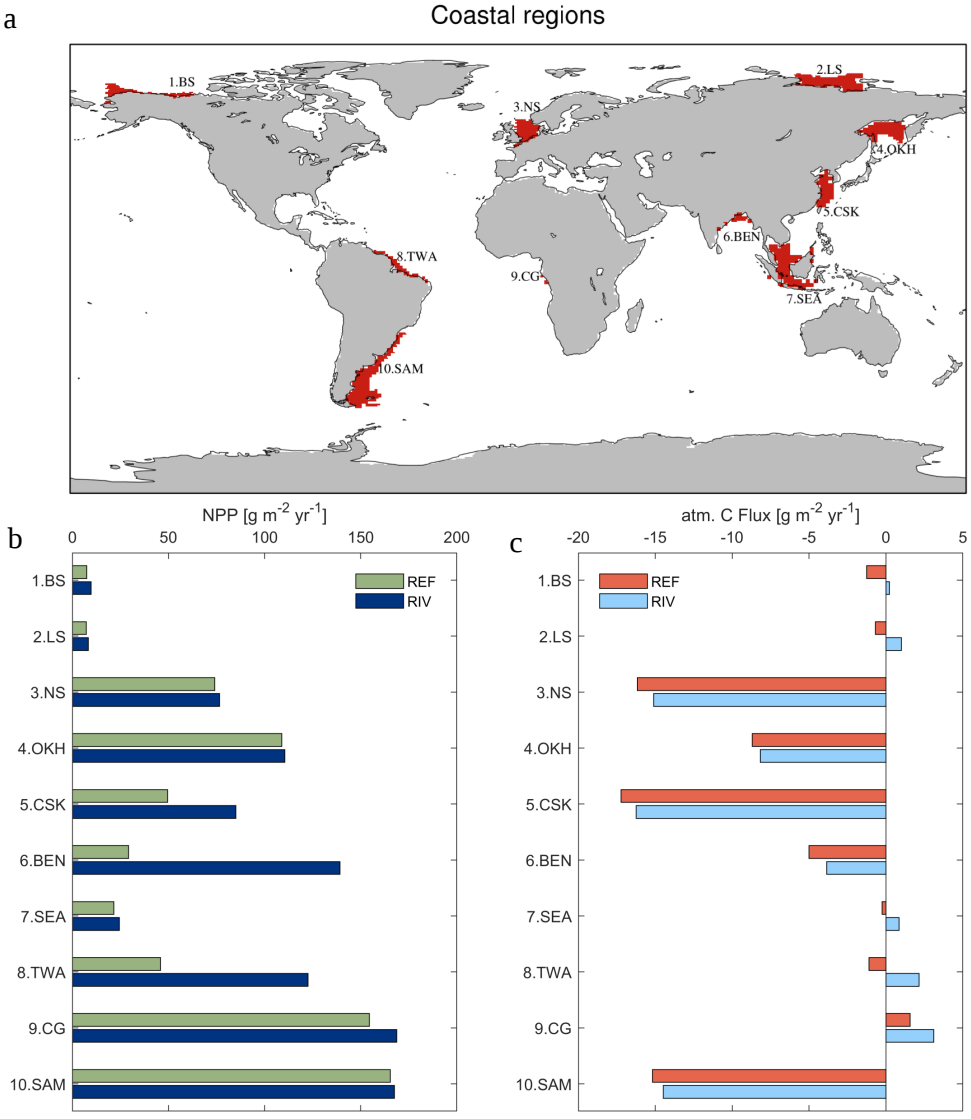

Figure 8. (a) Global map of the 10 chosen coastal regions with less than 250m depths~~and~~ , (b) pre-industrial annual NPP per area and (c) CO_2 flux in the given regions [g m^2 yr^{-1}]. In (c), a positive flux means a flux from the ocean to the atmosphere.

6 Origins and fate of riverine carbon

In our simplified ~~land-ocean system~~ model framework (Figure 9), we quantify the land sources of riverine carbon (**1**-**3**), its riverine transfer to the ocean (**4**), and the long-term fate of the riverine carbon in the ocean (**5-10**). Here, we briefly explain the fluxes to focus on their implications. While the terrestrial fluxes are derived from the weathering and organic matter export models, the long-term oceanic fluxes are based on fluxes given by the ocean biogeochemical model. The long-term oceanic CO_2 flux is furthermore decomposed to illustrate the contributions of inorganic and organic carbon inputs to the oceanic outgassing flux in a model equilibrium analysis. The detailed derivation of the land and ocean fluxes are explained in detail in the Appendix C (C1 for terrestrial and C2 for oceanic fluxes).

The ~~net~~ total pre-industrial terrestrial uptake of atmospheric CO_2 and its export ~~of~~ to rivers amounts to 529 Tg C yr^{-1} in our framework. The sink consists of 280 Tg C yr^{-1} from the CO_2 drawdown induced by weathering (**1**) and 249 Tg C yr^{-1} due to the ~~land~~ terrestrial biological uptake (**3**). During the weathering process, 94 Tg C yr^{-1} is moreover released from the lithology during carbonate weathering (**2**)~~, which is also reported in Hartmann et al. (2009)~~. During silicate weathering, all the carbon originates from atmospheric CO_2. The land biological uptake (**3**) is derived from the net global export of organic carbon to the ocean. It therefore implicitly takes into account the net ~~soil carbon uptake and~~ land biological uptake and its export to freshwaters, as well as all net sinks and sources in river systems. A total 603 Tg C yr^{-1} is transferred laterally to the ocean (**4**) while taking into consideration an endorheic catchment loss of 19 Tg C yr^{-1}.

In the ocean, riverine exports of carbon cause a long-term net annual carbon source of 231 Tg C yr^{-1}. We propose a decomposition of the long-term CO_2 flux into sources and sinks induced by the inputs of riverine ~~species~~ compounds (Appendix C.2). Assuming model equilibrium, the oceanic outgassing flux can be decomposed into a source from inorganic carbon supplied by weathering (183 Tg C yr^{-1}, **5**), a source from terrestrial organic carbon (128 Tg C yr^{-1}), **6**), a sink caused by the enhancement of the ~~biology~~ biological production due to the addition of dissolved inorganic nutrient and corresponding alkalinity production (69 Tg C yr^{-1}, **7**), and a sink due to disequilibrium at the atmosphere-water column interface in the model (11 Tg C yr^{-1}, **D1**). The production and the ~~sinking~~ downwards export of $CaCO_3$ and POM within the ocean lead to simulated sediment deposition fluxes of 188 Tg C yr^{-1} for $CaCO_3$ (inorg. C. flux, **8**) and 582 Tg C yr^{-1} for POM (org. C flux, **9**). The dissolution of $CaCO_3$ and the remineralization of POM within the sediment lead to a DIC flux from the sediment to the water column of 385 Tg C yr^{-1}. The net C flux at the sediment interface (**8+9-10**) is therefore a burial flux of 385 Tg C yr^{-1}. The calculated equilibrium carbon burial flux, which is the difference between the riverine carbon inputs and the equilibrium CO_2 outgassing (**4**-**5**-**6**+**7**), is 361 Tg C yr^{-1}, which implies that there is a deviation of 24 Tg C yr^{-1} (**D2**) towards the sediment in the simulated model burial (385 Tg C yr^{-1}) with respect to the calculated equilibrium state burial (361 Tg C yr^{-1}). The similar deviations from the equilibrium state at the atmosphere-water column and water column-sediment interfaces suggest that the model ~~drift in alkalinity, which most~~ disequilibrium, which likely originates from ~~disequilibrium~~ long time scales of the processes taking place in the sediment~~layers, translates~~ , translates relatively efficiently into a perturbation of the CO_2 flux at the atmosphere-water column interface.

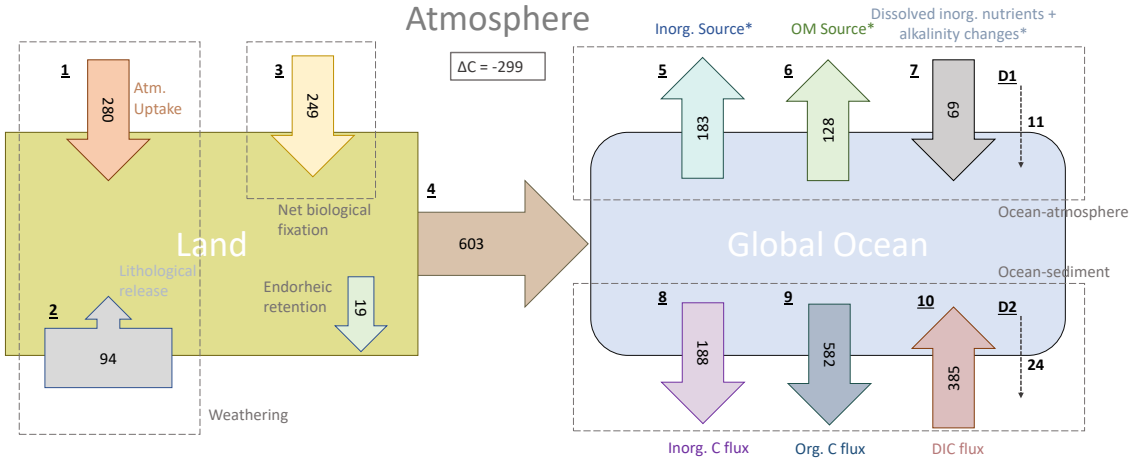

Figure 9. Origins and oceanic fate of riverine carbon in our ~~simplified land scheme coupled to HAMOCC (RIV simulation)~~ framework [Tg C yr^{-1}]. **1.** Land C uptake through weathering. **2.** Carbonate weathering lithological C flux. **3.** Net land biological C uptake (derived directly from riverine organic carbon exports). **4.** Riverine C exports. **5.** Oceanic outgassing from riverine DIC. **6.** Oceanic outgassing resulting ~~organic material (OM)~~ riverine tDOM loads. **7.** Oceanic C uptake due to the enhanced primary production by dissolved inorganic nutrients and the corresponding alkalinity production. **8.** Simulated inorganic C deposition to the sediment. **9.** Simulated net organic C deposition to sediment. **10.** Diffusive DIC flux from the sediment back to the water column. * are calculated fluxes for ocean model equilibrium, whereas the other fluxes are simulated fluxes by the terrestrial and ocean models. D1 and D2 are the calculated drifts between the oceanic modelled carbon fluxes and the calculated equilibrium fluxes (derived from model equations, Appendix C2) for the ocean-atmosphere and ocean sediment interfaces. See Appendix C for the derivation of the fluxes.

The riverine induced oceanic CO_2 outgassing flux of 231 Tg C yr^{-1} is consistent with the estimate range of 200-400 Tg C yr^{-1} given in Sarmiento and Sundquist (1992), who assume an annual riverine C flux of 300-500 Tg C, and with Jacobson et al. (2007) and Gruber et al. (2009), who suggest a slightly higher natural CO_2 outgassing flux of 450 Tg C yr^{-1}. Resplandy et al. (2018) suggest a higher land-ocean carbon (780 Tg C yr^{-1}) from the derivation of natural outgassing of carbon in the ocean. It is unclear if and how the ~~method~~ study considers oceanic carbon removal of the riverine-delivered carbon through sediment burial, leading to a much higher estimate than previously assumed.

Furthermore, we observe an imbalance in the calculated pre-industrial CO_2 land uptake from the atmosphere and the oceanic outgassing in our approach, with the land uptake outweighing the oceanic outgassing, resulting in a total net atmospheric sink of 299 Tg C yr^{-1}. Accounting for further sources of atmospheric CO_2 such as volcanic emissions and shale organic oxidation would therefore be necessary to achieve a stable atmospheric carbon budget in a fully coupled land-ocean-atmosphere setting, since Earth System Models assume constant pre-industrial atmospheric CO_2 levels. For instance, Mörner and Etiope (2002) suggest ~~long term~~ long-term volcanic annual emissions in the range of 80-160 Tg C yr^{-1}, whereas Burton et al. (2013) estimate ~~volcanic CO_2 fluxes~~ a long-term volcanic outgassing flux as high as that of silicate weathering drawdown~~, which would reduce~~

the disequilibrium in the pre-industrial atmospheric CO_2 budget. In our approach, the silicate weathering CO_2 drawdown is of 196 Tg C yr^{-1}. Additionally to the volcanic CO_2 emissions, the global atmospheric CO_2 land source from the oxidation of organic carbon in shale of around 100 Tg C yr^{-1} given by Sarmiento and Sundquist (1992) , due to the oxidation of organic carbon in rocks, would then approximately close the atmospheric carbon budget in our framework.

7 Approach advantages and limitations

7.1 Rivers in an Earth System Model setting

Our approach to represent riverine loads as a function of the climate variables runoff, precipitation and temperature can be used to estimate land-sea land-ocean fluxes in an Earth System Model (ESM) setting. For one, this could help tackle questions of the past, since weathering rates are dependent on climate variables (Berner, 1991). For instance, strong differences in weathering for the last glacial maximum have been suggested (Brault et al., 2017). The impacts of future climate change on weathering rates and land-sea fluxes could be addressed, as Gislason et al. (2009) and Beaulieu et al. (2012) suggest major changes in weathering due to changing climatic conditions on a decadal timescale. Furthermore, the RIV simulation can serve as a Our framework and simulations for the pre-industrial initial state to investigate temporal changes to the riverine loads over the 20th century, and in the future. Conclusions of Seitzinger et al. (2010) and Beusen et al. (2016) reveal strong increases DIP and DIN river loads during the 20th century, for which the oceanic impacts could be assessedstates of riverine loads and the ocean can be used as a baseline to assess oceanic impacts of perturbations of riverine loads due to temporal changes in weathering rates (Gislason et al., 2009), or due to increased anthropogenic P and N inputs to catchments (Seitzinger et al., 2010; Beusen et al., 2016).

Our approach provides a basis study relies on strong assumptions in order to address further questions regarding the land-ocean transfer dynamicsperform simulations at the global scale. Improvements within the framework are however possible. For one, improvements in the weathering mechanismsare possible (biological weathering enhancement and secondary mineral weathering). Ecosystem and the dynamical , the processing uptake of nutrients by the land biology, and their storage in the soil could be modelled, as well as considering terrestrial biology, the representation of hydrological flow characteristicsand river biogeochemical transformation processes . The consideration of groundwater fluxes could also be included. Coastal ocean dynamics could moreover be more accurately represented by using a higher modelresolution, and transformation processes and retention in rivers could all be represented more realistically. We also notably assumed fixed a N:P ratio for 16:1 for all catchments in this study. While N:P ratios are suggested to exceed this ratio at the global scale (29:1 by Seitzinger et al. (2010) and 21:1 by Beusen et al. (2016)), but denitrification in estuaries could compensate the excess of N with regard to a N:P ratio of 16:1 (see Supplementary Information 1.3), which we are incapable of representing in a global model. Furthermore, we assume a similar distribution of pre-industrial anthropogenic P inputs to catchments as for the present day. While comparing the chosen distribution with other approaches reveals the assumption to be plausible (Supplementary Information S.1), we acknowledge large uncertainty both in the magnitudes of anthropogenic inputs as well as in their distributions.

7.2 ~~Fate and consistence~~ Dynamics of terrestrial organic matter in the ocean

The composition of terrestrial organic matter, as well as its fate in the ocean ~~are associated with a large degree of uncertainty~~have been strongly debated in the past. Recent work shows that ~~tDOM is mineralized efficiently~~ despite its low biological reactivity, tDOM can be mineralized by abiotic processes ~~in the coastal zone (Fichot and Benner, 2014; Müller et al., 2016; Fichot and Benner, 2014)~~s as photodegradation in the ocean (Fichot and Benner, 2014; Müller et al., 2016; Aarnos et al., 2018), despite having already been strongly degraded along the land-ocean continuum. The global magnitude of this degradation is however strongly uncertain. On the other hand, few studies tackle the composition of POM, although it is thought to also be efficiently remineralized in the coastal zone sediment (Hedges et al., 1997; Cai, 2011). While the carbon loads from POM are the lowest loads of all carbon compounds considered in this study, a differing C:P ratio to the one chosen in this study would also affect the ~~model outgassing fluxestimated here~~modelled outgassing flux.

Rates of coastal remineralization processes have been suggested to differ from those of the open ocean (e.g. Krumins et al. (2013)). A higher sediment organic matter remineralization rate observed in coastal sediments (Krumins et al., 2013) could potentially reduce the coastal biogeochemical sink described in this study.

7.3 Arctic Ocean

The simulated nutrient concentrations in the Arctic Ocean are particularly high with regards to WOA data~~. Furthermore high dissolved organic material concentrations are found in observations for the Arctic (Benner et al., 2005). These characteristics suggest~~ , suggesting that this region with strong riverine inputs might be poorly represented in the ocean biogeochemistry model. Difficulties to represent the region could be due to fine circulation features, with outflows through narrow passages having been shown to be affected by model resolution (Aksenov et al., 2010). The modelled sea ice coverage, which is around 85% average for the Laptev Sea during the whole year, could be overestimated. Moreover, the primary production in the region might be underestimated due to photosynthesis taking place under ice, in ice ponds and over extended daytime periods in the summer months (Deal et al., 2011; Sørensen et al., 2017), all of which are not ~~represented~~ included in the model.

8 Summary and conclusions

In this study, we ~~provide global and spatial weathering release yields for P, Si, DIC and Alk, that are derived from driving spatially explicit models with MPI-ESM output of runoff, surface temperature and precipitation. These yields show good agreement with previous assessments found in published literature. The weathering yields are of disproportionate magnitude in warm and wet regions, confirming what has been suggested until now (Amiotte Suchet and Probst, 1995; Beusen et al., 2009; Hartmann et a~~ ~~Since ESMs tend to have substantial bias when quantifying the global runoff (Goll et al., 2014), runoff correction terms are needed to produce plausible weathering yields at the global scale. In the case of the MPI-ESM used in this study, which substantially underestimates the global runoff with regards to estimates of Dai and Trenberth (2002) and Fekete et al. (2002), a factor of 1.59 is necessary.~~

~~Accounting~~ account for weathering and non-weathering inputs to river catchments, which results in annual pre-industrial loads of 3.7 Tg P, 27 N, 168 Tg SiO_2, and 603 Tg C to the ocean. These loads are consistent with published literature estimates, although we acknowledge a certain degree of uncertainty regarding the magnitude of riverine fluxes. ~~Even for the present-day, substantial differences can be found between different approaches to derive land-ocean exports (Beusen et al., 2016).~~ While we omit the in-stream retention of P during its riverine transport, which reduces the global P exports to the ocean (Beusen et al., 2016), our estimate of ~~global~~ the global pre-industrial P export to the ocean is comparable in magnitude to an ~~approach~~ estimation that determines riverine P exports by upscaling from pristine river measurements (Compton et al., 2000).

We identify the tropical Atlantic catchments, the Arctic Ocean, Southeast Asia and Indo-Pacific islands as regions of dominant contributions of riverine supplies to the ocean. These 4 regions account for over 51% of land-ocean carbon exports in total, with tropical Atlantic catchments supplying around 20% of carbon to the ocean globally. We also observe that the contributions of different carbon species differ between the regions. Most prominently, the carbon supply of the Indo-Pacific islands is dominated by particulate organic carbon loads, which have been identified to be more strongly controlled by extreme hydrological events than other C species (Hilton et al., 2008).

In the ocean, riverine inputs of carbon lead to net global oceanic outgassing of 231 Gt C yr^{-1}, a comparable value with regards to previous estimates of 200-450 Tg C yr^{-1} (Sarmiento and Sundquist, 1992; Jacobson et al., 2007; Gruber et al., 2009). This outgassing flux can be decomposed into two source terms caused by inorganic C inputs (183 Tg C yr^{-1}) and organic C inputs (128 Tg C yr^{-1}), and a net sink term (80 Tg C yr^{-1}) caused by the enhanced biological C uptake due to riverine inorganic nutrient supplies, corresponding alkalinity production and a slight model drift in alkalinity. The magnitude of the outgassing is however strongly dependent on the magnitude of riverine carbon loads, for which uncertainties still exist.

We observe evidence of a substantial interhemispheric transport of carbon from the northern to the southern hemisphere, with a larger relative carbon outgassing flux in the southern hemisphere (49% of global outgassing) than its relative riverine carbon inputs to the ocean (36% of global C loads). We also show that the Southern Ocean outgasses 17 Tg of riverine carbon, despite not having a direct riverine source of carbon, meaning that riverine carbon is transported within the ocean interior to the Southern Ocean. This interhemispheric transfer of riverine carbon in the ocean has been previously suggested to contribute to the pre-industrial Southern Ocean source of atmospheric CO_2 for the pre-industrial time-frame (Sarmiento et al., 2000; Aumont et al., 2001; Gruber et al., 2009; Resplandy et al., 2018). Here we show that riverine carbon fluxes derived from state-of-the-art land export models confirm the larger contribution of the northern hemispheric terrestrial carbon supply to the ocean. Part of the uneven hemispheric terrestrial carbon supply is then compensated by the transport of carbon within the ocean and is outgassed remotely to the atmosphere.

Our results help identify oceanic regions that are sensitive to riverine fluxes. Riverine-induced changes in the regional NPP are mostly found in coastal regions, but significant riverine-derived CO_2 outgassing can also be observed in the open ocean of the tropical Atlantic. In general, latitudinal differences can also be observed in the sensitivity of the NPP and the CO_2 fluxes of various shallow shelves to riverine fluxes. While a high sensitivity in the NPP is found in tropical latitudes, with the tropical West Atlantic, the Bay of Bengal and the East China Sea showing large increases of 166%, 377% and 71% respectively, the relative changes in the regional CO_2 fluxes are larger at higher latitudes. For instance, the Laptev Sea and the Bay of Beaufort

become a atmospheric sources of 2.2 Tg C yr^{-1} and 2.3 Tg C yr^{-1} respectively, despite ~~previously~~ being sinks of atmospheric CO_2 ~~in the model~~without accounting for riverine inputs. While our analysis revolves around pre-industrial riverine exports, regions that show high sensitivity might also be more strongly affected by 20th century anthropogenic perturbations of land-ocean exports.

Deriving riverine exports as a function of Earth System Model variables (precipitation, temperature and runoff) enables a representation of the riverine loop, from the terrestrial uptake of carbon, its riverine export and to its long-term outgassing in the ocean and export to the oceanic sediment. In the case of implementing the framework in a coupled land-atmosphere-ocean setting such as an ESM, the atmospheric pre-industrial budget would have to be balanced. In our study, we emphasize the need to consider a ~~land~~ long-term terrestrial CO_2 source originating from long-term volcanic activity and from shale organic carbon oxidation in order to close the pre-industrial atmospheric C budget.

Throughout this study, we find global heterogeneity in the spatial features of weathering fluxes, riverine loads and their implications for the ocean biogeochemistry. ~~This, for instance, leads to the observed interhemispheric transfer of carbon in the ocean , with the dominance of northern hemispheric land-ocean carbon exports being evened out by remote oceanic carbon outgassing fluxes. Our results confirm the importance of nutrient and carbon fluxes for~~ We confirm that considering riverine exports to the ocean is central when assessing the biogeochemistry of ~~various shallow shelves and for the Arctic Ocean CO_2 flux~~coastal regions, but also find implications for open ocean regions (i.e. the tropical Atlantic). Our study also shows the necessity to account for the riverine-induced oceanic outgassing of carbon in ocean biogeochemistry models, since our conservative estimate consists of around 10% of the magnitude of the present-day ocean carbon uptake.

Code and data availability. Code, primary data and scripts needed to reproduce the analyses presented in this study are archived by the Max Planck Institute for Meteorology are available upon request (publications@mpimet.mpg.de)

Appendix A: ~~Freshwater Fluxes~~Ocean biogeochemistry model scheme

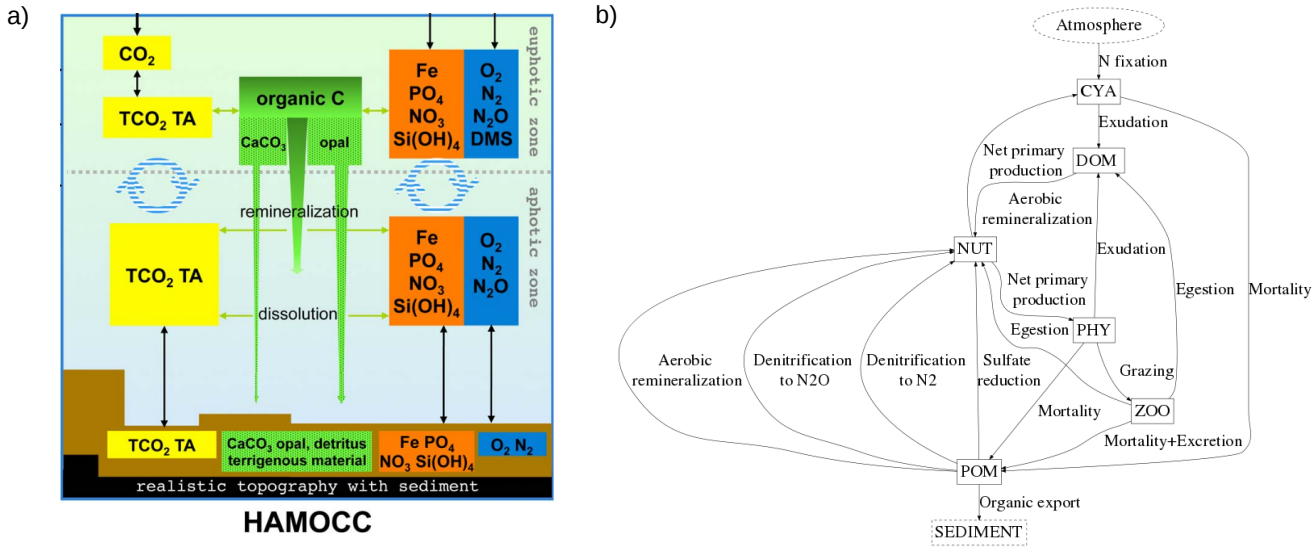

Figure A1. Scheme of model compartments in HAMOCC, modified from Ilyina et al. (2013), and (b) of the organic dynamics taking place in the model. The most central model parameters can be found in the Supplementary Information S.2.

Appendix B: Runoff, temperature and precipitation

The ~~freshwater loads from OMIP were already implemented in previous standard HAMOCC version, in order to close the hydrological cycle. Globally, they add 32,542 km^3 yr^{-1} of freshwater to the ocean. These impact the salinity and the ocean stratification in the proximity of our biogeochemical riverine inputs, and therefore their advection within the ocean~~weathering yields provided in this study are dependent on the MPI-ESM pre-industrial spatial representation of surface runoff, surface temperature and precipitation (Figure B1a,b,c).

Appendix C: ~~Coastal Salinity and Nutrient Profiles~~

~~Coastal vertical profiles show that despite the coarse resolution of our model, the features of salinity in selected coastal regions is comparable to WOA data, although vertical gradients are often not as strong as in the observational data (Figure A.2) . For the Amazon Northward section, we see a vertical the salinity gradient in the WOA data~~Previous work by Goll et al. (2014) describes the MPI-ESM performing well when estimating surface temperatures at single grid cells with regards to observations. The global precipitation is slightly higher than is reported in the Precipitation Climatology Project (GCPC) (Adler et al., 2003), which is ~~also reproduced albeit not extensively in the modelled data which induces stronger stratification of the water layers.~~

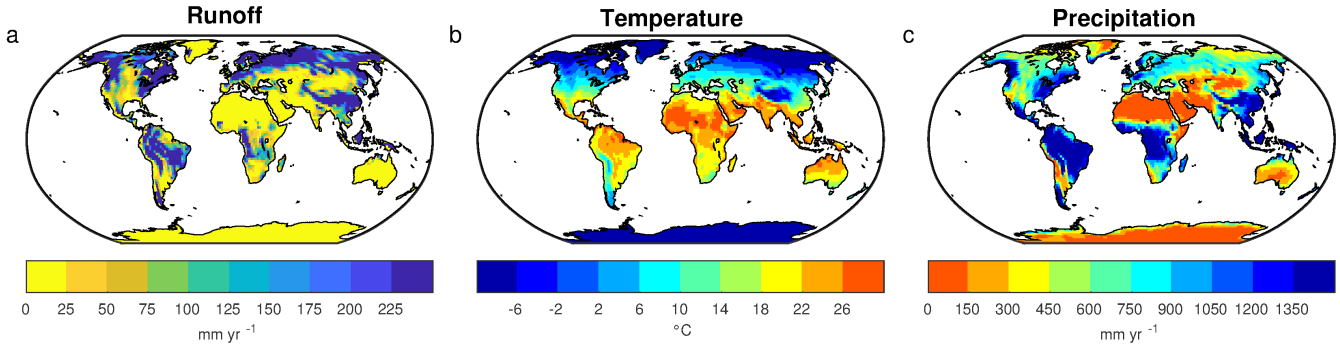

Figure B1. ~~Comparison of salinity from observational data~~ Modelled pre-industrial (~~WOA~~a) surface runoff [mm a^{-1}], (b) surface temperature[°C] and ~~modelled salinity in RIV (Salinity Model~~c) precipitation [mm a^{-1}] annual means.

~~In terms of absolute values the salinity is also well represented for the Ganges river, although the vertical stratification is also not quite as extensive further away from the coast. The bathymetry of the Laptev Sea at the Lena river mouth is poorly represented, as WOA data shows a height increase of the ocean floor at connection of the Sea with the Arctic Ocean, which is not represented in the model bathymetry. The salinity gradient in the East Chinese Sea is very strong due to currents parallel in the model which are also shown in observations (Ichikawa and Beardsley, 2002). Smaller currents in this region and in the Yellow Sea are however not well represented in~~ discussed along with spatial biases of the precipitation in Stevens et al. (2013). Most notably, the precipitation is too strong over extratropical land surface and too little over tropical land surface. Runoff on the other hand is less well reproduced globally. For the given time period of the CMIP5 simulation, the ~~model. The Congo river has a very steep coastal shelf, and therefore the salinity relatively strong vertical horizontal gradient, due to little bathymetry induced vertical mixing, as well as heating of the surface waters~~global runoff is 23,496 km^3 yr^{-1}. This is significantly lower than the global runoff estimations of 36,600-38,300 km^3 yr^{-1} (Fekete et al., 2002; Dai and Trenberth, 2002). The difficulty of representing several processes that control the runoff, such as evapotranspiration and condensation, is also reflected in the global runoff means of other Earth System Models, which range from 23,000 to 42,500 km^3 yr^{-1} (Goll et al., 2014). The spatial patterns in the CMIP5 simulation are however comparable with the mean annual runoff patterns reported in Fekete et al. (2002), with high surface runoff observed in the Amazon basin, West Africa, Indo-Pacific Islands, Southeast Asia, eastern North America, Northern Europe as well as in Siberia. Due to the strong underestimation of the model regarding the runoff in relation to the combined runoff mean of Fekete et al. (2002) and Dai and Trenberth (2002), we conclude that a scaling factor of 1.59 is necessary to produce runoff plausibly at the global scale. The global runoff from OMIP, which provides freshwater to the ocean model, is on the other hand more plausible (32,542 km^3 yr^{-1}), and was therefore not scaled.

~~Vertical profiles of the coastal bathymetry and salinity, along specific longitudes and longitudes for chosen river mouths. The left column (a-e) is made of WOA salinity profiles, whereas the right column (f-j) of profiles from model simulation RIV. a & f are shelf and salinity profiles at the Amazon river (TWA), b & g for the Ganges river, c & h Lena river, d & i Yangtze river, e & j Congo river.~~

Appendix C: Derivation of carbon fluxes in the simplified coupled system

C1 Terrestrial fluxes

1. Carbonate and silicate weathering cause a land uptake flux of 280 Tg C yr^{-1} from the atmosphere according to the weathering model simulations (Table ~~3~~2).

2. Carbonate mineral weathering causes a lithological carbon release flux of 94 Tg C yr^{-1} DIC, as shown in Section 3.2.

3. Carbon from terrestrial organic matter originates from the atmosphere (Meybeck and Vörösmarty, 1999). The net carbon uptake by the terrestrial and riverine biology is therefore the same as the lateral organic carbon export, which we derived from NEWS2 (Seitzinger et al., 2010) DOC and POC exports. The net uptake by the terrestrial biology, while taking into account all respiration processes on land and in rivers, is the sum of the lateral POC and DOC exports (249 Tg C yr^{-1}).

4. The riverine carbon export to the ocean consists of the sum of from weathering and organic matter carbon exports (623 Tg C yr^{-1}), minus a loss term due to endorheic rivers (19 Tg C yr^{-1}), which results in 603 Tg C yr^{-1} (values are rounded).

C2 Long-term ocean fluxes

In the model, riverine loads cause oceanic outgassing through the inputs of inorganic C and tDOM, while the inputs of dissolved inorganic nutrients cause a sink of atmospheric carbon through the biological enhancement of C uptake as well as increasing alkalinity while doing so.

The inorganic C is delivered by rivers as 1 mol DIC and 1 mol alkalinity (HCO_3^-) and exported as 0.5 mol DIC and 1 mol alkalinity ($CaCO_3$), leaving a surplus of 0.5 mol DIC and 0 mol alkalinity. Increasing the DIC pool without increasing the alkalinity directly increases the dissolved CO_2 concentrations, which in its turn causes outgassing:

$$H_2O+Ca^{2+}+2HCO_3^- => CaCO_3+CO_2+H_2O \quad \text{(C1)}$$

Equilibrium model outgassing caused by inorganic carbon inputs is therefore 0.5 fold of the riverine DIC loads.

tDOM model inputs, in contrary to POM, are not exported to the sediment. Outgassing from organic material results from the high C:P ratio of tDOM. It is mineralized in the ocean providing dissolved inorganic compounds in the C:P ratio of ~~2584~~2583:1, but the subsequent uptake of the released inorganic compounds happens at a C:P ratio of 122:1, resulting in a DIC overshoot. Since the net alkalinity over the entirety of Equation 15 is also constant, the DIC increase causes a pCO_2 increase (*simplified equation):

$$C_{2584\,2583}PN_{16}^* => 2584DIC\,2583DIC + DIP + 16DIN + ^* => C_{122}PN_{16}^* + 2462CO\,2461CO_2 \quad \text{(C2)}$$

The organic outgassing caused by organic matter inputs is therefore ~~2462~~2461/~~2584~~ 2583 multiplied with tDOM carbon loads.

The riverine loads of DIP and DIN on the other hand cause C uptake through their enhancement of biological primary production. DIC is thereby removed, thus sinking pCO_2 (*simplified equation):

$$DIP + 16DIN +^{*} + 122CO_2 => C_{122}PN^{*}_{16} \quad \text{(C3)}$$

The resulting C uptake from the equation is therefore 122-fold the mole DIP inputs. Additionally, alkalinity is produced in equation (16), which enhances C uptake. The uptake of DIN and DIP through primary production causes a net alkalinity increase by a factor of Alk:P = 17:1 (Wolf-Gladrow et al., 2007). The alkalinity is exported in a C:Alk ratio of 1:2 through ~~calcium carbonate~~ $CaCO_3$ production (Equation 14). The C uptake enhancement from the alkalinity increase is therefore the 17 * 1/2 - fold of the (bioavailable) DIP loads.

5. According to the $CaCO_3$ export equation (Eq ~~C1~~D1), half of the ~~DIC input (assuming HCO_3^-~~ riverine DIC input is exported to the sediment as $CaCO_3$ and the other half is outgassed as CO_2 in model equilibrium state. The contribution of outgassing caused by inorganic carbon in the ocean is therefore half (0.5-fold) the DIC inputs (366 Tg C yr^{-1}) and therefore 183 Tg C yr^{-1} assuming model equilibrium.

6. tDOM input C:P rations vastly exceed the oceanic sediment export C:P ratios of organic matter, which causes model equilibrium outgassing in the ocean. Equation C2 shows that for every mol tDOM supplied to the ocean, in model equilibrium 122/~~2584~~ 2583 of C is exported to the sediment and ~~2462~~2461/~~2584~~ 2583 of C increases the dissolved CO_2 pool, which is outgassed in the long term. The equilibrium outgassing is therefore the tDOM carbon load (134 Tg C yr^{-1}) multiplied by ~~2462~~2461/~~2584~~2583, which results in 128 Tg C yr^{-1}. In the case of POM, since the C:P ratio of the riverine input (122:1) is the same as the ratio of the export to the sediment in the ocean, there is no effect on the longterm equilibrium outgassing flux.

7. Since P has no further sinks or sources in the model other than riverine inputs and sediment burial as organic matter, in equilibrium the same amount of P supplied by rivers is buried in the sediment. When DIP is taken up by the biology and transformed to organic matter, carbon is also taken up in a mole ratio of C:P = 122:1. Accounting for this uptake through the biological production enhancement by DIP inputs (including bioavailable DIP) from rivers (~~(~~1.4 Tg P yr^{-1}) results in the uptake of 67 Tg C yr^{-1} ~~throug~~ through the biological enhancement. Furthermore, when DIP and DIN are transformed to organic matter as organic matter, an alkalinity increase of 17 mol per mol DIP uptake takes place (Eq. ~~C3~~D3, Wolf-Gladrow et al. (2007). This increase in alkalinity causes the further uptake uptake and export of 2 Tg C yr^{-1}, resulting in a total sink of 69 Tg C yr^{-1}.

D1. We attribute the difference between the equilibrium CO_2 flux of 242 Tg C yr^{-1} and the modelled net CO_2 flux of 231 Tg C yr^{-1} (=11 Tg C yr^{-1}) to the small surface alkalinity increase in the model due to slight disequilibrium over the analysis time period.

8. The simulated global particulate inorganic C sediment deposition flux in the ocean biogeochemistry model is 188 Tg C yr^{-1}.

9. The simulated global organic C sediment deposition flux in the ocean biogeochemistry model is 582 Tg C yr^{-1}.

10. The global modelled DIC flux from the sediment back to the water, which originates from POM remineralization in the sediment, column is 385 Tg C yr^{-1}.

D2. In model equilibrium the net sediment burial C flux is the total riverine C inputs of 603 Tg C yr^{-1} (**4**) subtracted by the equilibrium outgassing of 242 Tg C yr^{-1} (**5+6-7**), which results in 361 Tg C yr^{-1}. The simulated burial flux in the model of 385 Tg C yr^{-1} (**8+9-10**) deviates from the calculated model burial equilibrium flux. Therefore, the drift at the sediment-ocean interface is 24 Tg C yr^{-1} (385 Tg C yr^{-1} - 361 Tg C yr^{-1}).

Appendix D: Surface ~~Nutrient~~ nutrient profiles

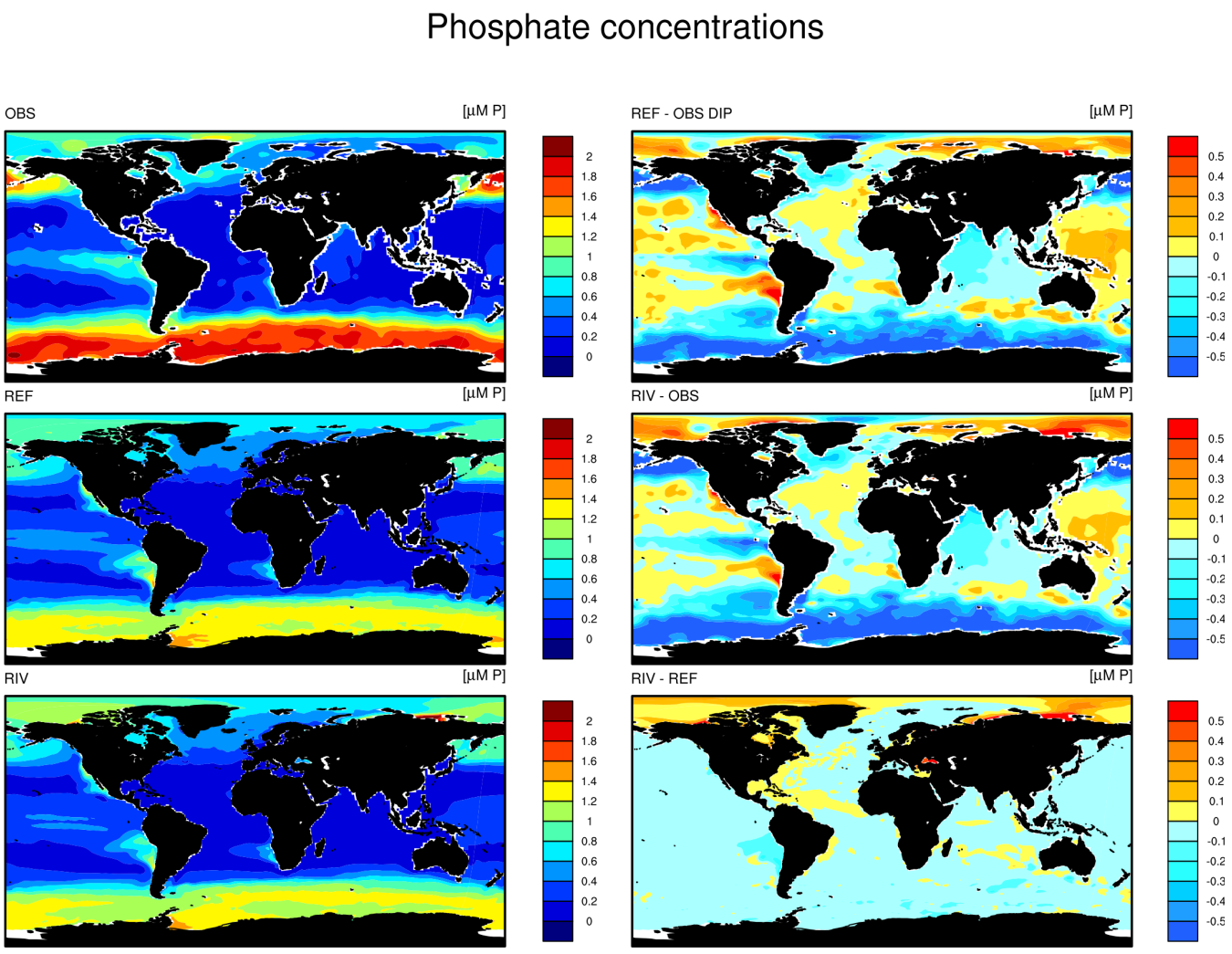

Figure E1. Phosphate (DIP) concentrations in OBS (WOA observations), REF and RIV.

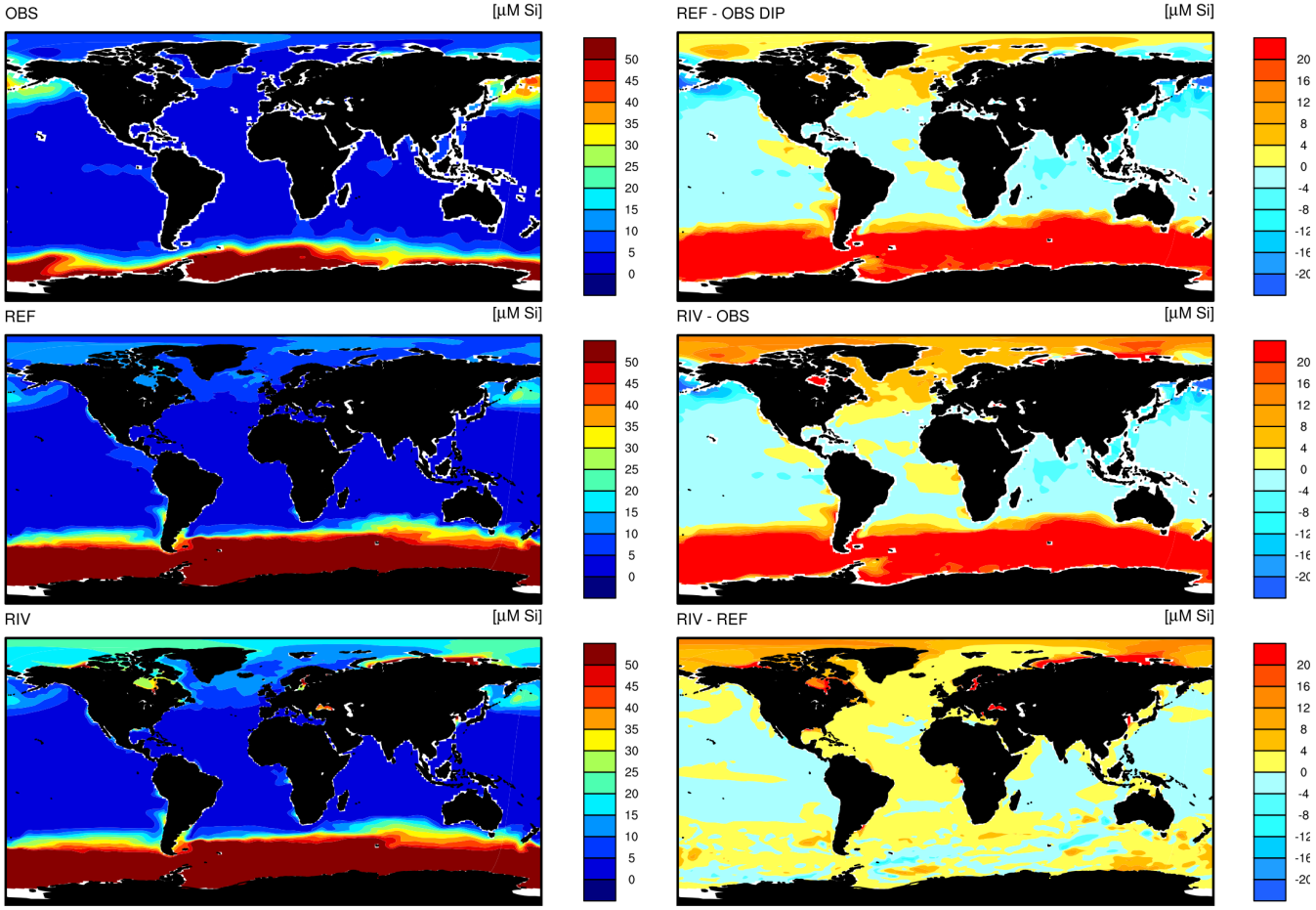

Figure F1. Dissolved silica (DSi) concentrations in OBS (WOA observations), REF and RIV.

Competing interests. All contributing authors declare that no competing interests are present.

Acknowledgements. All simulations were performed at the German Climate Computing Center (DKRZ). The research leading to these results has received funding from the European Union's Horizon 2020 research and innovation programme under the Marie Sklodowska-Curie grant agreement No 643052 (C-CASCADES project). We aknowledge constructive comments and suggestions received from Pierre Regnier, Irene Stemmler, Katharina Six and Philip Pika.

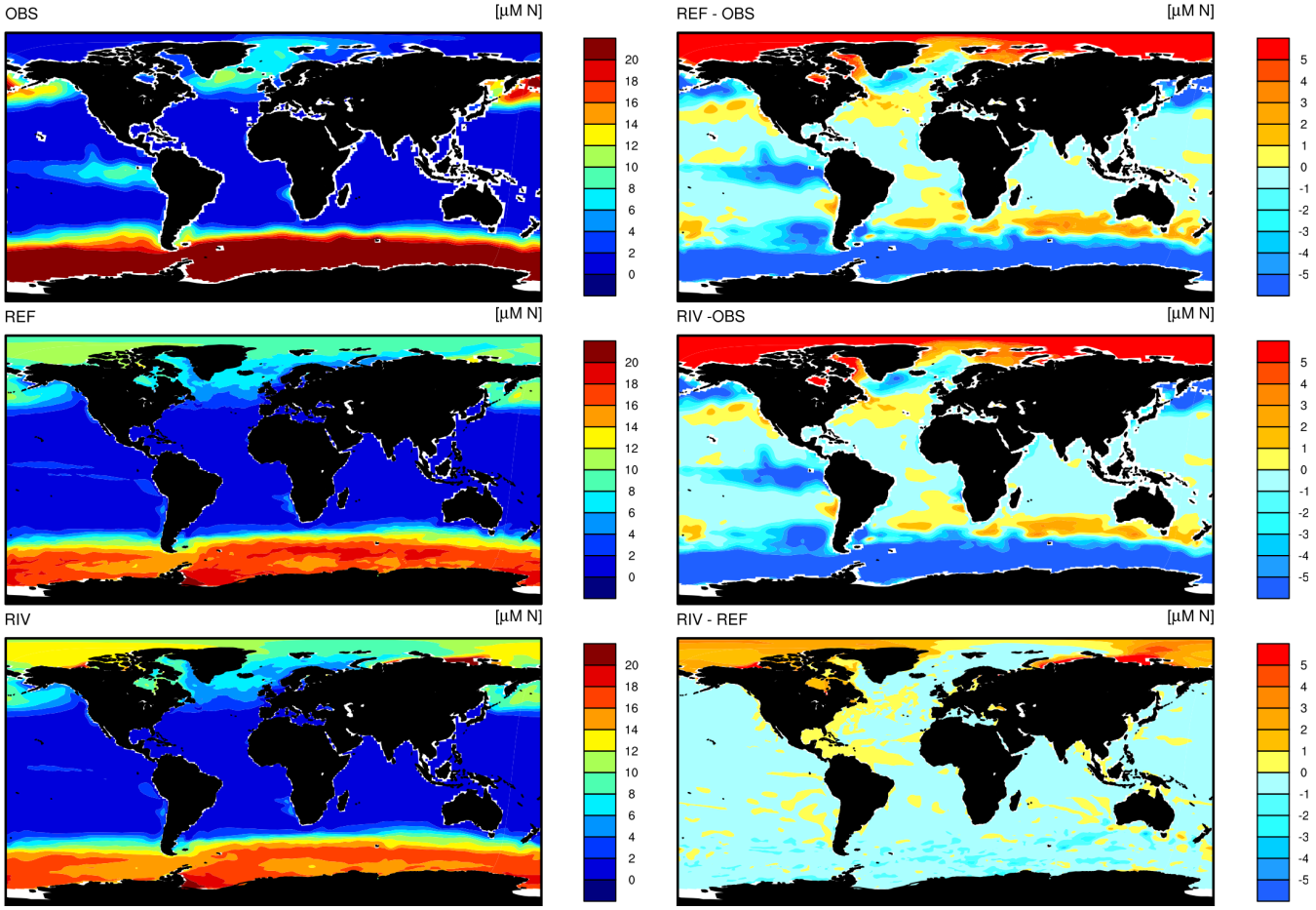

Figure G1. Nitrate (DIN) concentrations in OBS (WOA observations), REF and RIV.

References

Aarnos, H., Gélinas, Y., Kasurinen, V., Gu, Y., Puupponen, V.-M., and Vähätalo, A. V.: Photochemical Mineralization of Terrigenous DOC to Dissolved Inorganic Carbon in Ocean, Global Biogeochemical Cycles, 32, 250–266, https://doi.org/10.1002/2017GB005698, 2018.

Adler, R. F., Huffman, G. J., Chang, A., Ferraro, R., Xie, P.-P., Janowiak, J., Rudolf, B., Schneider, U., Curtis, S., Bolvin, D., Gruber, A., Susskind, J., Arkin, P., and Nelkin, E.: The Version-2 Global Precipitation Climatology Project (GPCP) Monthly Precipitation Analysis (1979–Present), Journal of Hydrometeorology, 4, 1147–1167, https://doi.org/10.1175/1525-7541(2003)004<1147:TVGPCP>2.0.CO;2, 2003.

Aksenov, Y., Bacon, S., Coward, A. C., and Holliday, N. P.: Polar outflow from the Arctic Ocean: A high resolution model study, Journal of Marine Systems, 83, 14–37, https://doi.org/https://doi.org/10.1016/j.jmarsys.2010.06.007, 2010.

Amiotte Suchet, P. and Probst, J. .-L.: A global model for presentday atmospheric/soil CO2 consumption by chemical erosion of continental rocks (GEMCO2), Tellus B, 47, 273–280, https://doi.org/10.1034/j.1600-0889.47.issue1.23.x, 1995.

Amiotte Suchet, P., Probst, J.-L., and Ludwig, W.: Worldwide distribution of continental rock lithology: Implications for the atmospheric/soil CO2 uptake by continental weathering and alkalinity river transport to the oceans, Global Biogeochemical Cycles, 17, https://doi.org/10.1029/2002GB001891, 2003.

Araujo, M., Noriega, C., and Lefèvre, N.: Nutrients and carbon fluxes in the estuaries of major rivers flowing into the tropical Atlantic, Frontiers in Marine Science, 1, 1–16, https://doi.org/10.3389/fmars.2014.00010, 2014.

Aumont, O., Orr, J. C., Monfray, P., Ludwig, W., Amiotte Suchet, P., and Probst, J.-L.: Riverinedriven interhemispheric transport of carbon, Global Biogeochemical Cycles, 15, 393–405, https://doi.org/10.1029/1999GB001238, 2001.

Batjes, N. H.: A world dataset of derived soil properties by FAO–UNESCO soil unit for global modelling, Soil Use and Management, 13, 9–16, https://doi.org/10.1111/j.1475-2743.1997.tb00550.x, 1997.

Batjes, N. H.: Revised soil parameter estimates for the soil types of the world, Soil Use and Management, 18, 232–235, https://doi.org/doi:10.1111/j.1475-2743.2002.tb00244.x, 2002.

Beaulieu, E., Goddéris, Y., Donnadieu, Y., Labat, D., and Roelandt, C.: High sensitivity of the continental-weathering carbon dioxide sink to future climate change, Nature Climate Change, 2, 346–349, https://doi.org/10.1038/nclimate1419, 2012.

Behrenfeld, M. and Falkowski, P.: Photosynthetic rates derived from satellite-based chlorophyll concentration, Limnology and Oceanography, 42, 1479–1491, https://doi.org/10.4319/lo.1997.42.1.0001, 1997.

Benner, R., Louchouarn, P., and Amon, R. M. W.: Terrigenous dissolved organic matter in the Arctic Ocean and its transport to surface and deep waters of the North Atlantic, Global Biogeochemical Cycles, 19, https://doi.org/10.1029/2004GB002398, 2005.

Bernard, C. Y., Dürr, H. H., Heinze, C., Segschneider, J., and Maier-Reimer, E.: Contribution of riverine nutrients to the silicon biogeochemistry of the global ocean – a model study, Biogeosciences, 8, 551–564, https://doi.org/10.5194/bg-8-551-2011, 2011.

Berner, R. A., Lasaga, A. C., and Garrels, R.: The carbonate-silicate geochemical cycle and its effect on atmospheric carbon dioxide over the past 100 million years, American Journal of Science, 283, 641–683, https://doi.org/10.2475/ajs.283.7.641, 1983.

Beusen, A. H. W., Dekkers, A. L. M., Bouwman, A. F., Ludwig, W., and Harrison, J.: Estimation of global river transport of sediments and associated particulate C, N, and P, Global Biogeochemical Cycles, 19, https://doi.org/10.1029/2005GB002453, 2005.

Beusen, A. H. W., Bouwman, A. F., Dürr, H., Dekkers, A. L. M., and Hartmann, J.: Global patterns of dissolved silica export to the coastal zone: Results from a spatially explicit global model, Global Biogeochemical Cycles, 23, https://doi.org/10.1029/2008GB003281, 2009.

Beusen, A. H. W., Bouwman, A. F., Van Beek, L. P. H., Mogollón, J. M., and Middelburg, J. J.: Global riverine N and P transport to ocean increased during the 20th century despite increased retention along the aquatic continuum, Biogeosciences, 13, 2441–2451, https://doi.org/10.5194/bg-13-2441-2016, 2016.

Bird, M. I., Robinson, R. A. J., Oo, N. W., Aye, M. M., Lu, X. X., Higgitt, D. L., Swe, A., Tun, T., Win, S. L., Aye, K. S., Win, K. M. M., and Hoey, T. B.: A preliminary estimate of organic carbon transport by the Ayeyarwady (Irrawaddy) and Thanlwin (Salween) Rivers of Myanmar, Quaternary International, 186, 113–122, https://doi.org/https://doi.org/10.1016/j.quaint.2007.08.003, 2008.

Björkman, K. M. and Karl, D. M.: Bioavailability of dissolved organic phosphorus in the euphotic zone at Station ALOHA, North Pacific Subtropical Gyre, Limnology and Oceanography, 48, 1049–1057, https://doi.org/10.4319/lo.2003.48.3.1049, 2003.

Bourgeois, T., Orr, J. C., Resplandy, L., Terhaar, J., Ethé, C., Gehlen, M., and Bopp, L.: Coastal-ocean uptake of anthropogenic carbon, Biogeosciences, 13, 4167–4185, https://doi.org/10.5194/bg-13-4167-2016, 2016.

Boyer, T. P., Antonov, J. I., Baranova, O. K., Garcia, H. E., Johnson, D. R., Mishonov, A. V., O'Brien, T. D., Seidov, D., Smolyar, I. I., Zweng, M. M., Paver, C. R., Locarnini, R. A., Reagan, J. R., Forgy, C., Grodsky, A., and Levitus, S.: World Ocean Database 2013, NOAA Atlas NESDIS 72, S. Levitus, Ed., A. Mishonov, Technical Ed.; Silver Spring, MD, 209, https://doi.org/10.7289/V5NZ85MT, 2013.

Brault, M.-O., Mysak, L. A., and Matthews, H. D.: Carbon cycle implications of terrestrial weathering changes since the last glacial maximum, FACETS, 2, 267–285, https://doi.org/10.1139/facets-2016-0040, 2017.

Burton, M. R., Sawyer, G. M., and Granieri, D.: Deep Carbon Emissions from Volcanoes, Reviews in Mineralogy Geochemistry, 75, 323–354, 2013.

Cai, W.-J.: Estuarine and Coastal Ocean Carbon Paradox: CO2 Sinks or Sites of Terrestrial Carbon Incineration?, Annual Review of Marine Science, 3, 123–145, https://doi.org/10.1146/annurev-marine-120709-142723, 2011.

Compton, J., Mallinson, D., Glenn, C., Filippelli, G., Föllmi, K., Shields, G., and Zanin, Y.: Variations in the global phosphorus cycle, IN:Marine Authigenesis: From Global to Microbial, Wiley-Blackwell, pp. 21–33, 2000.

Cooley, S. R., Coles, V. J., Subramaniam, A., and Yager, P. L.: Seasonal variations in the Amazon plume-related atmospheric carbon sink, Global Biogeochemical Cycles, 21, 1–15, https://doi.org/10.1029/2006GB002831, 2007.

Da Cunha, L., Buitenhuis, E. T., Le Quéré, C., Giraud, X., and Ludwig, W.: Potential impact of changes in river nutrient supply on global ocean biogeochemistry, Global Biogeochemical Cycles, 21, https://doi.org/10.1029/2006GB002718, 2007.

Dagg, M., Benner, R., Lohrenz, S., and Lawrence, D.: Transformation of dissolved and particulate materials on continental shelves influenced by large rivers: plume processes, Continental Shelf Research, 24, 833–858, https://doi.org/10.1016/j.csr.2004.02.003, 2004.

Dai, A. and Trenberth, K. E.: Estimates of Freshwater Discharge from Continents: Latitudinal and Seasonal Variations, Journal of Hydrometeorology, 3, 660–687, https://doi.org/10.1175/1525-7541(2002)003<0660:EOFDFC>2.0.CO;2, 2002.

Deal, C., Jin, M., Elliott, S., Hunke, E., Maltrud, M., and Jeffery, N.: Large-scale modeling of primary production and ice algal biomass within arctic sea ice in 1992, Journal of Geophysical Research: Oceans, 116, https://doi.org/10.1029/2010JC006409, 2011.

Dittmar, T. and Kattner, G.: The biogeochemistry of the river and shelf ecosystem of the Arctic Ocean: a review, Marine Chemistry, 83, 103–120, https://doi.org/https://doi.org/10.1016/S0304-4203(03)00105-1, 2003.

Dürr, H. H., Meybeck, M., and Dürr, S. H.: Lithologic composition of the Earth's continental surfaces derived from a new digital map emphasizing riverine material transfer, Global Biogeochemical Cycles, 19, https://doi.org/10.1029/2005GB002515, 2005.

Dürr, H. H., Meybeck, M., Hartmann, J., Laruelle, G. G., and Roubeix, V.: Global spatial distribution of natural riverine silica inputs to the coastal zone, Biogeosciences, 8, 597–620, https://doi.org/10.5194/bg-8-597-2011, 2011.

Edmond, J. M., Palmer, M. R., Measures, C. I., Grant, B., and Stallard, R. F.: The fluvial geochemistry and denudation rate of the Guayana Shield in Venezuela, Colombia, and Brazil, Geochimica et Cosmochimica Acta, 59, 3301–3325, https://doi.org/10.1016/0016-7037(95)00128-M, 1995.

Elser, J. J., Bracken, M. E. S., Cleland, E. E., Gruner, D. S., Harpole, W. S., Hillebrand, H., Ngai, J. T., Seabloom, E. W., Shurin, J. B., and Smith, J. E.: Global analysis of nitrogen and phosphorus limitation of primary producers in freshwater, marine and terrestrial ecosystems, Ecology Letters, 10, 1135–1142, https://doi.org/10.1111/j.1461-0248.2007.01113.x, 2007.

Etheridge, D. M., Steele, L. P., Langenfelds, R. L., Francey, R. J., Barnola, J.-M., and Morgan, V. I.: Natural and anthropogenic changes in atmospheric CO2 over the last 1000 years from air in Antarctic ice and firn, Journal of Geophysical Research: Atmospheres, 101, 4115–4128, https://doi.org/10.1029/95JD03410, 1996.

FAO/IIASA: Global Agro-Ecological Zones (Global-AEZ), Food and Agricul. Org. / Int. Inst. for Appl. Syst. Anal., Rome., https://doi.org/10.1029/2005GB002540, ttp://www.iiasa.ac.at/Research/LUC/GAEZ/index.htm.

Fekete, B. M., Vörösmarty, C. J., and Grabs, W.: High-resolution fields of global runoff combining observed river discharge and simulated water balances, Global Biogeochemical Cycles, 16, 10–15, https://doi.org/10.1029/1999GB001254, 2002.

Fernández-Martínez, M., Vicca, S., Janssens, I. A., Sardans, J., Luyssaert, S., Campioli, M., Chapin III, F., Ciais, P., Malhi, Y., Obersteiner, M., Papale, D., Piao, S. L., Reichstein, M., Rodà, F., and Peñuelas, J.: Nutrient availability as the key regulator of global forest carbon balance, Nature Climate Change, 4, 471, https://doi.org/10.1038/nclimate2177, 2014.

Fichot, C. G. and Benner, R.: The fate of terrigenous dissolved organic carbon in a river-influenced ocean margin, Global Biogeochemical Cycles, 28, 300–318, https://doi.org/10.1002/2013GB004670, 2014.

Filippelli, G. M.: The Global Phosphorus Cycle: Past, Present, and Future, Elements, 4, 89–95, https://doi.org/10.2113/GSELEMENTS.4.2.89, 2008.

Froelich, P. N.: Kinetic control of dissolved phosphate in natural rivers and estuaries: A primer on the phosphate buffer mechanism, Limnology and Oceanography, 33, 649–668, https://doi.org/10.4319/lo.1988.33.4part2.0649, 1988.

Gaillardet, J., Dupré, B., Louvat, P., and Allègre, C.: Global silicate weathering and CO2 consumption rates deduced from the chemistry of large rivers, Chemical Geology, 159, 3 – 30, https://doi.org/10.1016/S0009-2541(99)00031-5, 1999.

Giorgetta, M. A., Jungclaus, J., Reick, C. H., Legutke, S., Bader, J., Böttinger, M., Brovkin, V., Crueger, T., Esch, M., Fieg, K., Glushak, K., Gayler, V., Haak, H., Hollweg, H.-D., Ilyina, T., Kinne, S., Kornblueh, L., Matei, D., Mauritsen, T., Mikolajewicz, U., Mueller, W., Notz, D., Pithan, F., Raddatz, T., Rast, S., Redler, R., Roeckner, E., Schmidt, H., Schnur, R., Segschneider, J., Six, K. D., Stockhause, M., Timmreck, C., Wegner, J., Widmann, H., Wieners, K.-H., Claussen, M., Marotzke, J., and Stevens, B.: Climate and carbon cycle changes from 1850 to 2100 in MPI-ESM simulations for the Coupled Model Intercomparison Project phase 5, Journal of Advances in Modeling Earth Systems, 5, 572–597, https://doi.org/10.1002/jame.20038, 2013.

Gislason, S. R., Oelkers, E. H., Eiriksdottir, E. S., Kardjilov, M. I., Gisladottir, G., Sigfusson, B., Snorrason, A., Elefsen, S., Hardardottir, J., Torssander, P., and Oskarsson, N.: Direct evidence of the feedback between climate and weathering, Earth and Planetary Science Letters, 277, 213–222, https://doi.org/https://doi.org/10.1016/j.epsl.2008.10.018, 2009.

Goll, D. S., Moosdorf, N., Hartmann, J., and Brovkin, V.: Climate-driven changes in chemical weathering and associated phosphorus release since 1850: Implications for the land carbon balance, Geophysical Research Letters, 41, 3553–3558, https://doi.org/10.1002/2014GL059471, 2014.

Goudie, A. S. and Viles, H. A.: Weathering and the global carbon cycle: Geomorphological perspectives, Earth-Science Reviews, 113, 59–71, https://doi.org/10.1016/j.earscirev.2012.03.005, 2012.

Green, P. A., Vörösmarty, C. J., Meybeck, M., Galloway, J. N., Peterson, B. J., and Boyer, E. W.: Pre-industrial and contemporary fluxes of nitrogen through rivers: a global assessment based on typology, Biogeochemistry, 68, 71–105, https://doi.org/10.1023/B:BIOG.0000025742.82155.92, 2004.

Gruber, N., Gloor, M., Mikaloff Fletcher, S. E., Doney, S. C., Dutkiewicz, S., Follows, M. J., Gerber, M., Jacobson, A. R., Joos, F., Lindsay, K., Menemenlis, D., Mouchet, A., Müller, S. A., Sarmiento, J. L., and Takahashi, T.: Oceanic sources, sinks, and transport of atmospheric CO2, Global Biogeochemical Cycles, 23, https://doi.org/10.1029/2008GB003349, 2009.

Hagemann, S. and Dümenil, L.: A parametrization of the lateral waterflow for the global scale, Climate Dynamics, 14, 17–31, https://doi.org/10.1007/s003820050205, 1997.

Hagemann, S. and Gates, L. D.: Improving a subgrid runoff parameterization scheme for climate models by the use of high resolution data derived from satellite observations, Climate Dynamics, 21, 349–359, https://doi.org/10.1007/s00382-003-0349-x, 2003.

Harrison, J. A., Caraco, N., and Seitzinger, S. P.: Global patterns and sources of dissolved organic matter export to the coastal zone: Results from a spatially explicit, global model, Global Biogeochemical Cycles, 19, https://doi.org/10.1029/2005GB002480, 2005.

Harrison, W. and Cota, G.: Primary production in polar waters-relation to nutrient availability, Polar Research, 10, 87–104, https://doi.org/10.3402/polar.v10i1.6730, 1991.

Hart, M., Quin, B., and Long Nguyen, M.: Phosphorus Runoff from Agricultural Land and Direct Fertilizer Effects, Journal of environmental quality, 33, 1954–1972, 2004.

Hartmann, J. and Moosdorf, N.: Chemical weathering rates of silicate-dominated lithological classes and associated liberation rates of phosphorus on the Japanese Archipelago—Implications for global scale analysis, Chemical Geology, 287, 125–157, https://doi.org/https://doi.org/10.1016/j.chemgeo.2010.12.004, 2011.

Hartmann, J. and Moosdorf, N.: The new global lithological map database GLiM: A representation of rock properties at the Earth surface, Geochemistry, Geophysics, Geosystems, 13, https://doi.org/10.1029/2012GC004370, 2012.

Hartmann, J., Jansen, N., Dürr, H. H., Kempe, S., and Köhler, P.: Global CO2-consumption by chemical weathering: What is the contribution of highly active weathering regions?, Global and Planetary Change, 69, 185–194, https://doi.org/https://doi.org/10.1016/j.gloplacha.2009.07.007, 2009.

Hartmann, J., Moosdorf, N., Lauerwald, R., Hinderer, M., and West, A. J.: Global chemical weathering and associated P-release — The role of lithology, temperature and soil properties, Chemical Geology, 363, 145–163, https://doi.org/https://doi.org/10.1016/j.chemgeo.2013.10.025, 2014.

Hedges, J. I., Keil, R. G., and Benner, R.: What happens to terrestrial organic matter in the ocean?, Organic Geochemistry, 27, 195–212, https://doi.org/https://doi.org/10.1016/S0146-6380(97)00066-1, 1997.

Heinze, C., Maier-Reimer, E., Winguth, A. M. E., and Archer, D.: A global oceanic sediment model for longterm climate studies, Global Biogeochemical Cycles, 13, 221–250, https://doi.org/10.1029/98GB02812, 1999.

Hilton, R. G., Galy, A., Hovius, N., Chen, M.-C., Horng, M.-J., and Chen, H.: Nature Geoscience, p. 759, https://doi.org/https://doi.org/10.1038/ngeo333, 2008.

Ichikawa, H. and Beardsley, R. C.: The Current System in the Yellow and East China Seas, Journal of Oceanography, 58, 77–92, https://doi.org/10.1023/A:1015876701363, 2002.

Ilyina, T., Six, K. D., Segschneider, J., Maier-Reimer, E., Li, H., and NúñezRiboni, I.: Global ocean biogeochemistry model HAMOCC: Model architecture and performance as component of the MPI-Earth system model in different CMIP5 experimental realizations, Journal of Advances in Modeling Earth Systems, 5, 287–315, https://doi.org/10.1029/2012MS000178, 2013.

IPCC: Carbon and Other Biogeochemical Cycles, in: Climate Change 2013 – The Physical Science Basis: Working Group I Contribution to the Fifth Assessment Report of the Intergovernmental Panel on Climate Change, edited by Intergovernmental Panel on Climate Change, pp. 465–570, Cambridge University Press, Cambridge, https://doi.org/DOI: 10.1017/CBO9781107415324.015, 2013.

Ittekkot, V.: Global trends in the nature of organic matter in river suspensions, Nature, 332, 436, 1988.

Ittekkot, V., Humborg, C., and Schäfer, P.: Hydrological Alterations and Marine Biogeochemistry: A Silicate Issue?, BioScience, 50, 776, https://doi.org/10.1641/0006-3568(2000)050[0776:HAAMBA]2.0.CO;2, 2000.

Jacobson, A. R., Mikaloff Fletcher, S. E., Gruber, N., Sarmiento, J. L., and Gloor, M.: A joint atmosphere-ocean inversion for surface fluxes of carbon dioxide: 1. Methods and global-scale fluxes, Global Biogeochemical Cycles, 21, https://doi.org/10.1029/2005GB002556, 2007.

Jungclaus, J. H., Fischer, N., Haak, H., Lohmann, K., Marotzke, J., Matei, D., Mikolajewicz, U., Notz, D., and S., S. J.: Characteristics of the ocean simulations in the Max Planck Institute Ocean Model (MPIOM) the ocean component of the MPI-Earth system model, Journal of Advances in Modeling Earth Systems, 5, 422–446, https://doi.org/10.1002/jame.20023, 2013.

Krumins, V., Gehlen, M., Arndt, S., Van Cappellen, P., and Regnier, P.: Dissolved inorganic carbon and alkalinity fluxes from coastal marine sediments: Model estimates for different shelf environments and sensitivity to global change, Biogeosciences, 10, 371–398, https://doi.org/10.5194/bg-10-371-2013, 2013.

Lalonde, K., Vähätalo, A. V., and Gélinas, Y.: Revisiting the disappearance of terrestrial dissolved organic matter in the ocean: a δC13 study, Biogeosciences, 11, 3707–3719, https://doi.org/10.5194/bg-11-3707-2014, 2014.

Laruelle, G. G., Dürr, H. H., Lauerwald, R., Hartmann, J., Slomp, C. P., Goossens, N., and Regnier, P. A.: Global multi-scale segmentation of continental and coastal waters from the watersheds to the continental margins, Hydrology and Earth System Sciences, 17, 2029–2051, https://doi.org/10.5194/hess-17-2029-2013, 2013.

Laruelle, G. G., Lauerwald, R., Pfeil, B., and Regnier, P.: Regionalized global budget of the CO2 exchange at the air-water interface in continental shelf seas., Global Biogeochemical Cycles, pp. 1199–1214, https://doi.org/10.1002/2014GB004832.Received, 2014.

Laruelle, G. G., Landschützer, P., Gruber, N., Tison, J.-L., Delille, B., and Regnier, P.: Global high-resolution monthly pCO2 climatology for the coastal ocean derived from neural network interpolation, Biogeosciences, 14, 4545–4561, https://doi.org/10.5194/bg-14-4545-2017, 2017.

Le Fouest, V., Babin, M., and Tremblay, J.-É.: The fate of riverine nutrients on Arctic shelves, Biogeosciences, 10, 3661–3677, https://doi.org/10.5194/bg-10-3661-2013, 2013.

Lefèvre, N., Flores Montes, M., Gaspar, F. L., Rocha, C., Jiang, S., De Araújo, M. C., and Ibánhez, J. S. P.: Net Heterotrophy in the Amazon Continental Shelf Changes Rapidly to a Sink of CO2 in the Outer Amazon Plume, Frontiers in Marine Science, 4, 1–16, https://doi.org/10.3389/fmars.2017.00278, 2017.

Li, S. and Bush, R. T.: Changing fluxes of carbon and other solutes from the Mekong River, Sci. Rep., 26005, https://doi.org/10.1038/srep16005 (2015), 2015.

Ludwig, W., Probst, J.-L., and Kempe, S.: Predicting the oceanic input of organic carbon by continental erosion, Global Biogeochemical Cycles, 10, 23–41, https://doi.org/10.1029/95GB02925, 1996.

Ludwig, W., Amiotte Suchet, P., Munhoven, G., and Probst, J.-L.: Atmospheric CO2 consumption by continental erosion: present-day controls and implications for the last glacial maximum, Global and Planetary Change, 16-17, 107–120, https://doi.org/https://doi.org/10.1016/S0921-8181(98)00016-2, 1998.

Maavara, T., Dürr, H. H., and Van Cappellen, P.: Worldwide retention of nutrient silicon by river damming: From sparse data set to global estimate, Global Biogeochemical Cycles, 28, 842–855, https://doi.org/10.1002/2014GB004875, 2014.

Maavara, T., Lauerwald, R., Regnier, P., and Van Cappellen, P.: Global perturbation of organic carbon cycling by river damming, Nature Communications, 8, 15 347, https://doi.org/10.1038/ncomms15347, 2017.

Mackenzie, F. T., Lerman, A., and Ver, L. M. B.: Role of the continental margin in the global carbon balance during the past three centuries, Geology, 26, 423–426, 1998.

Mackenzie, F. T., Ver, L. M., and Lerman, A.: Century-scale nitrogen and phosphorus controls of the carbon cycle, Chemical Geology, 190, 13 – 32, https://doi.org/https://doi.org/10.1016/S0009-2541(02)00108-0, geochemistry of Crustal Fluids-Fluids in the Crust and Chemical Fluxes at the Earth's Surface, 2002.

Mahowald, N. M., Muhs, D. R., Levis, S., Rasch Philip, J., Yoshioka, M., Zender Charles, S., and Luo, C.: Change in atmospheric mineral aerosols in response to climate: Last glacial period, preindustrial, modern, and doubled carbon dioxide climates, Journal of Geophysical Research: Atmospheres, 111, https://doi.org/10.1029/2005JD006653, 2006.

Maier-Reimer, E. and Hasselmann, K.: Transport and storage of CO2 in the ocean ——an inorganic ocean-circulation carbon cycle model, Climate Dynamics, 2, 63–90, https://doi.org/10.1007/BF01054491, 1987.

Martin, J. H., Knauer, G. A., Karl, D. M., and Broenkow, W. W.: VERTEX: carbon cycling in the northeast Pacific, Deep Sea Research Part A. Oceanographic Research Papers, 34, 267–285, https://doi.org/https://doi.org/10.1016/0198-0149(87)90086-0, 1987.

Mauritsen, T., Bader, J., Becker, T., Behrens, J., Bittner, M., Brokopf, R., Brovkin, V., Claussen, M., Crueger, T., Esch, M., Fast, I., Fiedler, S., Fläschner, D., Gayler, V., Giorgetta, M., Goll, D. S., Haak, H., Hagemann, S., Hedemann, C., Hohenegger, C., Ilyina, T., Jahns, T., de la Cuesta Otero, D., Jungclaus, J., Kleinen, T., Kloster, S., Kracher, D., Kinne, S., Kleberg, D., Lasslop, G., Kornblueh, L., Marotzke, J., Matei, D., Meraner, K., Mikolajewicz, U., Modali, K., Möbis, B., Müller, W. A., Nabel, J. E. M. S., Nam, C. C. W., Notz, D., Nyawira, S.-S., Paulsen, H., Peters, K., Pincus, R., Pohlmann, H., Pongratz, J., Popp, M., Raddatz, T., Rast, S., Redler, R., Reick, C. H., Rohrschneider, T., Schemann, V., Schmidt, H., Schnur, R., Schulzweida, U., Six, K. D., Stein, L., Stemmler, I., Stevens, B., von Storch, J.-S., Tian, F., Voigt, A., de Vrese, P., Wieners, K.-H., Wilkenskjeld, S., Winkler, A., and Roeckner, E.: Developments in the MPI-M Earth System Model version 1.2 (MPI-ESM 1.2) and its response to increasing CO2, Journal of Advances in Modeling Earth Systems, 0, https://doi.org/10.1029/2018MS001400, 2018.

Mayorga, E., Seitzinger, S. P., Harrison, J. A., Dumont, E., Beusen, A. A. H. W., Bouwman, A. F., Fekete, B. M., Kroeze, C., and Drecht, G. V.: Global Nutrient Export from WaterSheds 2 (NEWS 2): Model development and implementation, Environmental Modelling & Software, 25, 837–853, https://doi.org/https://doi.org/10.1016/j.envsoft.2010.01.007, 2010.

Meybeck, M.: Carbon, Nitrogen, and Phosphorus Transport by World Rivers, Am. J. Sci., 282, 1982.

Meybeck, M.: C, N, P and S in Rivers: From Sources to Global Inputs, in: Interactions of C, N, P and S Biogeochemical Cycles and Global Change, edited by Wollast, R., Mackenzie, F. T., and Chou, L., pp. 163–193, Springer Berlin Heidelberg, Berlin, Heidelberg, 1993.

Meybeck, M. and Vörösmarty, C.: Global transfer of carbon by rivers, Global Change News Lett, 26, 1999.

Meybeck, M., Dürr, H. H., and Vörösmarty, C. J.: Global coastal segmentation and its river catchment contributors: A new look at land-ocean linkage, Global Biogeochemical Cycles, 20, https://doi.org/10.1029/2005GB002540, 2006.

Morée, A. L., Beusen, A. H. W., Bouwman, A. F., and Willems, W. J.: Exploring global nitrogen and phosphorus flows in urban wastes during the twentieth century, Global Biogeochemical Cycles, 27, 836–846, https://doi.org/10.1002/gbc.20072, 2013.

Mörner, N.-A. and Etiope, G.: Carbon degassing from the lithosphere, Global and Planetary Change, 33, 185–203, https://doi.org/https://doi.org/10.1016/S0921-8181(02)00070-X, 2002.

Müller, D., Warneke, T., Rixen, T., Müller, M., Mujahid, A., Bange, H. W., and Notholt, J.: Fate of terrestrial organic carbon and associated CO2 and CO emissions from two Southeast Asian estuaries, Biogeosciences, 13, 691–705, https://doi.org/10.5194/bg-13-691-2016, 2016.

Nixon, S. W., Ammerman, J. W., Atkinson, L. P., Berounsky, V. M., Billen, G., Boicourt, W. C., Boynton, W. R., Church, T. M., Ditoro, D. M., Elmgren, R., Garber, J. H., Giblin, A. E., Jahnke, R. A., Owens, N. J. P., Pilson, M. E. Q., and Seitzinger, S. P.: The fate of nitrogen and phosphorus at the land-sea margin of the North Atlantic Ocean, pp. 141–180, Springer Netherlands, Dordrecht, 1996.

Orr, J. C., Najjar, R. G., Aumont, O., Bopp, L., Bullister, J. L., Danabasoglu, G., Doney, S. C., Dunne, J. P., Dutay, J.-C., Graven, H., Griffies, S. M., John, J. G., Joos, F., Levin, I., Lindsay, K., Matear, R. J., McKinley, G. A., Mouchet, A., Oschlies, A., Romanou, A., Schlitzer, R., Tagliabue, A., Tanhua, T., and Yool, A.: Biogeochemical protocols and diagnostics for the CMIP6 Ocean Model Intercomparison Project (OMIP), Geoscientific Model Development, 10, 2169–2199, https://doi.org/10.5194/gmd-10-2169-2017, 2017.

Paulsen, H., Ilyina, T., Six, K. D., and Stemmler, I.: Incorporating a prognostic representation of marine nitrogen fixers into the global ocean biogeochemical model HAMOCC, Journal of Advances in Modeling Earth Systems, 9, 438–464, https://doi.org/10.1002/2016MS000737, 2017.

Plummer, L. and Busenberg, E.: The solubilities of calcite, aragonite and vaterite in CO2-H2O solutions between 0 and 90°C, and an evaluation of the aqueous model for the system CaCO3-CO2-H2O, Geochimica et Cosmochimica Acta, 46, 1011–1040, https://doi.org/10.1016/0016-7037(82)90056-4, 1982.

Ramirez, A. J. and Rose, A. W.: Analytical geochemistry of organic phosphorus and its correlation with organic carbon in marine and fluvial sediments and soils, American Journal of Science, 292, 421–454, https://doi.org/10.2475/ajs.292.6.421, 1992.

Raymond, P. A., McClelland, J. W., Holmes, R. M., Zhulidov, A. V., Mull, K., Peterson, B. J., Striegl, R. G., Aiken, G. R., and Gurtovaya, T. Y.: Flux and age of dissolved organic carbon exported to the Arctic Ocean: A carbon isotopic study of the five largest arctic rivers, Global Biogeochemical Cycles, 21, https://doi.org/10.1029/2007GB002934, 2007.

Regnier, P., Friedlingstein, P., Ciais, P., Mackenzie, F. T., Gruber, N., Janssens, I. A., Laruelle, G. G., Lauerwald, R., Luyssaert, S., Andersson, A. J., Arndt, S., Arnosti, C., Borges, A. V., Dale, A. W., Gallego-Sala, A., Goddéris, Y., Goossens, N., Hartmann, J., Heinze, C., Ilyina, T., Joos, F., LaRowe, D. E., Leifeld, J., Meysman, F. J. R., Munhoven, G., Raymond, P. A., Spahni, R., Suntharalingam, P., and Thullner, M.: Anthropogenic perturbation of the carbon fluxes from land to ocean, Nature Geoscience, 6, 597, 2013.

Resplandy, L., Keeling, R. F., Rödenbeck, C., Stephens, B. B., Khatiwala, S., Rodgers, K. B., Long, M. C., Bopp, L., and Tans, P. P.: Revision of global carbon fluxes based on a reassessment of oceanic and riverine carbon transport, Nature Geoscience, 11, 504–509, https://doi.org/10.1038/s41561-018-0151-3, 2018.

Roelandt, C., Goddéris, Y., Bonnet, M.-P., and Sondag, F.: Coupled modeling of biospheric and chemical weathering processes at the continental scale, Global Biogeochemical Cycles, 24, https://doi.org/10.1029/2008GB003420, 2010.

Romero-Mujalli, G., Hartmann, J., and Börker, J.: Temperature and CO2 dependency of global carbonate weathering fluxes – Implications for future carbonate weathering research, Chemical Geology, https://doi.org/https://doi.org/10.1016/j.chemgeo.2018.08.010, 2018.

Röske, F.: A global heat and freshwater forcing dataset for ocean models, Ocean Modelling, 11, 235–297, https://doi.org/https://doi.org/10.1016/j.ocemod.2004.12.005, 2006.

Sarmiento, J. and Sundquist, E.: Revised budget for the oceanic uptake of anthropogenic carbon dioxide, Nature, 356, 589–593, https://doi.org/10.1038/356589a0, 1992.

Sarmiento, J. L., Monfray, P., Maier-Reimer, E., Aumont, O., Murnane, R. J., and Orr, J. C.: Sea-air CO2 fluxes and carbon transport: A comparison of three ocean general circulation models, Global Biogeochemical Cycles, 14, 1267–1281, https://doi.org/10.1029/1999GB900062, 2000.

Seitzinger, S. P. and Sanders, R. W.: Contribution of dissolved organic nitrogen from rivers to estuarine eutrophication, Marine Ecology Progress Series, 159, 1–12, 1997.

Seitzinger, S. P., Harrison, J. A., Dumont, E., Beusen, A. H. W., and Bouwman, A. F.: Sources and delivery of carbon, nitrogen, and phosphorus to the coastal zone: An overview of Global Nutrient Export from Watersheds (NEWS) models and their application, Global Biogeochemical Cycles, 19, https://doi.org/10.1029/2005GB002606, 2005.

Seitzinger, S. P., Mayorga, E., Bouwman, A. F., Kroeze, C., Beusen, A. H. W., Billen, G., Drecht, G. V., Dumont, E., Fekete, B. M., Garnier, J., and Harrison, J. A.: Global river nutrient export: A scenario analysis of past and future trends, Global Biogeochemical Cycles, 24, https://doi.org/10.1029/2009GB003587, 2010.

Sharples, J., Middelburg, J. J., Fennel, K., and Jickells, T. D.: What proportion of riverine nutrients reaches the open ocean?, Global Biogeochemical Cycles, 31, 39–58, https://doi.org/10.1002/2016GB005483, 2017.

Six, K. D. and Maier-Reimer, E.: Effects of plankton dynamics on seasonal carbon fluxes in an ocean general circulation model, Global Biogeochemical Cycles, 10, 559–583, https://doi.org/10.1029/96GB02561, 1996.

Song, H., Marshall, J., Follows, M. J., Dutkiewicz, S., and Forget, G.: Source waters for the highly productive Patagonian shelf in the southwestern Atlantic, Journal of Marine Systems, 158, 120–128, https://doi.org/https://doi.org/10.1016/j.jmarsys.2016.02.009, 2016.

Sørensen, H. L., Thamdrup, B., Jeppesen, E., Rysgaard, S., and Glud, R. N.: Nutrient availability limits biological production in Arctic sea ice melt ponds, Polar Biology, 40, 1593–1606, https://doi.org/10.1007/s00300-017-2082-7, 2017.

Stallard, R. F.: Tectonic, Environmental, and Human Aspects of Weathering and Erosion: A Global Review using a Steady-State Perspective, Annual Review of Earth and Planetary Sciences, 23, 11–39, https://doi.org/10.1146/annurev.ea.23.050195.000303, 1995.

Stepanauskas, R., Jørgensen, N. O. G., Eigaard, O. R., Žvikas, A., Tranvik, L. J., and Leonardson, L.: Summer Inputs of riverine nutrients to the Baltic Sea: bioavailability and eutrophication relevance, Ecological Monographs, 72, 579–597, https://doi.org/10.1890/0012-9615(2002)072[0579:SIORNT]2.0.CO;2, 2002.

Stevens, B., Giorgetta, M., Esch, M., Mauritsen, T., Crueger, T., Rast, S., Salzmann, M., Schmidt, H., Bader, J., Block, K., Brokopf, R., Fast, I., Kinne, S., Kornblueh, L., Lohmann, U., Pincus, R., Reichler, T., and Roeckner, E.: Atmospheric component of the MPIM earth system model: ECHAM6, Journal of Advances in Modeling Earth Systems, 5, 146–172, https://doi.org/10.1002/jame.20015, 2013.

Stramski, D., Boss, E., Bogucki, D., and Voss, K. J.: The role of seawater constituents in light backscattering in the ocean, Progress in Oceanography, 61, 27–56, https://doi.org/10.1016/j.pocean.2004.07.001, 2004.

Takahashi, T., Wallace, S. B., and Langer, S.: Redfield ratio based on chemical data from isopycnal surfaces, Journal of Geophysical Research: Oceans, 90, 6907–6924, https://doi.org/10.1029/JC090iC04p06907, 1985.

Tank, S. E., Raymond, P. A., Striegl, R. G., McClelland, J. W., Holmes, R. M., Fiske, G. J., and Peterson, B. J.: A land-to-ocean perspective on the magnitude, source and implication of DIC flux from major Arctic rivers to the Arctic Ocean, Global Biogeochemical Cycles, 26, https://doi.org/10.1029/2011GB004192, 2012.

Tao, Y., Wei, M., Ongley, E., Zicheng, L., and Jingsheng, C.: Estuarine , Coastal and Shelf Science Long-term variations and causal factors in nitrogen and phosphorus transport in the Yellow River , China, Estuarine, Coastal and Shelf Science, 86, 345–351, https://doi.org/10.1016/j.ecss.2009.05.014, 2010.

Tréguer, P. J. and De La Rocha, C. L.: The World Ocean Silica Cycle, Annual Review of Marine Science, 5, 477–501, https://doi.org/10.1146/annurev-marine-121211-172346, 2013.

Turner, R. E., Rabalais, N. N., Justic', D., and Dortch, Q.: Global patterns of dissolved N, P and Si in large rivers, Biogeochemistry, 64, 297–317, https://doi.org/10.1023/A:1024960007569, 2003.

Tyrrell, T.: The relative influences of nitrogen and phosphorus on oceanic primary production, Nature, 400, 525–531, https://doi.org/10.1038/22941, 1999.

Vodacek, A., Blough, N. V., DeGrandpre, M. D., DeGrandpre, M. D., and Nelson, R. K.: Seasonal variation of CDOM and DOC in the Middle Atlantic Bight: Terrestrial inputs and photooxidation, Limnology and Oceanography, 42, 674–686, https://doi.org/10.4319/lo.1997.42.4.0674, 2003.

Wang, Y. P., Law, R. M., and Pak, B.: A global model of carbon, nitrogen and phosphorus cycles for the terrestrial biosphere, Biogeosciences, 7, 2261–2282, https://doi.org/10.5194/bg-7-2261-2010, 2010.

Wolf-Gladrow, D., Zeebe, R., Klaas, C., Körtzinger, A., and Dickson, A. G.: Total alkalinity: the explicit conservative expression and its application to biogeochemical processes, Marine Chemistry, 106, 287–300, https://doi.org/10.1016/j.marchem.2007.01.006, 2007.

Yoshimura, C., Zhou, M., Kiem, A. S., Fukami, K., Prasantha, H. H. A., Ishidaira, H., and Takeuchi, K.: Science of the Total Environment 2020s scenario analysis of nutrient load in the Mekong River Basin using a distributed hydrological model, Science of the Total Environment, The, 407, 5356–5366, https://doi.org/10.1016/j.scitotenv.2009.06.026, 2009.